CHALMERS
UNIVERSITY OF TECHNOLOGY

Anchorage of plain, naturally corroded reinforcement bars with end-hooks

Master's thesis in Master Program Structural engineering and building technology

Litong Zheng
Sining Liu

Department of Architecture and Civil Engineering
Division of Structural Engineering
Concrete Structures
CHALMERS UNIVERSITY OF TECHNOLOGY
Gothenburg, Sweden 2021

Anchorage of plain, naturally corroded reinforcement bars with end-hooks

Master's thesis in Master Program Structural engineering and building technology

Litong Zheng
Sining Liu

CHALMERS
UNIVERSITY OF TECHNOLOGY

Department of Architecture and Civil Engineering
Division of Structural Engineering
Concrete Structures
Chalmers University of Technology
Gothenburg, Sweden 2021

Anchorage of plain, naturally corroded reinforcement bars with end-hooks

Master's thesis in Master Program Structural engineering and building technology

Litong Zheng
Sining Liu

Supervisor: Professor Karin Lundgren, Department of Architecture and Civil Engineering
Supervisor: PhD candidate Samanta Robuschi, Department of Architecture and Civil Engineering
Supervisor: PhD Mohammad Tahershamsi, WSP
Examiner: Professor Karin Lundgren, Department of Architecture and Civil Engineering

Department of Architecture and Civil Engineering
Division of Structural Engineering
Concrete Structures Group
Chalmers University of Technology
SE-412 96 Gothenburg
Telephone +46 31 772 1000

Cover: An illustration of reinforcement bar terminating in end hook.

Department of Architecture and Civil Engineering
Gothenburg, Sweden 2021

Anchorage of plain, naturally corroded reinforcement bars with end-hooks
Master's thesis in Master Program Structural engineering and building technology

Litong Zheng
Sining Liu
Department of Architecture and Civil Engineering
Division of Structural Engineering
Concrete Structures
Chalmers University of Technology

ABSTRACT

Following the developments since 1960, plain reinforcement bars have been replaced by ribbed reinforcement bars in the design of concrete structures. However, some of the existing old structures with plain reinforcement bars are still in use and there is insufficient knowledge available for the assessment of structures with plain reinforcement bars.

The aim of this thesis was to evaluate the anchorage capacity of naturally corroded plain reinforcement bars with end-hooks. The studied specimens were earlier cut from edge beams of a decommissioned bridge. There were two types of beams: with one or two pairs of hooks. Three-point bending tests of the beams had been carried out before this thesis project. Digital Image Correlation was used to monitor deflections and crack developments. In this thesis, the structural behavior of both types of beams was evaluated. The yield penetration and corrosion level of plain reinforcement bars with end-hooks were evaluated from 3D scanned data. Further, the bond stress in the yielded zone and the force anchored by the hooks were assessed. Finally, the experimental results were compared to the design capacity in accordance with two different available codes, BBK 04[3] and ACI[1].

In comparison, the beams with two pairs of hooks showed a larger load-carrying capacity. The end-hook of beams with one pair of hooks managed to carry the yield force in some cases, while for the beams with two pairs of hooks, shear failure limited the deformation capacity of the beams. The results showed that the average corrosion level varied from 0% to 2%. The bond stress in the yielded zone was found to vary between 0 MPa and 4.5 MPa. The force anchored by the hooks varied depending on the assumed value of the bond stress in the unyielded zone. For an assumed bond stress ranging from 1 MPa to 12 MPa, the evaluated force anchored by the hooks was similar in both types of beams and varied between 32 kN and 53 kN. The calculated force anchored by the hooks in the experiments was on average 84% and 64% of the code results according to BBK 04[3] and ACI[1], respectively.

Key words: Natural corrosion, plain reinforcement bars, reinforced concrete, anchorage, bond stress, DIC, 3D scanning

Contents

1 Introduction **1**
- 1.1 Background . . . 1
- 1.2 Scope and Objectives . . . 2
- 1.3 Method . . . 2
- 1.4 Limitations . . . 3
- 1.5 Original features . . . 3
- 1.6 Outline . . . 3

2 Theoretical background **5**
- 2.1 Plain reinforcement bars with end-hooks . . . 5
- 2.2 Effect of corrosion . . . 8

3 Methodology **11**
- 3.1 Specimen . . . 11
  - 3.1.1 Geometry . . . 11
  - 3.1.2 Material . . . 15
- 3.2 Structural tests . . . 16
  - 3.2.1 Three-point bending tests . . . 16
  - 3.2.2 DIC . . . 19
- 3.3 Post processing . . . 19
  - 3.3.1 Extraction of the rebar, labelling and cutting . . . 19
  - 3.3.2 Sandblasting . . . 20
  - 3.3.3 3D scanning . . . 21
- 3.4 Evaluation of corrosion level and yield penetration . . . 23
  - 3.4.1 Corrosion level . . . 23
  - 3.4.2 Yield penetration . . . 25
- 3.5 Remaining capacity of the end hooks . . . 28
  - 3.5.1 Bond stress in the yielded zone . . . 29
  - 3.5.2 Force anchored by the hook . . . 30
- 3.6 Capacity calculation of the hooks according to ACI Journal and Swedish Handbook for Concrete Structures (BBK 04) . . . 31
- 3.7 Shear capacity of the beams . . . 32

4 Results **33**

4.1 General behavior of the structural tests . . . 33
4.1.1 Load versus deflection curves . . . 33
4.1.2 Crack patterns . . . 38
4.1.3 Differences between plain rebars with and without end-hooks . 40
4.1.4 Shear capacity of beams with two pairs of hooks . . . 41
4.1.5 Deformation of hook ends after the three-point bending tests . 42
4.2 Corrosion level . . . 43
4.3 The average bond stress in the yielded zone . . . 45
4.4 Force anchored by the hooks . . . 48
4.4.1 Force anchored by the hooks during the tests . . . 48
4.4.2 The impact of corrosion . . . 50
4.4.3 The impact of casting positions . . . 52
4.5 Comparison of anchorage strength calculated by design provisions . . 52

5 Conclusion and recommendations for further studies 57
5.1 Conclusion . . . 57
5.2 Recommendations for further studies . . . 58

References 58

A Appendix i
A.1 Corrosion level and yield penetration . . . i
A.2 Calculation of correlation coefficient . . . xxv
A.3 Source code in MATLAB file for figures . . . xl

B Appendix li
B.1 Corrosion data in Excel . . . li

C Appendix lv
C.1 Beam 1 . . . lv
C.2 Beam 18H . . . lxv
C.3 Beam 19 . . . lxxii
C.4 Beam 10D . . . lxxx
C.5 Beam 13G . . . lxxxvi
C.6 Beam 16K . . . xcii
C.7 Shear capacity . . . xcviii

Preface

In this work, the effects of natural corrosion on the structural behaviour of concrete beams containing reinforcement bars with end hooks was studied. The work was carried out from January 2021 to September 2021 at the Department of Architecture and Civil Engineering, Division of Structural Engineering at Chalmers University of Technology.

During the work, we have been fortunate to have the guidance of many people with a wealth of experience and knowledge, and we would like to thank them.

We would like to thank our supervisor Samanta Robuschi for your experience and guidance. You have always scheduled time to answer our questions and provide ideas, which helped us a lot during the Master thesis work. We would also like to thank our supervisor at WSP, Mohammad Tahershamsi, for your kind input.

We also want to thank our opponents Malik Sheraz Nazam and Maharaghni Chennapragada for their ideas and opinions, and it is great pleasure for us to be able to communicate and cooperate with them.

Finally, we would like to thank our examiner Karin Lundgren for your support to this work. We thank you for your encouragement and inspiration to keep us progressing and overcoming difficulties.

Gothenburg, October 2021

Litong Zheng

Sining Liu

1

Introduction

1.1 Background

In recent years, sustainability has become increasingly important in our society. As such, in the future of structural engineering, more efforts will be put onto assessing, repairing and strengthening the existing structures. Reinforced concrete uses large amounts of cement, which at production requires large energy consumption, which in turn produces carbon dioxide. Starting from the concept of sustainable development, it is essential to research and maintain the existing old reinforced concrete structures and make full use of them in order to reduce the negative environmental impacts of newly constructed reinforced concrete structures. Under the precondition of safety, the service life of structures should be prolonged as much as possible, in order to avoid waste of resources.

Older reinforced concrete structures are characterized by the use of plain reinforcement bars. Generally speaking, plain reinforcement bars are those with no surface deformations. After decades of development, plain reinforcement bars have been gradually replaced by ribbed reinforcement bars, since the latter one has surface ribs that will increase its bond strength when used in reinforced concrete. Past research has shown that bond strength between reinforcement bars and concrete consists of three main mechanisms: chemical adhesion, friction and mechanical interlock. Friction and chemical adhesion usually play a fundamental role for plain reinforcement bars compared with ribbed reinforcement bars, while mechanical interlock contributes only at the micro-level for plain reinforcement bars. As a result, the bond of plain reinforcement bars will be naturally lower and weaker than that of ribbed reinforcement bars.

In fact, concrete structures reinforced with plain reinforcement bars were quite common up to 40s. In many cases, the reinforcement bars ended with hooks in the anchorage zone to increase the anchorage capacity and compensate for the weak bond. Many structures from that time are still in use. Currently however, there is insufficient knowledge available for the assessment of structures with plain reinforcement bars since corrosion effects on bond is unknown.

It is well known that under the influence of various environmental factors, these reinforced concrete structures are bound to suffer different degrees of corrosion. Corrosion is the most common cause of deterioration in reinforced concrete structures. Corrosion is commonly due to chloride contamination. Corrosion results in a reduction in the effective cross-sectional area of reinforcement bars. Further, corro-

sion products occupy a larger volume than the steel they originate from, which can cause cracking of the concrete cover, and thus further deterioration.

Since the mechanical behaviors of plain reinforcement bars and ribbed reinforcement bars differ, their bond behaviors are expected to be different after the reinforcement bars are corroded. However, there is little knowledge on the effect of corrosion on the structural behavior of reinforced concrete structures with plain reinforcement bars, which may lead to unnecessary demolishment and reconstruction.

Before this thesis work, seven naturally corroded reinforced concrete beams were tested in three-point bending tests in Structures Laboratory at Chalmers University of Technology. Three of the beams included spliced reinforcement bars with hooks and four included reinforcement bars that were anchored by hooks at their ends. Depending on the hook positioning, the failure modes varied between shear and bending failure.

1.2 Scope and Objectives

The aim of this thesis was to acquire knowledge on the structural behavior of end hook anchorage in naturally corroded reinforced concrete structures with plain bars. More specifically, the overall aim was to evaluate the anchorage capacity of naturally corroded, plain reinforcement bars with end-hooks. To reach this aim, the following objectives were identified:

- To study the effect on structural behavior of plain rebars with end-hooks under the influence of corrosion;
- To study and assess the load-carrying capacity of the beams with corroded reinforcement bars anchored with end-hooks.

1.3 Method

In three-point bending tests had been carried out earlier, mid-span deflections and crack developments were monitored by Digital Image Correlation(DIC). After the tests, the reinforcement bars were extracted for further evaluation.

With the aim of obtaining data, the reinforcement bars were cut and sandblasted. Geometrical data were acquired by 3D scanning and processed by software VX elements and GOM Inspect for further evaluation of yield penetration and corrosion level. A set of current MATLAB codes were modified and used to evaluate the corrosion level of the reinforcement bars. At the same time, the plot of both cross-sectional perimeter and area along the longitudinal reinforcement bars was obtained. The yield penetration was evaluated by comparing the trends of the cross-sectional perimeter and area. Further, the forces anchored by the hooks were calculated from the evaluated corrosion level and yield penetration, and on an assumed bond stress in the straight part of the reinforcement bars. The value of this assumed bond stress was based on a literature study. The theoretical design capacity of hooks was also calculated, from two different codes, BBK 04[3] and ACI[1]. Finally, the calculated

force anchored by the hooks were compared to the theoretical design capacity.

1.4 Limitations

- The structural tests had already been carried out before this thesis work started, this project focused on interpretation of the results and an analytical study.
- The specimens were originally parts taken from a decommissioned bridge. The corrosion level influenced by environment, geometry of the beams could thus not be controlled.
- Due to the limited space of the sandblasting machine compared with the reinforcement bars dimensions, the reinforcement bars were cut into two separate sections. This implies that information on the corrosion status might be lost at the cutting area.

1.5 Original features

The original features of this study are as follows:

- Beams from an 80-year old bridge including naturally corroded reinforcement bars with end hooks were investigated.
- Corrosion level and yield penetration for each reinforcement bar were identified.

1.6 Outline

The outline of the thesis is as follows:

Chapter 1 introduces background, aim, method, limitations and original features of the study.

Chapter 2 provides an overview of structural behavior of naturally corroded plain bars with hooks and on the effect of corrosion by reviewing existing literature.

Chapter 3 focuses on the methodology of obtaining the geometry of the bars and the post-processing as well as the calculation and analysis of the data.

Chapter 4 presents the structural behaviour of the beams, and the results of yield penetration and corrosion level of the bars. The force anchored by the hooks is also calculated and compared to the design capacity.

Chapter 5 discusses the results.

Chapter 6 concludes the study.

2

Theoretical background

The purpose of this chapter is to provide theoretical support for this study, and to gradually establish a rational theoretical framework. In particular, the effect of corrosion on the bond of plain reinforcement bars is discussed. Additionally, the bond of plain bars is discussed with particular attention to the role of end-hooks.

2.1 Plain reinforcement bars with end-hooks

Due to the widespread utilization of ribbed rebars in concrete structures, a large number of research papers exist that investigates the bond of ribbed rebars. Plain reinforcement bars have been replaced in the design of concrete structures following developments in the understanding of the steel/concrete bond mechanism since 1960 (Cairns & Feldman, 2018)[5]. However, plain reinforcement bars are still present in large quantities in many existing structures in European countries, and the requirements for load-carrying capacity have gradually increased. Additionally, such structures are likely to be affected by corrosion, which is the most common cause of deterioration for reinforced concrete structures (Bell, 2004)[2].

The bond mechanism of plain bars is different from those of ribbed bars. The introduction of ribs allows the ribbed reinforcement bars to interlock better with the surrounding concrete, thus increasing the bond capacity. The bond mechanism is the interaction between reinforcement and concrete. The ability that makes it possible to combine the compressive strength of concrete and the tensile strength of reinforcement in reinforced concrete structures is also attributable to this transfer of stress (Lundgren, 2005a)[15]. In general, bond is considered to be a result of three different mechanisms: chemical adhesion, friction and mechanical interlocking between the ribs of the reinforcement bars and the concrete (Lundgren, 2007)[17]. The basic behaviors of the structures are greatly influenced by these bond mechanisms, which are manifested in many aspects such as crack development and spacing, crack width and ductility (Lundgren, 2005a)[15].

For ribbed bars, the bond strength principally depends on the bearing, or mechanical interlock (Cairns et al., 2006)[4]. The inclined forces generated by the bond action of the ribs continue to transmit forces between the reinforcement and concrete even after the chemical adhesion has disappeared. The inclined stress can be resolved into parallel and radial components. The component parallel to the direction of the reinforcement axis is called bond stress and is a function of the normal confining

pressure exerted by the surrounding concrete on the surface of the reinforcement. Perpendicular to the direction of the reinforcement axis is the radial stress, also referred to as the splitting stress (Sæther, 2011)[20], see Figure 2.1. In other words, the introduction of ribs can improve the bond capacity of the reinforcement by increasing the mechanical interlocking.

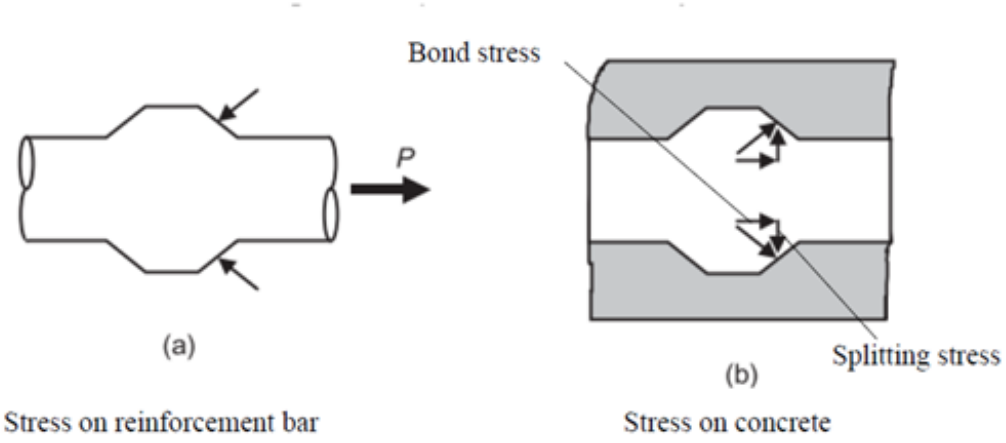

Figure 2.1: Bond and splitting stresses between a ribbed bar and the surrounding concrete, from Magnusson (2000)

However, plain rebars with a smooth surface have significantly weaker bond capacity compared to ribbed rebars. More specifically, friction is the major component of bond resistance of plain bars, which usually fail by pulling out of the concrete, leaving the cover uncracked (Cairns & Feldman, 2018)[5]. In addition, the role of adhesion can no longer be ignored since the splitting force is much smaller for plain reinforcement bars.

Among the existing studies on bond of plain reinforcement bars, Cairns et al. (Cairns et al., 2006)[4] observed that the casting position has an effect on the bond strength. Their experiments showed that in the absence of corrosion, the bond strength of top-cast bars was weaker than that of bottom-cast bars, more specifically by an average of 55%. Subsequently they also suggested the use of a reduction factor of 0.5 for the bond of plain reinforcement bars in poor casting position. In addition to this, they concluded that an increase in concrete cover may improve the bond strength of plain bars. Further studies seem to confirm that minimum cover has a strong influence on bond resistance (Cairns & Feldman, 2018)[5].

Currently, most of the buildings from the 60s and 70s in European countries, especially in Italy, are somewhat under-designed (Fabbrocino et al., 2002)[8]. These structures were reinforced with plain bars and exhibited poor bond, and thus many used specific anchoring end details to ensure a satisfactory interaction with concrete.

Anchor end-hooks, used to increase the bond capacity of plain reinforcement bars, are typically bent at 90, 135 and 180 degrees angles (Fabbrocino et al., 2002)[7]. Fabbrocino et al. noted that the end detail of rebars are essential for the devel-

opment of the strength and the deformation mechanisms in the beam to column region. Figure 2.2 showed the force transfer for the behavior of the tensile reinforcement bar. The anchored bar is divided into two parts: one straight region and the anchorage region, indicated by a circular hook, see Figure 2.3 for more details. From a theoretical point of view, the end anchorage results in a restraint for the inner end of straight part of the rebar. Figure 2.3 highlights two boundary conditions for the straight region. One case is when the end detail is ideally free, which means the anchorage is not present, and slip occurs at the unloaded end ($s \neq 0$), but the bar stress is zero. The other case is when the anchorage is ideally rigid and the bar stress is not zero when the unloaded end slip is zero ($s = 0$) because of high ratio between the applied force and the anchorage reaction force. The stress-slip response of common anchorages lies between these two bounds, so that neither the slip nor its derivative is zero.

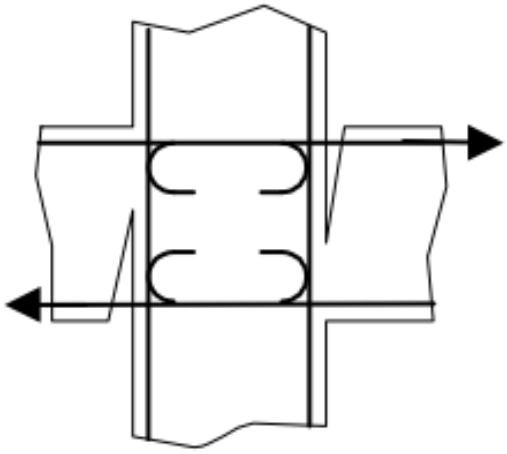

Figure 2.2: Global joint deformation: the slippage of anchored reinforcement. (Fabbrocino et al., 2002)[7]

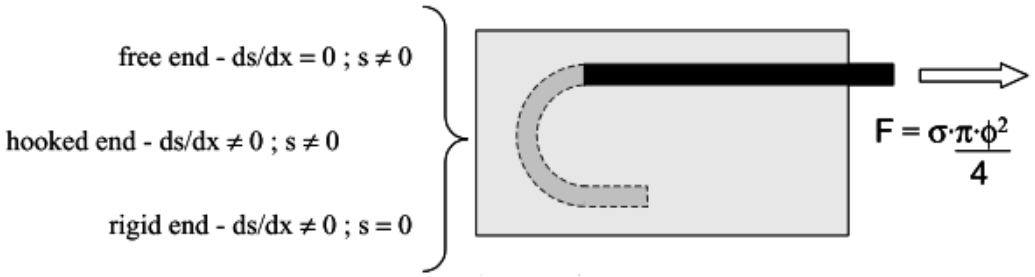

Figure 2.3: The anchored plain reinforcement bar. (Fabbrocino et al., 2002)[7]

Rigid anchorage allows full development of flexural strength and is thus effective in avoiding premature anchorage failure. On the other hand, it produced the minimum

values of slippage at the loaded end. Thus, the actual stress-slip response of the anchors is in the shaded area, see Figure 2.4 (Fabbrocino et al., 2004)[9]. From the pull-out tests on hook anchorages in their research, the results showed that the slip of the hook at yielding is constant. Furthermore, they concluded that the mechanism of the stress-slip response of the hook reduced the yield penetration in the anchorage device.

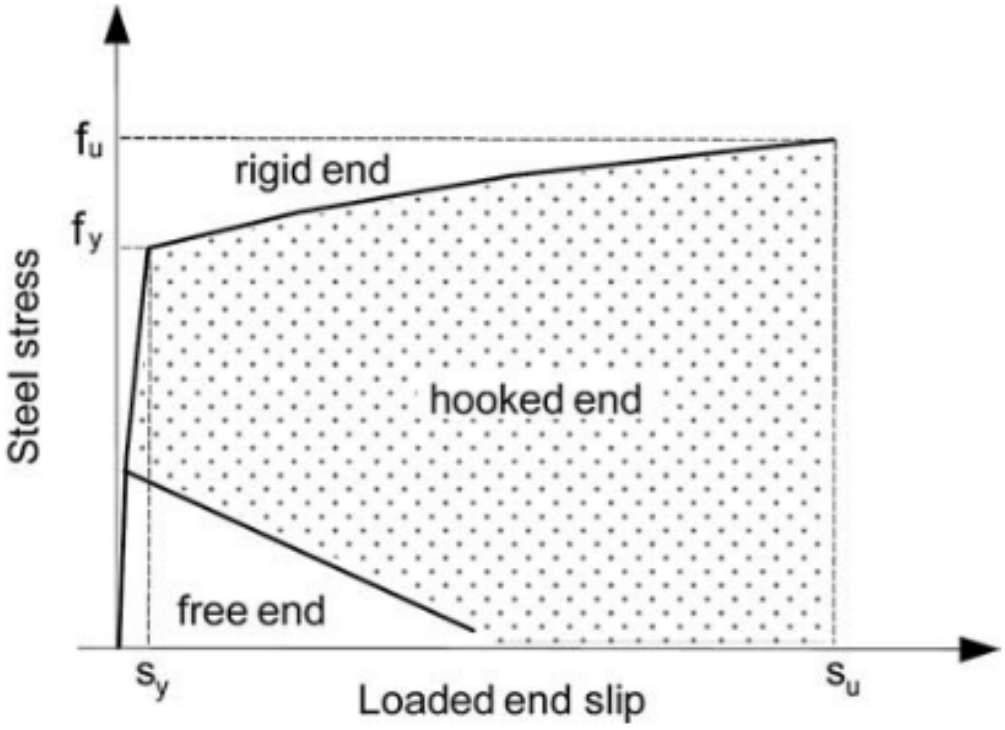

Figure 2.4: Stress vs. loaded end slip of anchored smooth bars. (Fabbrocino et al., 2004)[9]

2.2 Effect of corrosion

Corrosion of embedded reinforcement is a major cause of deterioration of concrete structures, with the result that the service life of the structure is usually limited. The direct impact of corrosion on reinforcement bars is reflected in the main points: loss of bar cross-section; the oxide produced by corrosion of the reinforcement bars occupies a larger volume than the parent metal, and the increase in volume caused by corrosion products leads to an increase in the stresses on the concrete, eventually leading to cracking and spalling of the concrete cover; and the formation of corrosion products changes the properties of the interface between the concrete and bar (Cairns et al., 2006)[4]. Therefore, the effects of corrosion on the residual structural capacity can be divided into effects on the reinforcement itself, effects on the surrounding concrete, and effects on the bond between the two. A detailed diagram of effect of corrosion on plain round bars is shown in Figure 2.5.

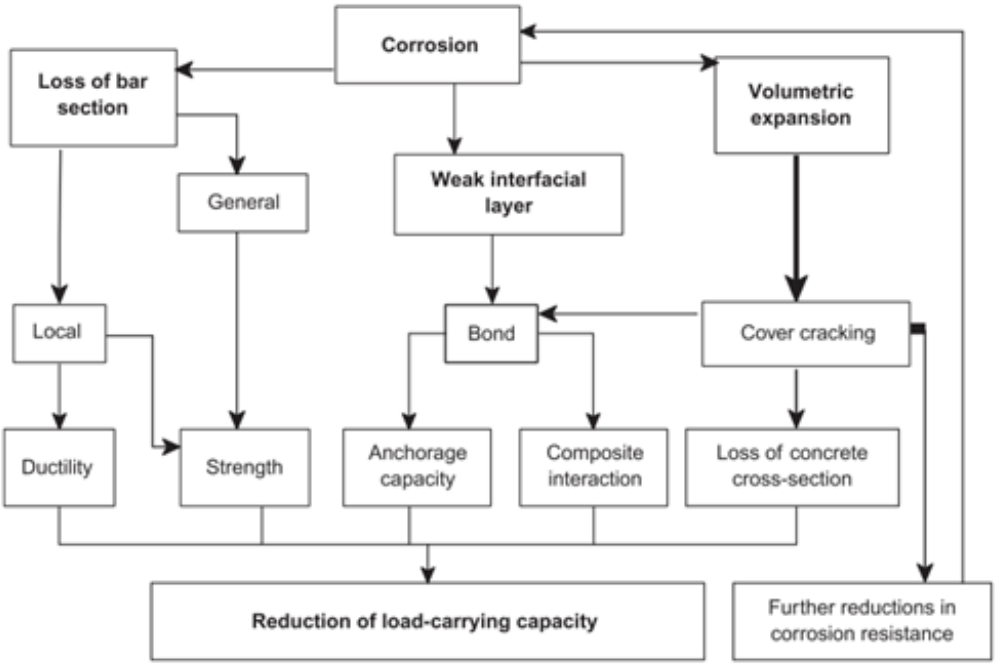

Figure 2.5: Effects of corrosion on residual strength (plain round bars). (Cairns et al., 2006)[4]

Corrosion of reinforcement is caused by many factors, the most prevalent of which are carbonation and chloride penetration. Corrosion occurs on the bar surface in the presence of water and oxygen when the protective layer on the steel surface is damaged by chloride or carbonation ions. It is possible for both types of corrosion to occur simultaneously. Carbonation, also known as general corrosion, has a mechanism of action in which the protective layer is completely dissolved, resulting in a general loss of reinforcement bar cross-section. Chloride ingress (pitting corrosion) leads to localized destruction of the protective layer, resulting in a greater local loss of the reinforcement bar cross-section.

At the initial stage of the corrosion process, corrosion products accumulate on the surface of the reinforcement, resulting in an increase in the radial compressive stress between the reinforcement and the concrete, thus increasing the frictional component of the bond (Sæther, 2011)[20]. This, however, eventually causes spalling of the cover (Lundgren, 2005b)[16].

With reference to previous studies, there are many parameters that affect the bond strength between reinforcement and concrete, such as the reinforcement bar type, the diameter, and the thickness of concrete cover (Fang et al., 2006)[12](Fang et al., 2004)[11](Wu et al., 2016)[22](Yalciner et al., 2012)[23].

It is well known that the different types of reinforcement, such as plain and ribbed reinforcement, have effect on the bond strength (Fang et al., 2006)[12]. The results of a study by Wu et al. (Wu et al., 2016)[22] in which different diameters of ribbed reinforcement were used in the experiments showed that the tendency of the deterioration to affect the bond strength also varies depending on the size of

the reinforcement diameter, probably also because of the varying thicknesses of the protective concrete.

Previously, Yalciner et al. have compared and evaluated the bond strength of different concrete cover depths by pull-out tests (Yalciner et al., 2012)[23]. They took the same diameter size for all the ribbed bars and set three different cover thicknesses. It was found that the bond strength of the specimens in the uncorroded condition increased with the ratio of c/D (cover-to-bar-diameter ratio), where the highest ultimate bond strength was obtained for this value of 3.2.

Williamson and Clark (Williamson & Clark, 2002)[21] studied the effect of corrosion and loading on the bond strength, and showed that corrosion enhances the bond strength of plain bars unless cracking and loss of confinement is severe.

Fang et al. performed pull-out tests to assess the effect of corrosion on bond and bond-slip behavior, where the specimens also contained plain rebars (Fang et al., 2004)[11]. In these tests, it was found that for unconfined plain rebars, the bond strength increases with the corrosion level when the corrosion level is low, and the ultimate bond strength can be 2.5 times that of non-corrosion; while the bond strength decreases rapidly when the corrosion level is high. 2-4% of the corrosion level was found to be a breaking point in their tests. When it comes to plain rebars with confinement, the situation is slightly different. The bond strength can increase with the degree of corrosion up to a relatively high degree of corrosion. Other experiments tested the bond stress-slip response of corroded reinforcement to concrete under cyclic loading; these also involved plain reinforcement bars (Fang, et al., 2006)[10]. Their experiments showed that the bond behavior of plain reinforcement bars, whether confined or unconfined, is significantly reduced under cyclic loading.

In the long term, if proper measures are not taken and corrosion is allowed to develop on the surface of the reinforcement, the bond strength between the reinforcement and the surrounding concrete will be seriously affected and, more seriously, the safety and integrity of the building structure will be reduced. Thus, the assessment and repair of plain reinforcement bats, for which there are relatively few references, will continue to be an important topic.

3

Methodology

Gullspång bridge was located in central Sweden, close to the Sweden's largest inner lake, Vänern. During an 81-year service life, the bridge had been exposed to deicing salts, resulting in visible corrosion damages. After the demolishment of the bridge, the edge beams were divided into segments and used for research. This thesis focuses on analyzing the results from the structural tests of the edge beams, particularly on the remaining capacity of the end-hooks of the plain reinforcement bars. The study was divided into two parts. The first part is mostly experimental, focusing on obtaining data, such as the geometry of the bars, including the corrosion level, and on post-processing of data from the structural tests of the edge beams. In the second part, the obtained data, the corrosion level, yield penetration and the remaining capacity of the hooks are compared with equations in code provisions.

3.1 Specimen

3.1.1 Geometry

Seven beams, cut from the edge beams of Gullspång bridge, were tested in three-point bending in 2018. The edge beams were reinforced with plain reinforcement bars ending in hooks. The reinforcement bars had 16 mm diameter, further the beams included stirrups of 6 mm diameter. The distribution of the stirrups varied a lot from beam to beam. The straight bars at the cut ends of the beams were prevented from slipping by the use of the bolts and washers applied prior to the structural test. In this study, one beam (named as beam 11) was excluded from the evaluations; this was due to that the beam had been repaired during the service life of the bridge with a welded end steel plate. This was discovered after extracting the reinforcement bars from the beam. The tested beams were classified into two categories. One was beams with one pair of hooks at both top and bottom layers, defined as beams with one pair of hooks (1); the other was beams with two pairs of hooks at both top and bottom layers, defined as beams with two pairs of hooks (2). These two types of beams also had different distributions of reinforcement bars. In the first case, the hooks were located at one end of the beam (see Figure 3.1), while in the second case the hooks were located at the middle part of the beam (see Figure 3.2). The cross-sectional dimensions of the beams are illustrated in Figure 3.3. In Figure 3.3, the left figure showed the cross section of the beams with one pair of hooks and the right figure showed the cross section of the beams with

two pairs of hooks. The reinforcement bars in the beams with one pair of hooks were labelled as TI-Top Inner; TO-Top Outer; BI-Bottom Inner; BO-Bottom Outer; The reinforcement bars in the beams with two pairs of hooks were labelled as TI-Top Inner; TO-Top Outer; TICR-Top Inner Center to Right; TOCR-Top Outer Center to Right; BI-Bottom Inner; BO-Bottom Outer; BICR-Bottom Inner Center to Right; BOCR-Bottom Outer Center to Right; Both the top and bottom mentioned referred to the original position of the reinforcement bar in the bridge. The left side of the cross sections was the inner side of the beams. The concrete cover, which is the distance from the bars towards to the top or bottom, and the configuration of the hooks are listed in Table 3.1 to Table 3.2.

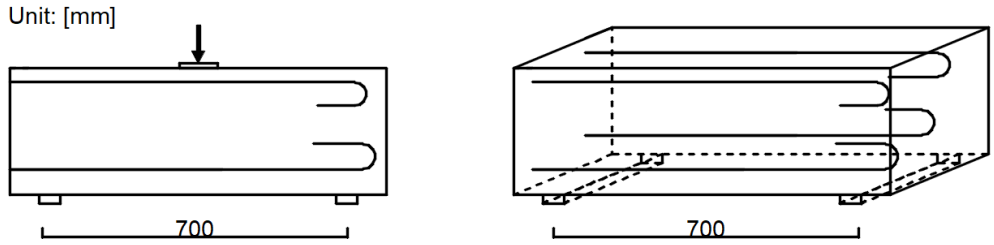

Figure 3.1: Beam with one pair of hooks

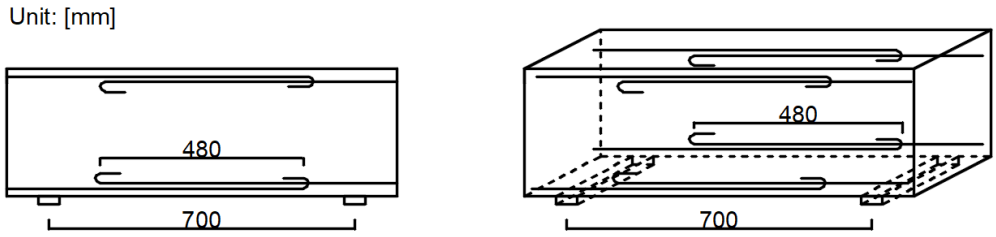

Figure 3.2: Beam with two pairs of hooks

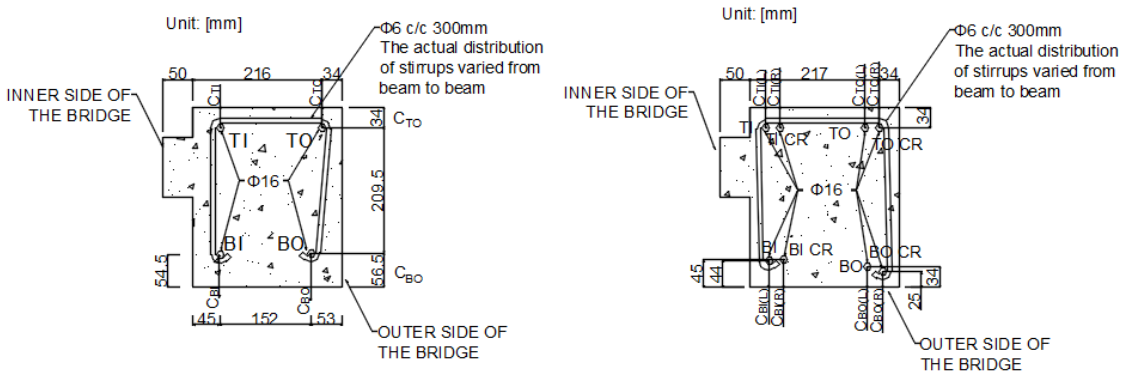

Figure 3.3: Cross section of edge beam. Rebars in the beams with one pair of hooks (left figure) were labelled as following: TO - Top Outer; TI - Top Inner; BO - Bottom Outer; BI - Bottom Inner. Rebars in the beams with two pairs of the hooks (right figure) were labelled as following: TI - Top Inner; TO - Top Outer; TICR - Top Inner Center to Right; TOCR - Top Outer Center to Right; BI - Bottom Inner; BO - Bottom Outer; BICR - Bottom Inner Center to Right; BOCR - Bottom Outer Center to Right

Table 3.1: Geometry of the beams with one pair of hooks

Beam ID	Length (mm)	$c_{TI}(mm)$	$c_{TO}(mm)$	$c_{BI}(mm)$	$c_{BO}(mm)$
1	885	54.5	56.5	34	34
18H	880	34	34	17	19
19	912.5	71	415	34	34

Table 3.2: Geometry of the beams with two pairs of hooks

Beam ID	Length (mm)	c_{TI} (mm)	c_{TO} (mm)	c_{BI} (mm)	c_{BO} (mm)
10D	920	45(R) 33(L)	25(R) 34(L)	34	34
13G	995	34(R) 38(L)	36(R) 24(L)	34	34
16K	895	68(R) 52(L)	35(R) 38(L)	34	34

In Figure 3.3, the label CR of beams with two pairs of hooks stands for center to the right which means that hook positioned in the center and the bar ends on the right side, see the labels of bottom reinforcement bars in Figure 3.4.

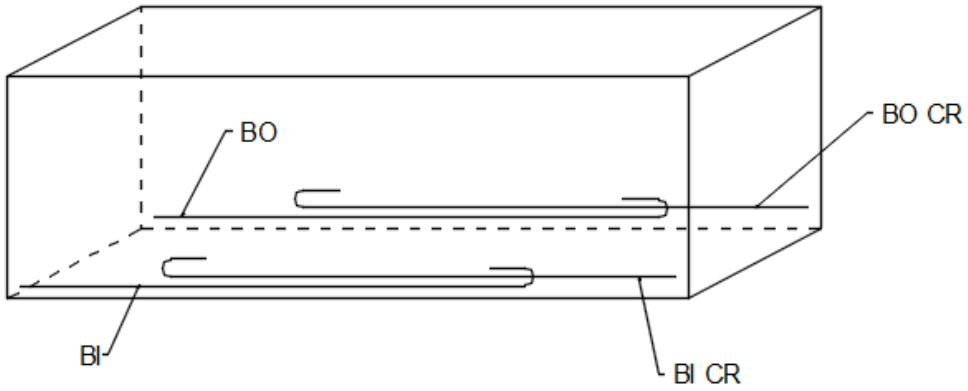

Figure 3.4: Labels for reinforcement bars in the beams with two pairs of hooks at bottom layer

Beams with two pairs of hooks were upside down during the tests and only the tensile reinforcement bars were saved, which were originally top reinforcement bars in the bridge. For Beam 18H, only the bottom reinforcement bars were saved after the test. Through measuring the configuration of the hook, it could be seen whether the hook was deformed during the structural test. The measurement of lengths and distances are illustrated in Figure 3.5, and the results for each bar are shown in Table 3.3.

Beam		Labelling of bars	Distance 1 (mm)	Distance 2 (mm)	Distance 3 (mm)	Length 1 top (mm)	Length 2 mid (mm)	Length 3 straight (mm)
Beams with two pairs of hooks	10D	TI	52	52	52	100	150	690
		TO	53	54	55	111	167	702
		TI CR	61	63	64	120	173	717
		TO CR	59	60	61	122	173	835
	13G	TI	61	63	64	117	169	883
		TO	59	60	60	127	184	904
		TI CR	56	52	50	117	169	710
		TO CR	58	58	58	113	168	734
	16K	TI	65	71	76	138	192	714
		TO	59	59	59	104	157	709
		TI CR	57	57	57	121	173	608
		TO CR	53	54	54	127	177	651
Beams with one pair of hooks	18H	BI	57	57	57	113	164	841
		BO	53	55	54	106	153	1050
	19	BI	59	60	60	115	169	817
		BO	59	61	62	114	162	852
		TI	56	57	58	117	170	853
		TO	56	56	55	121	171	875
	1	BI	60	61	62	163	214	783
		BO	65	70	75	145	195	848
		TI	61	63	64	163	213	753
		TO	62	72	78	145	200	794

Table 3.3: Labelling of the reinforcement bars in beams and the corresponding configuration of the hooks

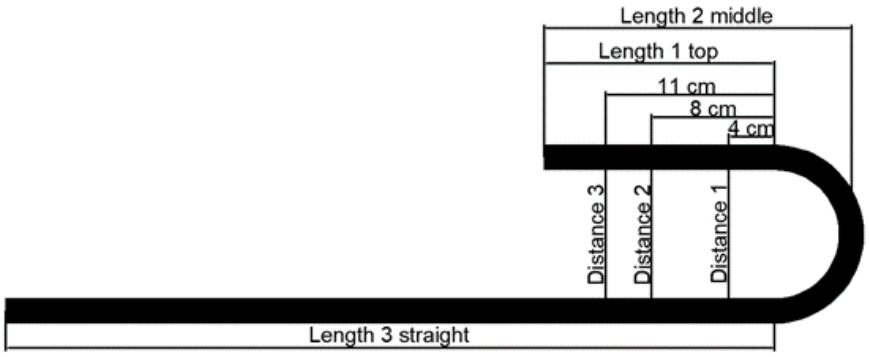

Figure 3.5: The configuration of the hooks

3.1.2 Material

Concrete

The bridge was older than 80-year-old, there was no vibration of concrete during casting, but tamped. Eight concrete cylinders with a 100 mm diameter were drilled from the edge beams of the bridge and subjected to compression tests according to SS-EN 12390-3:2009/AC:2011 (Robuschi et al., 2018). The results of the compression tests are shown in Table 3.4[18]. The average compressive strength of concrete in those tests was measured to be about 45.55 MPa with a standard deviation of 4.6 MPa. This compressive strength has thus been used in the subsequent analytical calculations.

Test datum: 2018-05-18

Label	Height [mm]	Diameter [mm]	Density [kg/m3]	Max. load [kN]	Compressive strength [MPa]
17D 200	198	100	2400	402	51.0
10G1 200	200	100	2380	378	49.0
14D	198	100	2380	346	43.9
18A 200	197	101	2360	388	48.9
10C 200	199	100	2380	358	45.4
16B 200	196	100	2390	293	37.1
14H 200	198	100	2370	382	48.5
10G2	200	100	2380	328	41.6

Table 3.4: Results of compression test

Steel

Uncorroded sections of plain reinforcement bars were extracted from the edge beams of Gullspång bridge and were tested in tension to characterize the stress-strain curve of the steel. The relation between stress and strain is illustrated in Figure 3.6. The result of test showed that average yield strength of the plain reinforcement bars was to be about 252 MPa. The deviation of 10.1 MPa for yield strength was determined in Robuschi et al.(2020). Therefore, 252 MPa was used as the yield strength of reinforcement bars in further calculations.

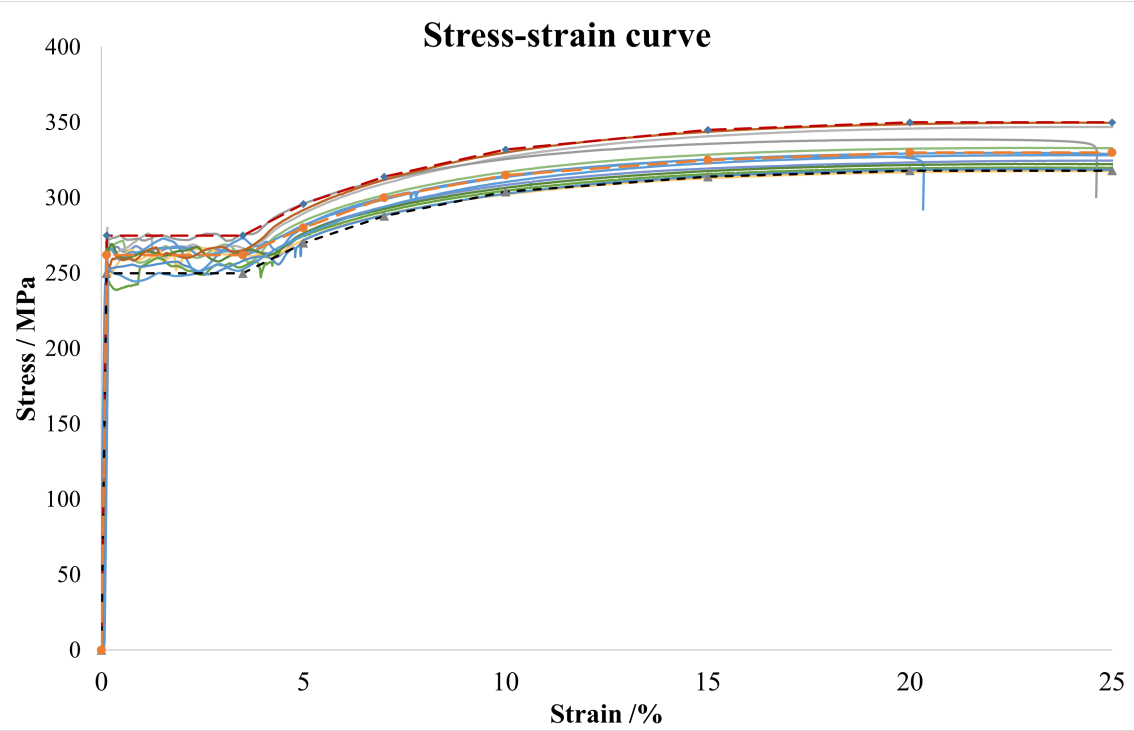

Figure 3.6: Stress-strain curves of the reinforcement bars of Gullspång bridge. Higher and lower bond is given with dotted line, an average is provided in orange.

3.2 Structural tests

3.2.1 Three-point bending tests

The beams were placed on two 50 mm wide supports under the whole width for all beams, the span of the beam between the supports was 700 mm. The beams were between 880 mm and 1000 mm in length and 300 mm in height, and the center of the support was positioned between 90 to 148 mm from the beam end on each side depended on the length of the beams, as shown in figure 3.7 and 3.8. The reinforcement bars were restrained at the end of the beam by the use of the bolts and washers to prevent the reinforcement bars from failing in anchorage. The stirrups were positioned with different spacing of c/c distance in each beam, as shown in Figure 3.7 and 3.8. All beams except Beam 18H were placed upside down during the test relative to their original placements on the bridge. The load was applied in the mid-span on a 90 mm wide plate to avoid the crushing of concrete. The test was displacement-controlled at the mid-span: a loading rate of 2 mm/min was used up to 35 kN, while compressing the wood layers underneath the load and support plates. The load rate was then changed to 1 mm/min up to 60 kN. From 60 kN, the loading rate was set to 0.4 mm/min, to capture the pre-cracking behaviour of the beam in detail. It was increased again to 1 mm/min after the recorded deformation had reached 10 mm.

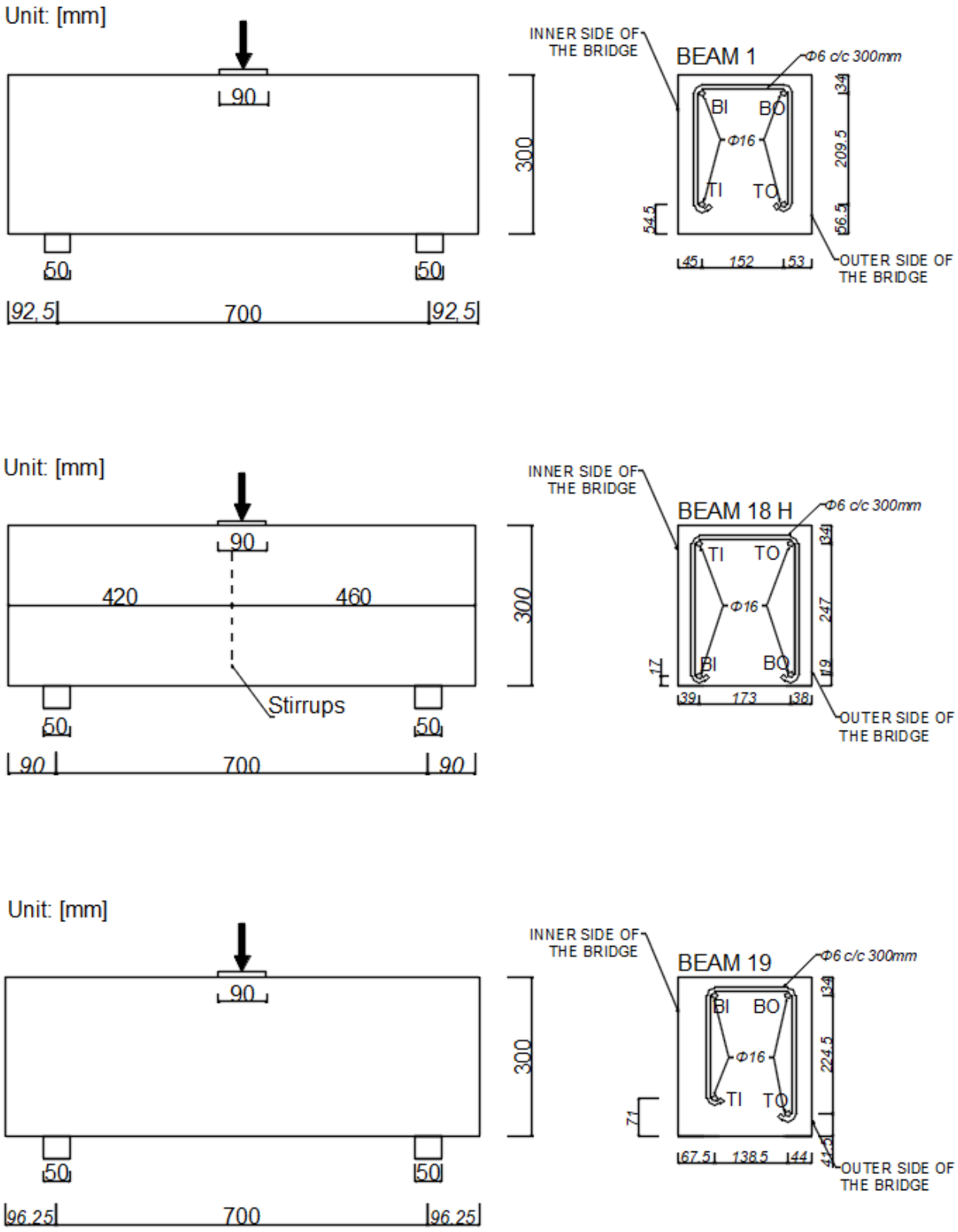

Figure 3.7: Three-point bending test for the beams with one pair of hooks: Beam 1, Beam 18H, Beam 19. Nominal measurement values are giving in italics.

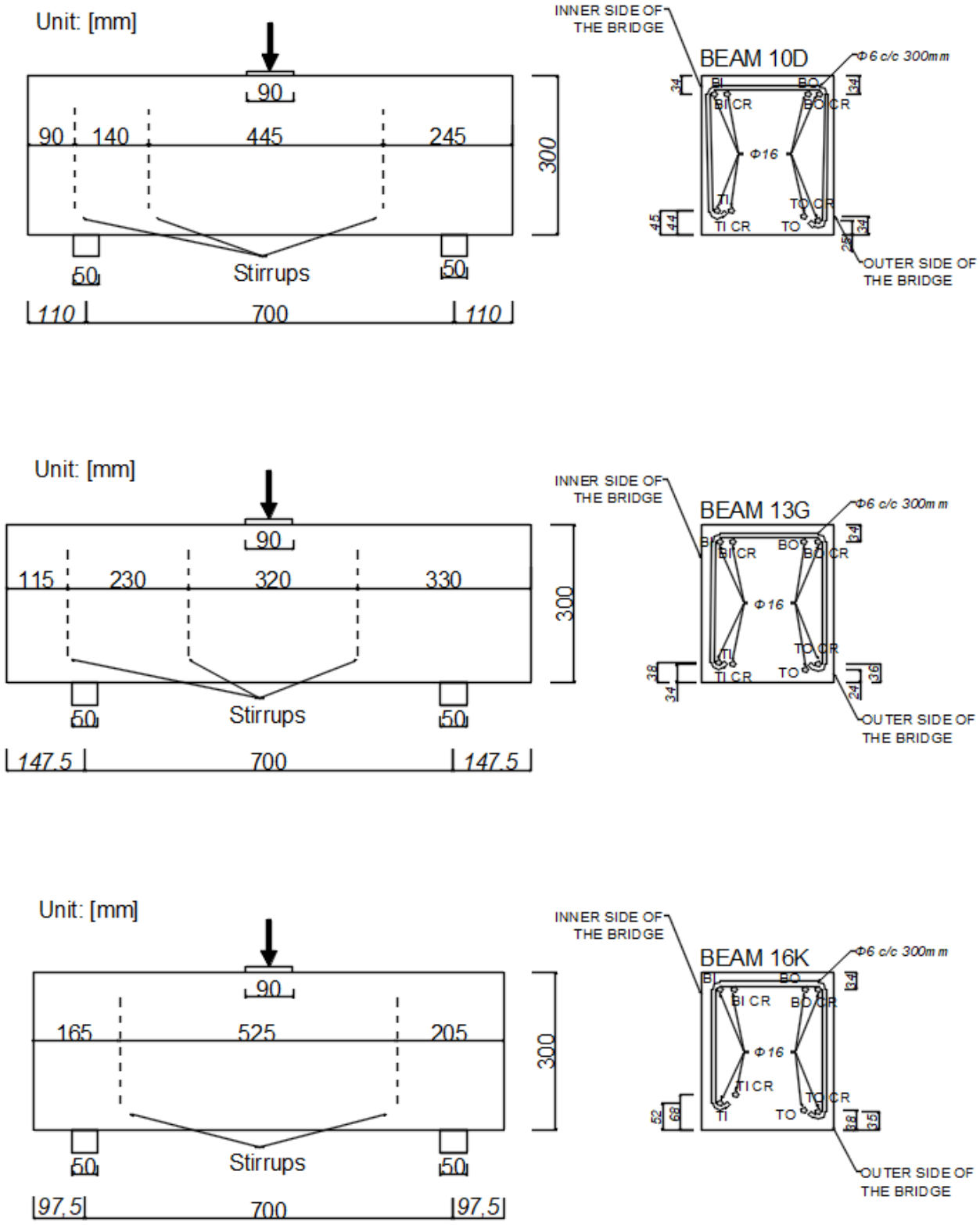

Figure 3.8: Three-point bending test for the beams with two pairs of hooks: Beam 10D, Beam 13G, Beam 16K. Nominal measurement values are giving in italics.

3.2.2 DIC

In the structural tests, DIC (Digital image correlation) method was used to measure the displacements of the specimens. Images of the tests were acquired at a rate of 1/7 Hz. DIC was set to monitor the external side of each beam, i.e. the outer side of the edge beams as positioned on the bridge. An ARAMIS® adjustable stereo camera system was used. The surface of each beam was painted in white. Subsequently, black paint was applied with the help of a brush to generate a random pattern that would allow the acquisition of geometrical data. The results were subsequently processed by using the software GOM® Correlate. In the GOM Correlate, an extensometer tool was used to monitor changes in the distance between two points. Extensometers were used at the supports and at the mid-span to document the mid-span deflection. Further, extensometers were also used to document the width of the cracks at different load levels, see Figure 3.9.

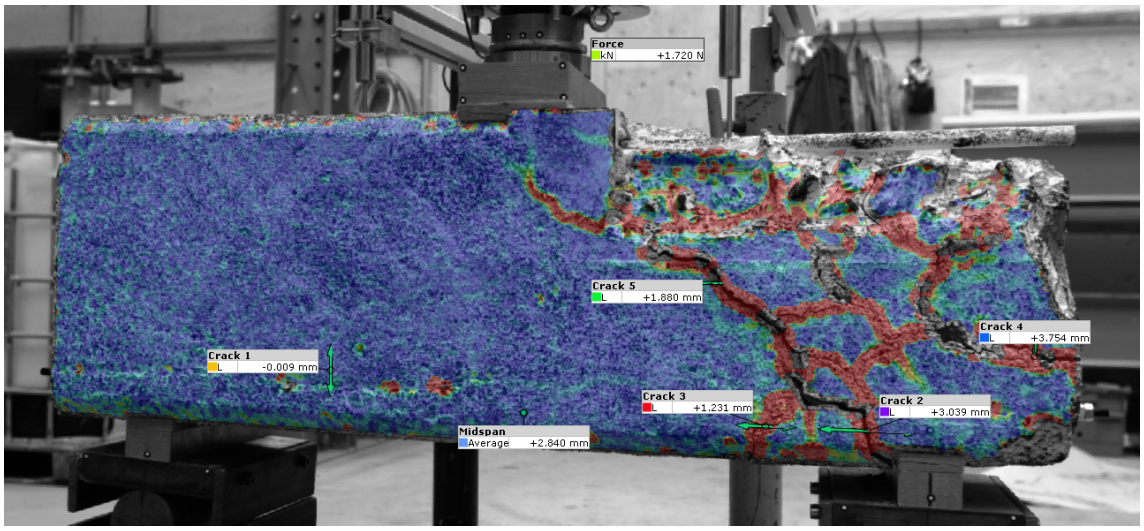

Figure 3.9: Contour plot of principal strains in Beam 10D, measured by the DIC method

3.3 Post processing

After the bending test, the bars were extracted from the beams. The reinforcement bars were corroded and slightly damaged on the surface. The reinforcement bars were cut, cleaned with sandblasting and 3D scanned for further evaluation.

3.3.1 Extraction of the rebar, labelling and cutting

The original lengths of the reinforcement bars was between 60 and 100 cm depending on the hook configuration. Due to the limitation on the length of the sandblasting machine, the reinforcement bars were cut into segments with an appropriate length. In addition, the three-point bending tests caused some bending in the reinforcement bars. Thus, the reinforcement bars were cut at the position where the largest displacement took place to keep each segment as straight as possible. This was done

to minimize the errors in calculating the cross-section areas, the corrosion level and the yield penetration from the 3D scanned data.
The reinforcement bars taken out were named according to their position inside the beam, as shown in Figure 3.10. The different parts of the reinforcement bar were named 1 of 2, for the section with the hook, named 2 of 2, for the straight section, respectively, see Figure 3.10.

Figure 3.10: Division of rebar

The rebar cutter RC-20 was used to apply lateral force in the direction perpendicular to the reinforcement bars. The shear force of the reinforcement bars reached the maximum strength, and the plastic fracture was seen on the cutting surface. Due to the lateral extrusion of the machine, a local elliptical deformation also appeared near the cut. Therefore, the reinforcement bars were locally damaged because of the rebar cutter. The sections with hammer damage or cutting damage were removed in software GOM Inspect to ensure that only the corrosion damage was included.

3.3.2 Sandblasting

When the reinforcement bars were taken out from the concrete beams, rust and concrete particles where still attached on the surface, as shown in Figure 3.11. It was therefore necessary to clean the reinforcement bars before acquiring the geometry of the reinforcement bars by 3D scanning. Sandblasting was considered an appropriate method that can clean the surface without damaging the surface (Fernandez et al., 2018)[13]. A sandblasting cabinet was used to spray sand particles on the surface of the reinforcement bars to clean and smooth the outer surface. After sandblasting, the rust and concrete particles attached to the surface were removed, see Figure 3.12.

Figure 3.11: Reinforcement bar 16K TO CR before sandblasting

Figure 3.12: Reinforcement bar 16K TO CR after sandblasting

3.3.3 3D scanning

Handy Scan 700TM from Crea-Form was utilized for the acquisition and optimization of 3D data. The mesh length corresponded to 0.2 mm, which was considered to be a suitable accuracy. The scanning procedure started with setting up a suitable frame and reference points setting. The frame with reference points was needed to establish a reference system in the 3D space, that could be used to export the geometry of the reinforcement bars. The software was in fact able to construct a 3D reference coordinate system from the scanned reference points. Further clipping planes were used to define the scanning space. Finally, the geometry of the reinforcement bars was acquired. Once the geometric data of the reinforcement bar was obtained, the file was imported into the software VXelement for the first processing step, which consisted in the alignment of the non-bend part of the reinforcement bar. The axis of the coordinate system were aligned to the cross-section of the straight bar, and the origin of the coordinates was located at one of the extremities of the bar, see Figure 3.13 and Figure 3.14.

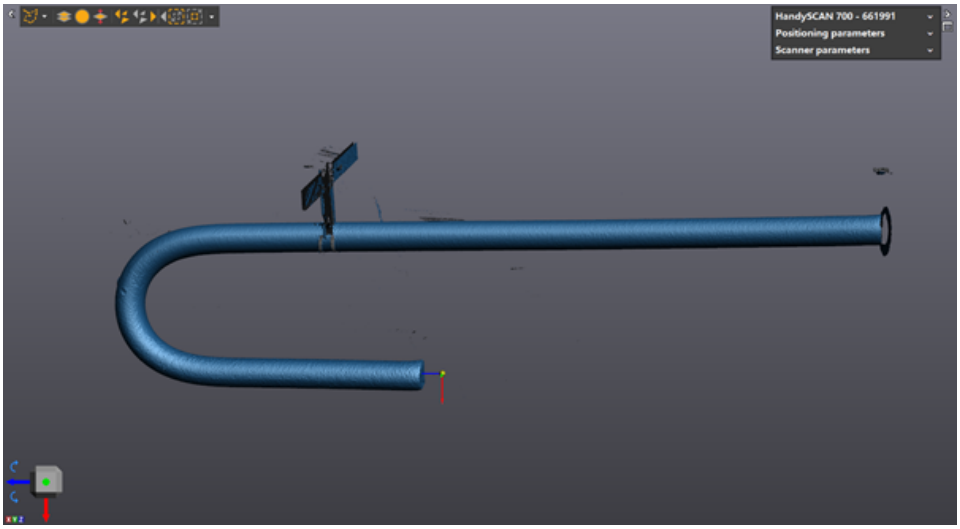

Figure 3.13: Axis setting of hook part

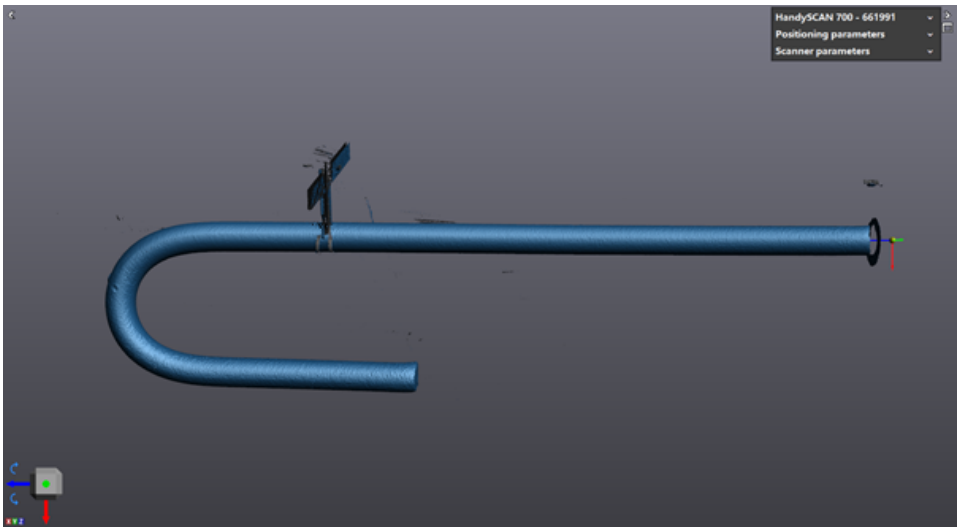

Figure 3.14: Axis setting of straight part

Corrosion in the bent part of the bar was estimated only at those locations where corrosion damages were observed. The segment with corrosion was selected and the axis of the coordinate system were set as in Figure 3.15, with the Z-axis parallel to the selected segment, and the XY-plane parallel to the cross section. The yellow border indicates the selected part as shown below. In general, the coordinates was set in the part further away from the end-hook.

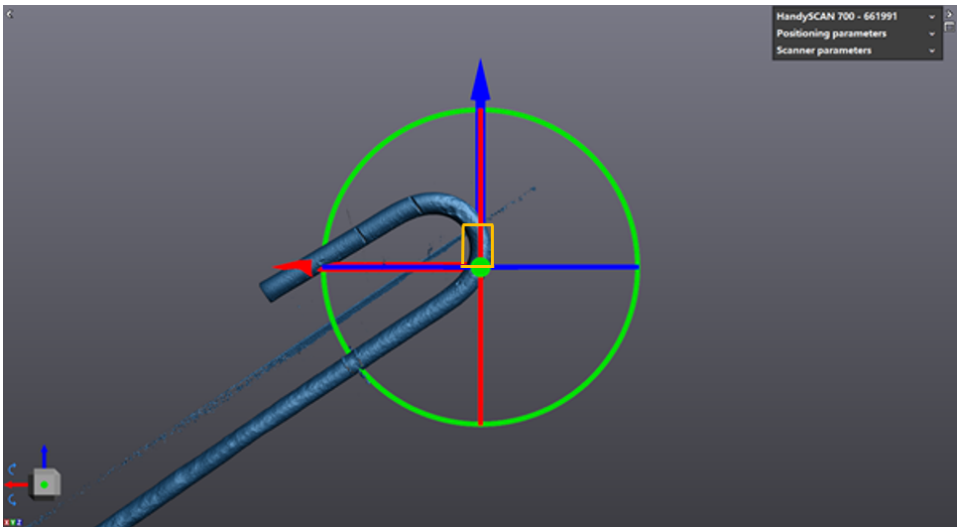

Figure 3.15: Plot of axis setting of the corroded section at bent part, selected area is marked by the yellow box, and the red and blue axes indicate the X-axis and Y-axis respectively

The second part of the process to obtain the geometric data of the bars was to import the obtained mesh into GOM Inspect. Here, noise and frames supporting the reinforcement bars during scanning were removed, allowing more accurate geometrical data to be collected.

3.4 Evaluation of corrosion level and yield penetration

3.4.1 Corrosion level

The data obtained by 3D scanning was then used to calculate the perimeter and area of the reinforcement bar at different cross-sections. By using MATLAB, the data in Cartesian coordinate system was converted into polar coordinate system to calculate the radius of the cross section along the length. Afterwards, the codes calculated two different types of diameter, based on cross-sectional area and perimeter respectively. They were compared to each other to find acceptable cross-sections which had a small deviation between two types of diameters. By filtering away the diameters with large deviations, the remaining data kept a high degree of consistency of two types of diameters which means that the data used in following corrosion level calculation was refined and more accurate. Plotting the obtained cross-sectional areas and perimeters of each bar along the length allowed to observe the distribution of corrosion damages, but also to observe that some of the bars yielded during the three-point bending test. In Figure 3.16, the cross-sectional area and perimeter of the reinforcement bar 10D TO CR 2of2 is shown, and in Figure 3.17 the area variation due to corrosion along the length. The nominal area of the reinforcement bar is as well shown in Figure 3.18.

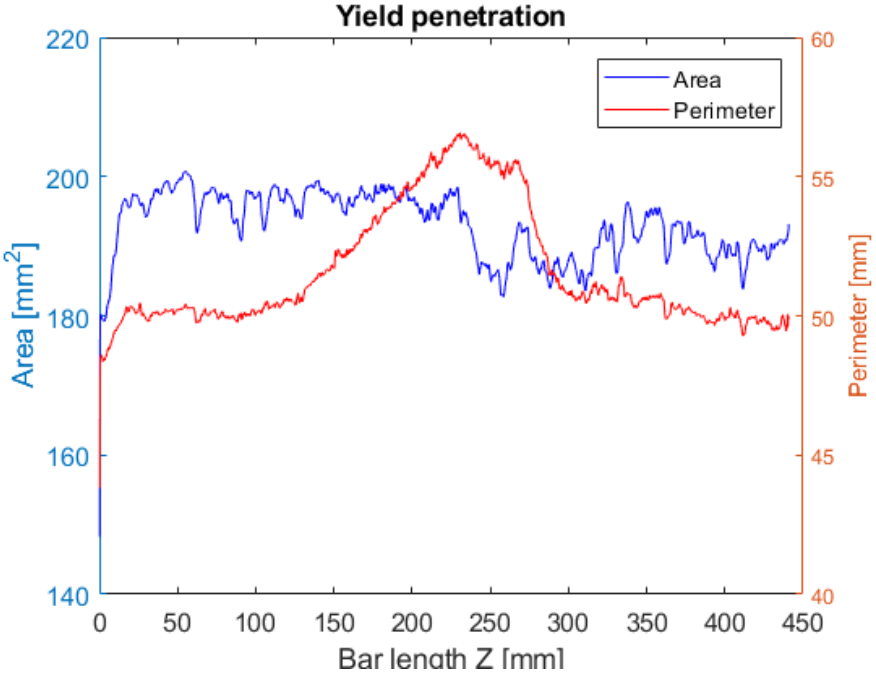

Figure 3.16: The cross-sectional area and perimeter along length for 10D TO CR 2of2

Figure 3.17: 10D TO CR 2of2 after sandblasting

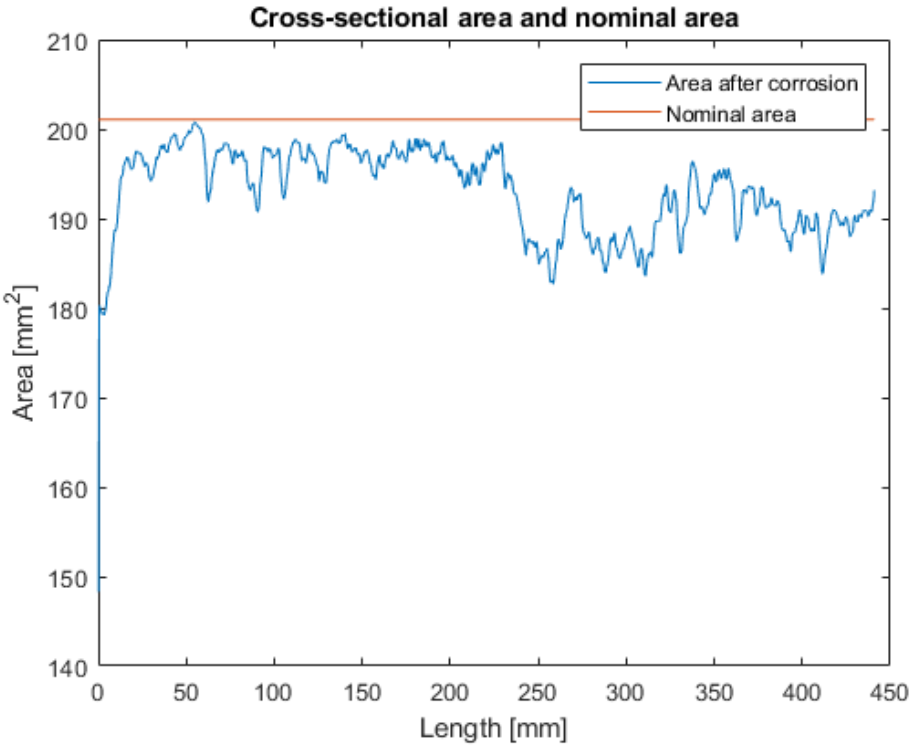

Figure 3.18: The cross-sectional area and the nominal area along length for 10D TO CR 2of2

The results of a study by Robuschi et al. (Robuschi al., 2020) showed that there was a variation in the diameter of the reinforcement bars. The nominal perimeter was 50.65 mm with a deviation of 0.39 mm. The cross-sectional area decreased after corrosion. On the other hand, the perimeter tended to increase due to the irregularity of the corrosion damages. The corrosion level was expressed as the ratio of loss of cross-sectional area after corrosion and the cross-sectional area before corrosion. For peak corrosion level:

$$C_{peak} = \frac{A_n - A_{peak}}{A_n} * 100\,[\%] \tag{3.1}$$

For mean corrosion level:

$$C_{mean} = \frac{A_n - A_{mean}}{A_n} * 100\,[\%] \tag{3.2}$$

In the above formulas, C is the corrosion level and is expressed in percentage, A_n is the nominal cross-sectional area of the reinforcement bar, calculated from the uncorroded cross-sections in the unyielded zone. A_{mean} and A_{peak} are, respectively, the average area along the reinforcement bar in the unyielded zone and the minimum area of the reinforcement bar in the unyielded zone.

Calculating the cross-sectional area of the section with the hook was challenging, since the angle between the reinforcement bars and coordinate axis was constantly changing. The standard coordinate system was not appropriate for calculating the geometrical properties of the part of the reinforcement bar with the end-hook. To simplify the problem, the reinforcement bars were divided in three different zones: two straight parts and a hook part, as illustrated in Figure 3.19. In the hook part, the corrosion level was estimated separately, and local axis was fitted to the specific section, to minimize the effect of the curvature. Specifically, the sections showing signs of corrosion were selected for corrosion level calculation. The rest of the sections were assumed to be uncorroded and the average cross-sectional area of this part was based on the adjacent uncorroded parts in the hook.

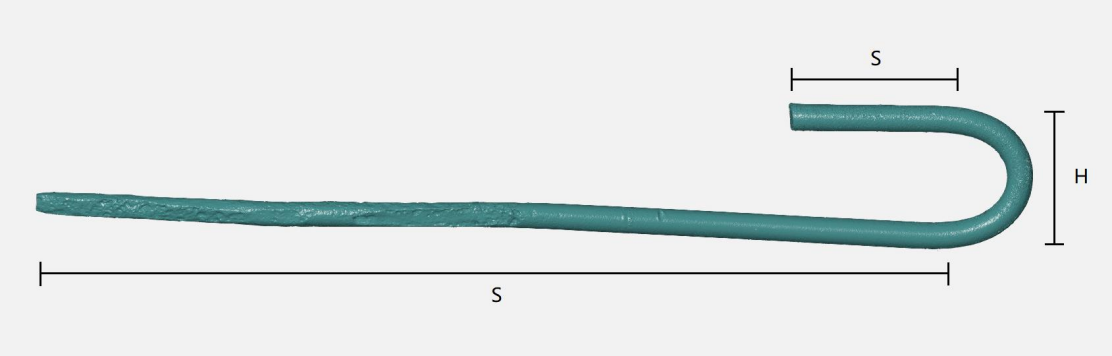

Figure 3.19: Illustration of the division of the straight parts and the hook part. S-straight part, H-hook part.

3.4.2 Yield penetration

Yield could be observed from the perimeter and area variation along the length of the reinforcement bar. Yield was identified as a continuous segment where both the perimeter and the area significantly decreased, as shown in the black box in the Figure 3.20. Additionally, the yielded part was not considered in the evaluation of the average corrosion level of the bar, since the yield also caused area loss and affected the accuracy of the corrosion analysis. The yield penetration was evaluated in Appendix A.1 and the results were attached in Appendix B.

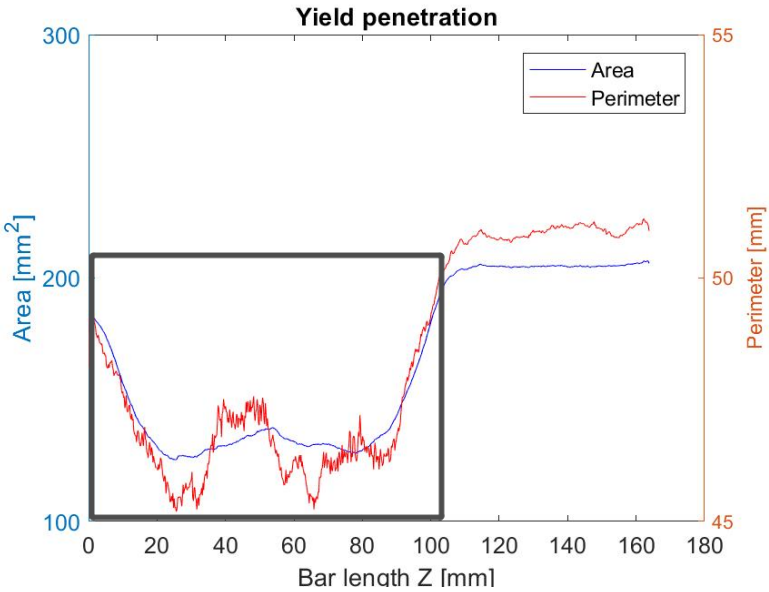

Figure 3.20: Yield, here in the marked zone, was identified when both perimeter and area were decreasing and formed a shape of basin.

Besides the evaluation of the yield penetration, total length, unyielded length and length of the hook end for all bars were also evaluated in order to observe the location of the main crack where maximum tensile force occured in relation to the yield penetration, as shown in Figure 3.21 and Figure 3.22. The results was attached in Appendix B.

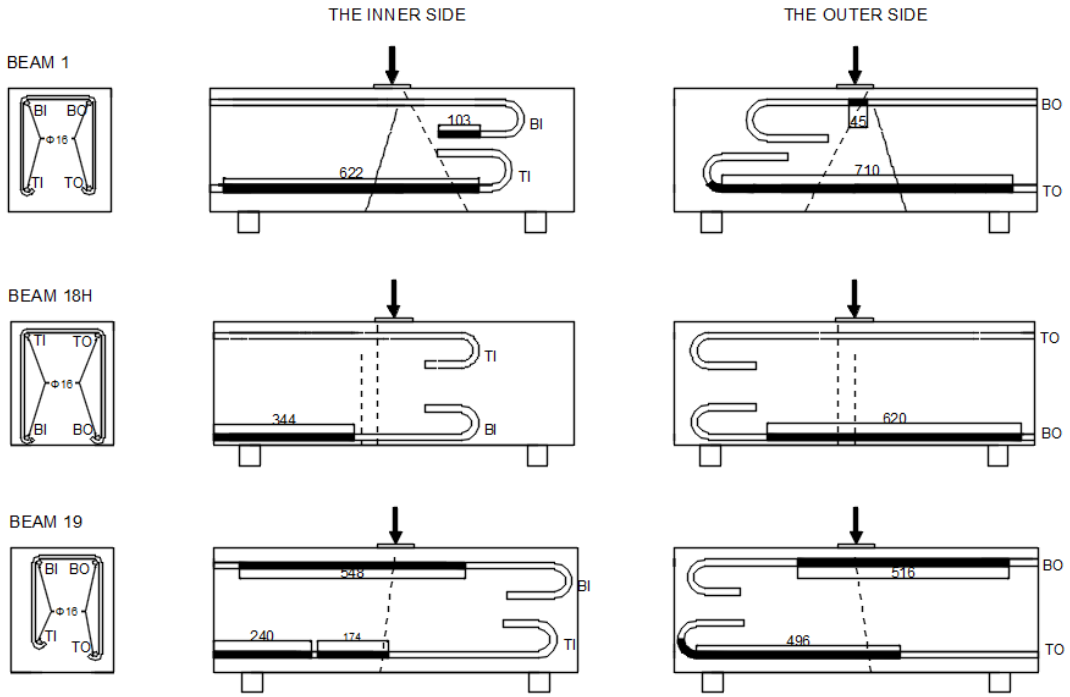

Figure 3.21: Yield penetration of the beams with one pair of hooks. The black hatched zone in the reinforcement bars was the yield penetration.

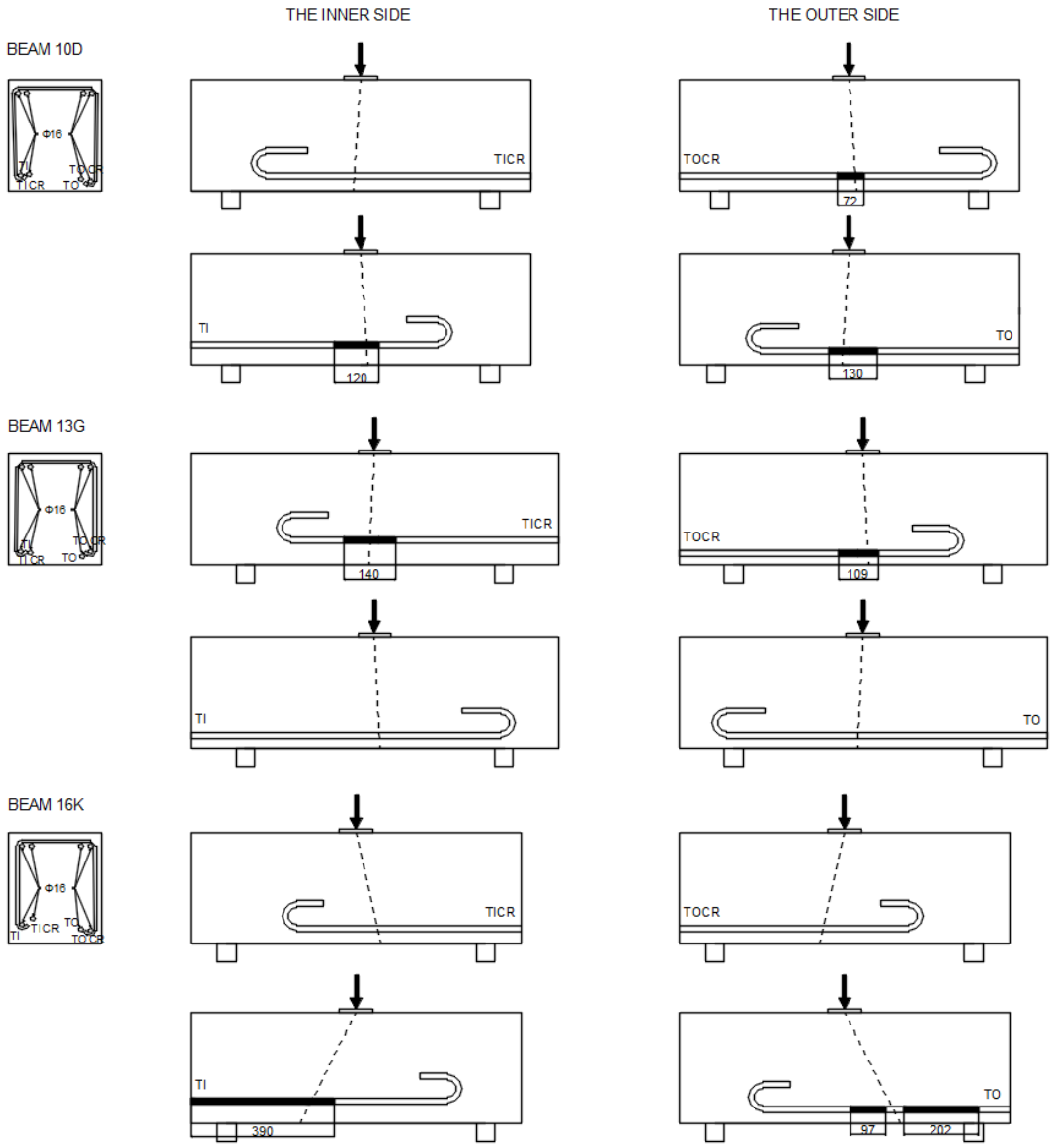

Figure 3.22: Yield penetration of the beams with two pairs of hooks. The black hatched zone in the reinforcement bars was the yield penetration.

3.5 Remaining capacity of the end hooks

In the three-point bending tests, the capacity of the beams was evaluated from the maximum applied load. After taking out the reinforcement bars and evaluating the corrosion level and yield penetration, the overall length of reinforcement bar was divided into the yield penetration and the unyielded length of the straight part and the hook part; the forces changed along the length of reinforcement bar concerning the yield, as shown in Figure 3.23.

The tensile force in the reinforcement bar was evaluated from the applied load. In Figure 3.23, the maximum tensile force was usually appeared in the cracked section in the mid-span of the beam and was defined as F_t. Since this thesis focuses on

the hook part, only the length of the cross section where maximum tensile force was located towards the side where the end hook was located was evaluated in the subsequent calculations. The yield force was defined as F_y at the cross section where yielded zone changed to unyielded zone. The length between the cross section where the maximum tensile force was located and the section where the unyielded length began was the yield penetration, defined as L_y. The bond stress in the yield penetration was defined as τ_y. At the cross section, where it went from yield penetration to unyielded length, L_{uy}, the bars carried the yield force. The force anchored by the hooks was complementary with the bond capacity, and defined as F_h. F_h in this thesis was estimated from an assumed bond capacity in the unyielded zone.

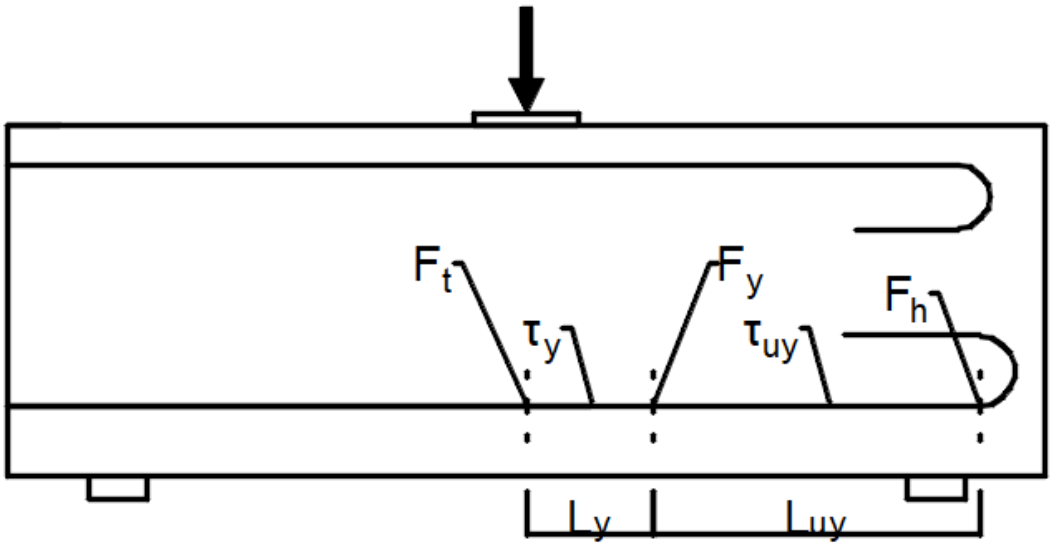

Figure 3.23: The reinforcement bars were divided into yield penetration and unyielded length with respect to the yielding.

3.5.1 Bond stress in the yielded zone

The bond stress of the reinforcement bars was affected by yielding. The maximum load applied on the beam was found in the diagram of applied load versus mid-span deflection obtained from three-point bending test results. The bending moment corresponding to the maximum load was then calculated equilibrium, see Eq. 3.3.

$$M = \frac{F_{max} * L}{2} \tag{3.3}$$

M = bending moment in middle section
F_{max} = the maximum applied load
L = the length of the span between centre line of supports

The tensile forces in the reinforcement bars were at the mid-span calculated from the maximum moment, Eq. 3.4.

$$F_t = \frac{M}{0.9 * d * n} \tag{3.4}$$

F_t = tensile force in reinforcement bar at mid-span
d = effective height, average distance between tensile reinforcement bars and top of the cross section. The commonly used approximate assumption of the inner level arm is that to be 90% of the effective height was used in this equation, Eurocode 2[14].
n = amount of reinforcement bars in the cross section

The reinforcement bars had reached yield at the maximum loads in all beams. This could clearly be seen both from the applied load versus mid-span deflection curves for all beams, and also in the 3D scanned results of the reinforcement bars after the tests. The yield penetration was described in Section 3.4.2. The yield force was calculated in Eq. 3.5

$$F_y = f_y * A_n \tag{3.5}$$

F_y = yield force
f_y = yield strength, defined in Section 3.1.2
A_n = nominal cross-sectional area

The bond stress in the yielded zone was calculated in Eq. 3.6. which related to the perimeter, tensile force and the yield penetration. The yield penetration was considered from the crack to the beginning of unyielded section.

$$\tau_y = \frac{F_t - F_y}{P_n * L_y} \tag{3.6}$$

τ_y = bond stress in yielded zone
P_n = nominal cross-sectional perimeter, defined in Section 3.4.1
L_y = yield penetration, evaluated from Section 3.4.2
F_y = yield force, from Eq. 3.5
F_t = tensile force, from Eq. 3.4

3.5.2 Force anchored by the hook

Beside the evaluation of yield penetration, unyielded length was also evaluated in the most cases, L_{uy} shown in Figure 3.23. The exact bond stress in the unyielded zone was unknown. In order to be able to calculate the force from the bond in unyielded zone, an assumed bond stress, τ_{uy}, was used in Eq 3.7.

The force in the cross section where L_y changes to L_{uy}, as shown in Figure 3.23, was the yield force. Concerning the force equilibrium, the force anchored by the hooks was equal to the difference between the yield force and the force from the bond in the unyielded zone, as shown in Eq. 3.8.

$$F_u = \tau_{uy} * L_{uy} * P_n \tag{3.7}$$

τ_{uy} = assumed bond stress in the unyielded zone
L_{uy} = the length of unyielded zone, evaluated from Section 3.4.2
P_n = the nominal cross-sectional perimeter, defined in Section 3.4.1

$$F_h = F_y - F_u \tag{3.8}$$

F_h = force anchored by the hook
F_y = yield force
F_u = force from bond in the unyielded zone, from Eq. 3.7

3.6 Capacity calculation of the hooks according to ACI Journal and Swedish Handbook for Concrete Structures (BBK 04)

There are different codes containing formulas to calculate the anchorage capacity of hooks, ACI 318-71[1] and BBK 04[3]. Since the reinforcement bars were corroded, the average corrosion level was considered when using the geometric data of reinforcement bars, such as the average cross-sectional area.

Marques and Jirsa studied the strength of hooks through experiments in 1975 and concluded that the strength of the hook was related to the diameter of the steel bar and the compressive strength of the concrete. The relation was expressed in Eq. 3.9. (J. Marques, J. Jirsa. 1975)[1].

$$f_h = 700(1 - 0.3d_b)\psi\sqrt{f'_c} <= f_y \tag{3.9}$$

f_h = strength of hook in psi
d_b = diameter of the reinforcement bar in inch
f'_c = concrete compressive strength
ψ = coefficient which depends on the size of the bar, the length of the lead straight embedment, side concrete cover and cover extension of the tail

In accordance with the handbook published by Swedish Boverket (Boverket, 2004)[3], the concentrated anchorage force carried by hook could be calculated by using Eq. 3.10.

$$F_a = A_s * f_{cc} * \epsilon \tag{3.10}$$

A_s = the cross-sectional area of reinforcement bars
f_{cc} = the compression strength of concrete
ϵ = factor which depends on the outline and angle of the hooks, is 90 for plain

reinforcement bar terminating in end hook

3.7 Shear capacity of the beams

Since shear cracking took place in the beams with two pairs of hooks, it was of interest to calculate the shear capacity of the beams. The c/c distance of stirrups in the beams with two pairs of hooks varied a lot from beam to beam, as shown in Figure 3.8. The shear capacity of reinforced concrete beams with stirrups was calculated according to Eurocode 2: Design of concrete structures[14] for every beam with two pairs of hooks, in Eq. 3.11.

$$V_{Rd,c} = n * f_{ywd} * A_{sw} \tag{3.11}$$

$V_{Rd,s}$ = shear capacity in a reinforced concrete beam with vertical stirrups
n = amount of stirrups that shear crack has passed, in Figure 3.8
f_{ywd} = yield strength of stirrups, defined in Section 3.1.2
A_{sw} = cross-sectional area of stirrups, defined in Section 3.1.1

4

Results

This chapter is divided into four parts. First, the structural behavior of the specimens under three-point bending test is described, subsequently, the corrosion level of the reinforcement bars and the yield penetration are presented, and their effects on bond stress are analyzed. Finally, the force in the end-hooks is evaluated, and compared to code provisions.

4.1 General behavior of the structural tests

Six beams were analyzed in this study. Three beams with one pair of hooks (1, 18H, and 19), and three beams with two pairs of hooks (10D, 13G, and 16K).

4.1.1 Load versus deflection curves

The deformation and crack-opening of the beams under the three-point bending tests were recorded by using Digital Image Correlation (DIC) method. From these measurements, the mid-span deflection was evaluated. In Figure 4.1, the applied load versus mid-span deflection of the tested beams for all tests is shown. Specifically, Figure 4.1a shows the load versus mid-span deflection curve of the three beams with one pair of hooks (Beam 1, 18, 19), and Figure 4.1b shows the load versus mid-span deflection curve of the three beams with two pairs of hooks (Beam 10D, 13G, 16K).

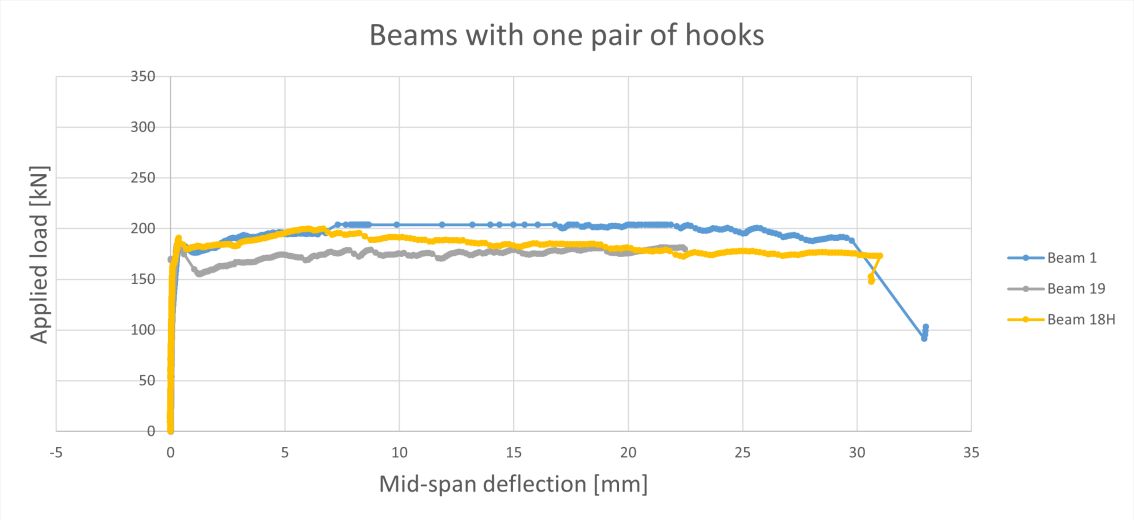

(a) Applied load versus mid-span deflection for beams with one pair of hooks

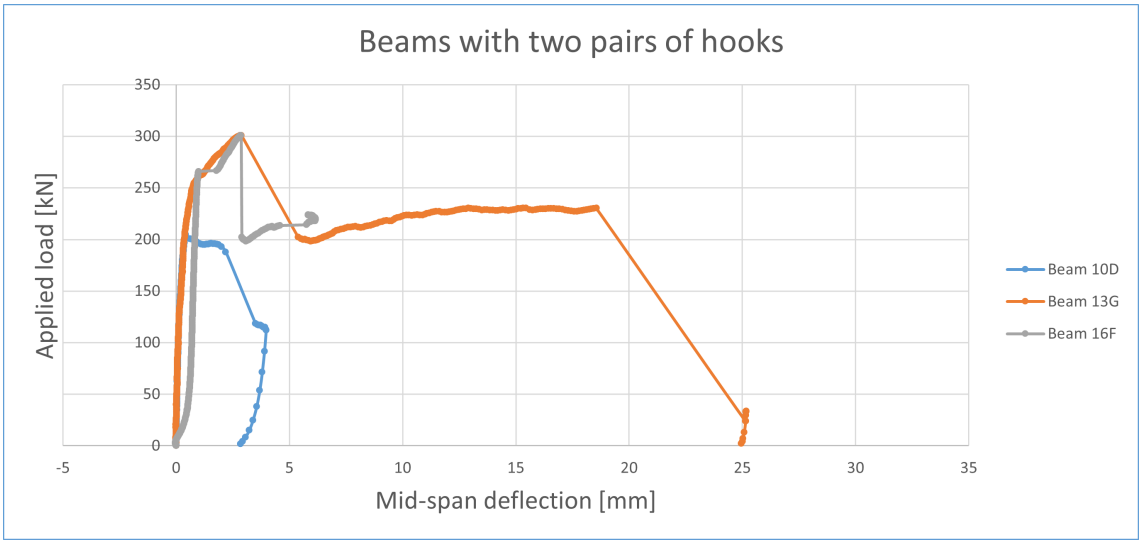

(b) Applied load versus mid-span deflection for beams with two pairs of hooks

Figure 4.1: Applied load versus mid-span deflection in the three-point bending tests

Regarding the beams with one pair of hooks, the applied load developed linearly with the mid-span deflection for small deflections. As the load continued to increase, small cracks appeared and the beams went from stage I to stage II, and the curves slightly deviated from the initial elastic status. When the applied load reached approximately 180 kN in all tests of beams with one pair of hooks, there was a visible load-drop in the load-deflection curves. By comparing Figure 4.1a. with corresponding DIC measurements as illustrated in Figure 4.2a: when the applied load reached between 175 kN and 190 kN, a visible crack appeared in the beams. After a load-drop, cracks in concrete passed the bottom reinforcement layer, the reinforcement bars were activated and started to engage (Figure 4.2b). With contribution from steel hardening, the beams showed an increase of load-carrying capacity of about

20 kN to 30 kN and reached the maximum load. Thus, the beams had a non-linear ductile behavior. Failure took place in the bolts restricting the reinforcement bars on one end of the beam, at approximately 30 mm mid-span deflection.

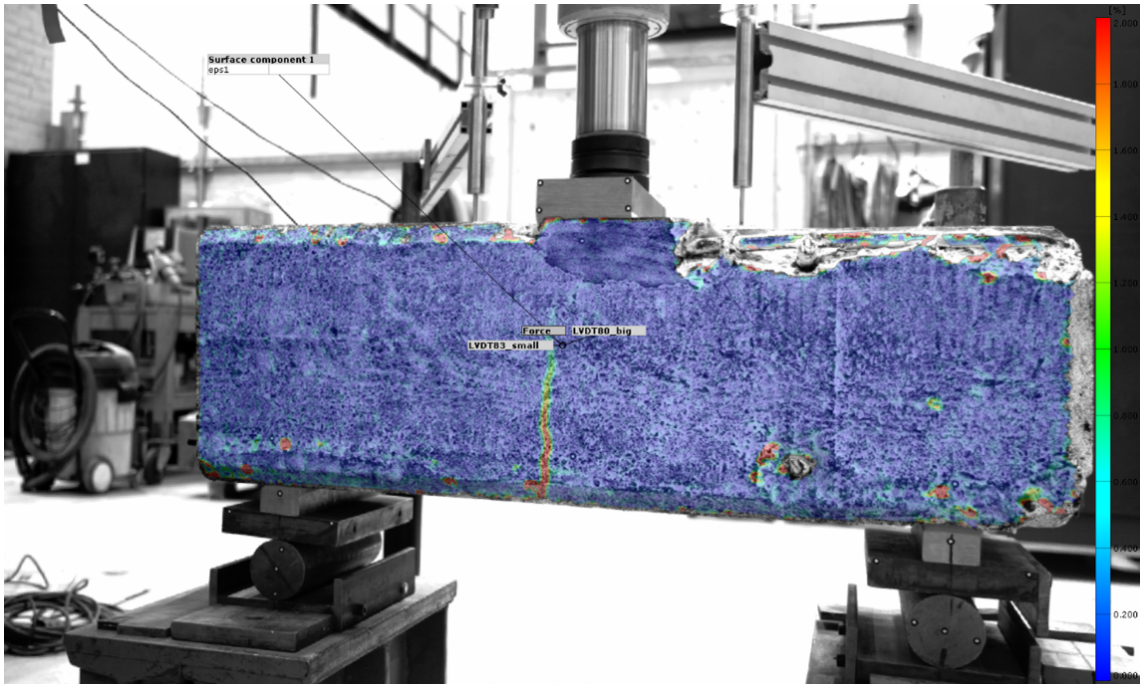

(a) Crack on Beam 19 before load-drop. Load 183 kN. Mid-span deflection 0.3 mm.

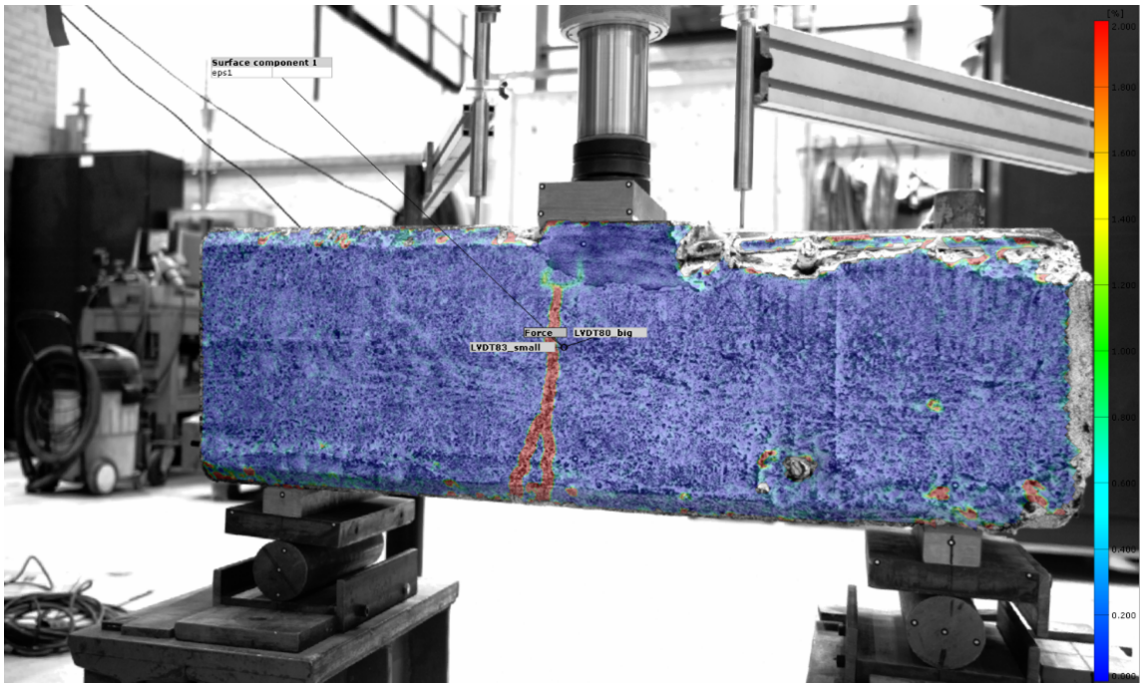

(b) Beam 19 after first load-drop. Load 155 kN. Mid-span deflection 1.3 mm.

Figure 4.2: Crack development of a beam with one pair of hooks, before and after load-drop

The beams with two pairs of hooks had a different structural behavior from the beams with one pair of hooks. As shown in Figure 4.1b, the beams with two pairs of hooks had a brittle failure, but carried a much higher applied load. In the beginning, the beams showed a linear behavior with small deflection. By increasing the load, the beams went from the stage I to stage II and deviated from the linear development. The beams with two pairs of hooks showed an increase of load-carrying capacity in most cases due to the presence of one extra pair of reinforcement bars both at top and bottom layers and the hardening of reinforcement bars. The hardening of the beams with two pairs of hooks provided about 10 kN extra load-carrying capacity, which was less than the beams with one pair of hooks since there was less required contribution from each reinforcement bar. Figure 4.3 showed an example of Beam 13G before and after load-drop. For beams 13G and 16K, a slow development of bending cracks on the mid-span was first observed, and when the maximum applied load of about 300 kN was reached, multiple shear cracks suddenly appeared. When the shear cracks appeared, an obvious load-drop caused by the shear failure of the beam was observed.

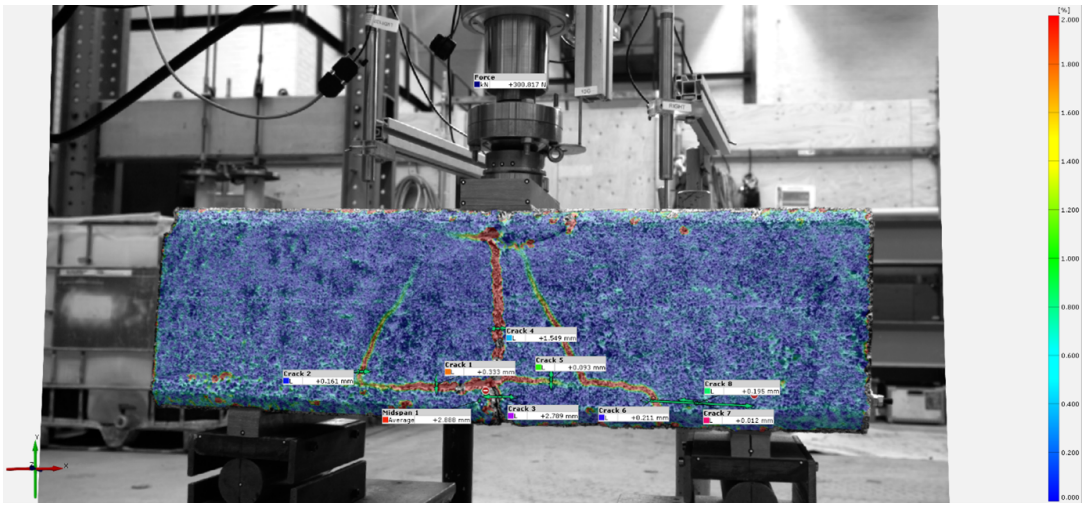

(a) Beam 13G before load-drop. Load 300 kN. Mid-span deflection 2.9 mm.

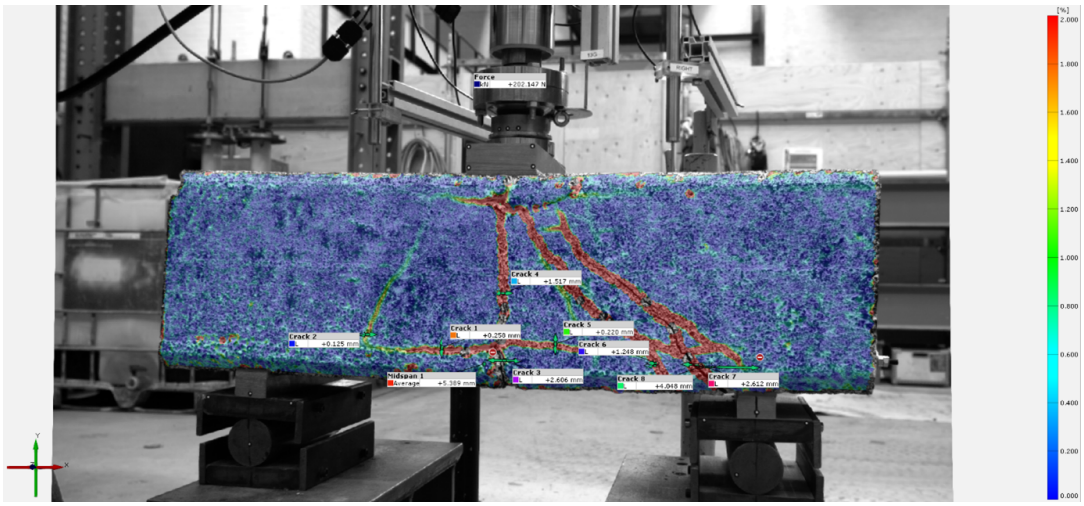

(b) Beam 13G after load-drop. Load 202 kN. Mid-span deflection 5.4 mm.

Figure 4.3: Crack development of a beam with two pairs of hooks, before and after load-drop

Beam 13G showed a more ductile behavior than beam 16K, as shown in Figure 4.1. Beam 10D failed due to shear cracks as well, but with less load than the other beams with two pairs of hooks, probably mainly due to the damaged concrete of the beam before tests as shown in Figure 4.4.

Figure 4.4: Damaged concrete before test, beam 10D

Compared to the beams with one pair of hooks, the beams with two pairs of hooks had a higher load-carrying capacity, but showed a more brittle behavior and failed with less mid-span deflection. The higher load-carrying capacity was due to the presence of more reinforcement bars in the beams.

4.1.2 Crack patterns

During the tests, all beams were observed to get significant cracks. One or at most two major bending cracks could be observed for all beams with one pair of hooks. The bending cracks were located in the middle of the span, underneath the load plate, see Figure 4.5 and 4.6. In addition, the top edge of Beam 18H was damaged due to corrosion before test. It could be observed, from the DIC measurements, that the concrete in the upper right corner of Beam 18H did not cover the hooks of the top reinforcement bars due to the severe damage of the concrete, as shown in Figure 4.5(c). Moreover, rupturing of one of the two reinforcement bars was observed in this test (Beam 18H). The end of the ruptured reinforcement bar was observed to have an unyielded part, thus bond stress must have been transferred in the yielded zone. Further, it was interesting to note that the reinforcement bar was ruptured instead if the hook being pulled out.

In contrast, the beams with two pairs of hooks in both top and bottom layers, including beams 10D, 13G and 16K, usually produced multiple cracks with more complex shapes and orientations, and were mostly located on the right side of the inner side plane, as shown in Figure 4.6. For beam 13G and 16K, there were visible bending cracks in the middle; these cracks developed in the beginning of the test. Because of the presence of four more reinforcement bars in the beams, the beams carried larger applied load with increasing crack-opening in the middle of the span. However, for large loads, shear cracks were generated towards the support on the right side; these thereafter developed quicker than the bending cracks in the middle. At the maximum load, the beams failed in shear failure.

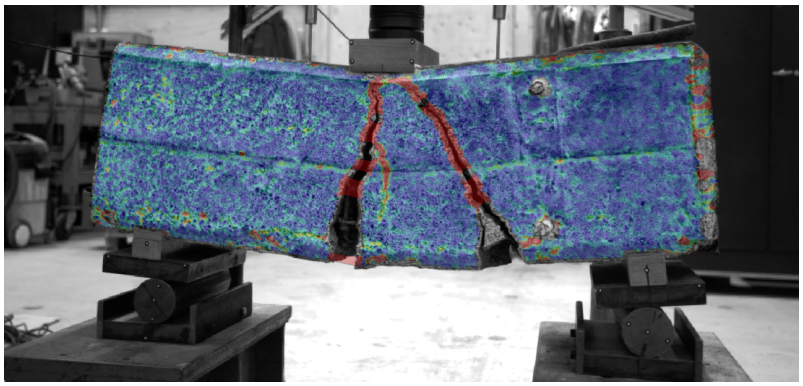

(a) Crack patterns of Beam 1

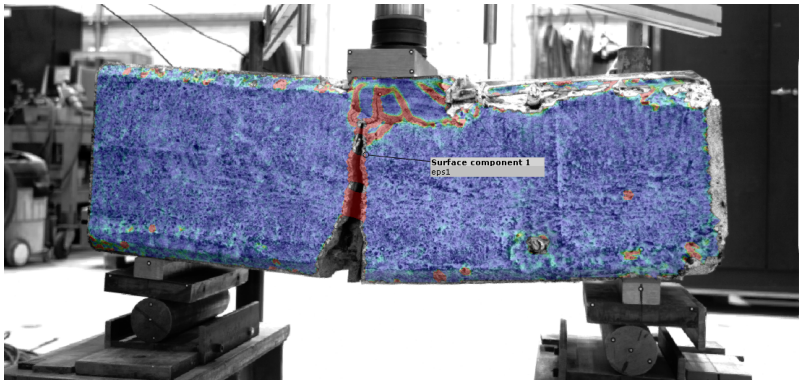

(b) Crack patterns of Beam 19

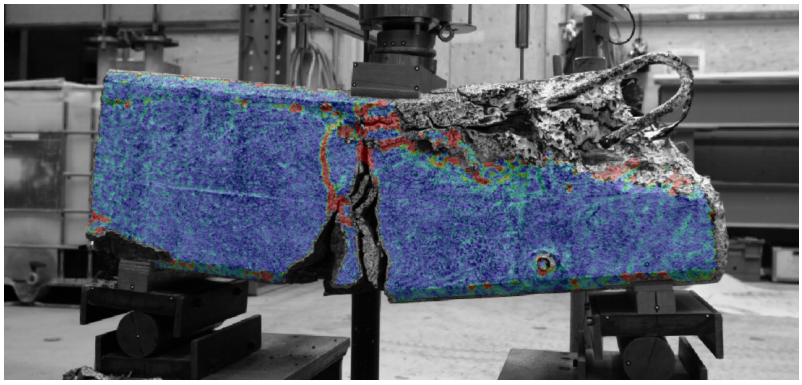

(c) Crack patterns of Beam 18H

Figure 4.5: Beams with one pair of hooks tested in three-point-bending, crack pattern at failure.

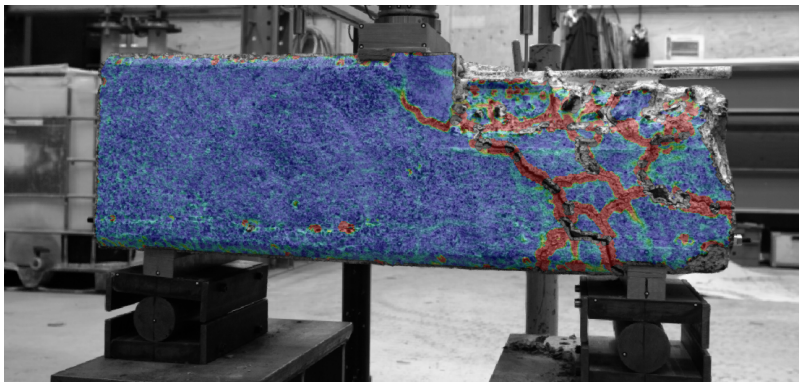

(a) Crack patterns of Beam 10D

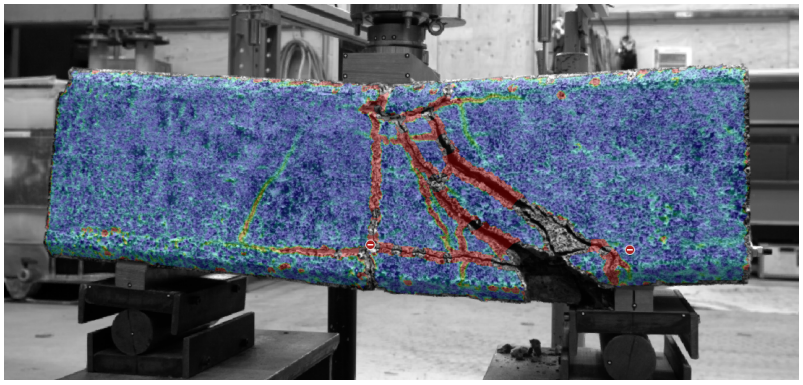

(b) Crack patterns of Beam 13G

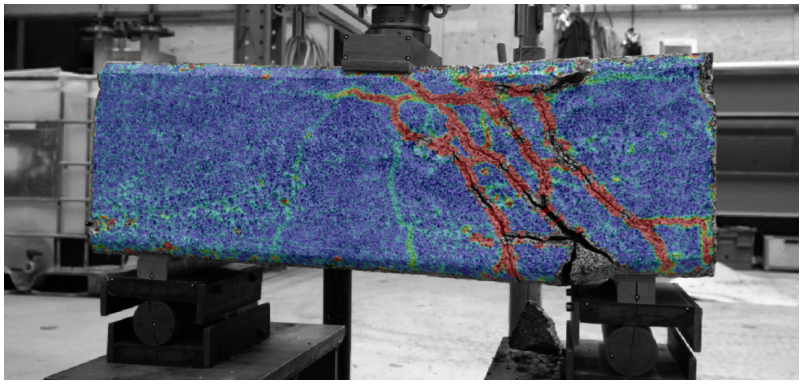

(c) Crack patterns of Beam 16K

Figure 4.6: Beams with two pairs of hooks tested in three-point-bending, crack pattern at failure.

4.1.3 Differences between plain rebars with and without end-hooks

In an earlier study, twenty beams with naturally corroded plain reinforcement bars from Gullspång bridge were tested in three-point bending (Robuschi et al., 2020)[19]. The load versus mid-span deflection curves for these beams are shown in Figure 4.7. As can be seen, the maximum mid-span deflections varied between 10 and 25 mm. The deflection increased with the increasing applied load before reaching the peak

load. At the peak load, the first end-slip was triggered in most cases.

By terminating the reinforcement bars with hooks, the structural behavior became different from the beams with the ordinary plain reinforcement bars. The maximum mid-span deflection of the beams with one pair of hooks were between 20 and 33 mm as illustrated in Figure 4.1a. Thus, compared to beams with ordinary plain reinforcement bars, the hooks improved the ductility of the beam. The beams with plain reinforcement bars ending in hooks showed a 24% ~50% deflection increase compared to the beams with ordinary plain reinforcement bars.

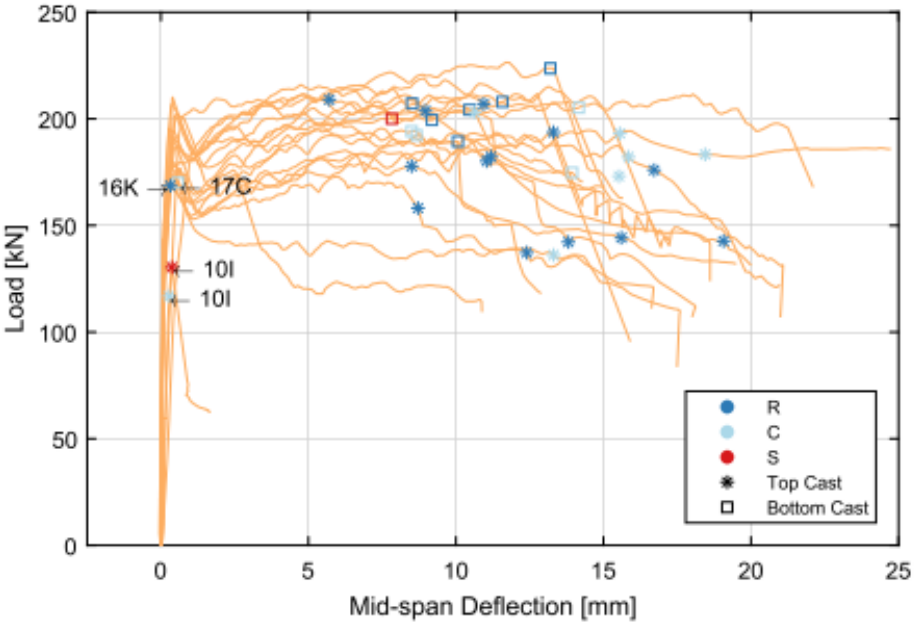

Figure 4.7: Load-mid-span deflection curves for the three-point bending tests. (Robuschi et al., 2020)[19]

4.1.4 Shear capacity of beams with two pairs of hooks

Since the beams with two pairs of hooks were observed to fail in shear, it was of interest to compare the shear capacity of the beams to codes. The shear capacity of the beams with two pairs of hooks was calculated according to Eurocode 2 in order to compare with the maximum applied load during the tests, see Appendix C.7. According to Eurocode 2, all the shear force was carried by the stirrups[14]. The shear crack inclination was measured in accordance with DIC measurements for all beams with two pairs of hooks, as shown in Table 4.1. As shown in Figure 3.8, the number of the stirrups that the shear cracks went through was one pair for all beams with two pairs of hooks. The design shear capacity of the beams was 14.25 kN, which was about one tenth of the maximum applied during the tests. As mentioned above, beam 10D had slightly less capacity, due to the concrete damage; the design shear capacity was about one seventh of the maximum applied. In addition, Figure 3.8 showed that there were one more pair of stirrups in the left side of the inner side

of the observation plane of Beam 10D and Beam 13G, but this extra pair of the stirrups was not in the shear span.

Beams	Shear crack angle (Exp.) [deg]	Max. shear force (Exp.) [kN]	Shear capacity (Theor.)
10D	37	102	14.25
13G	39	150	14.25
16K	43	150	14.25

Table 4.1: Shear capacity and the shear crack angle of the beams with two pairs of hooks

4.1.5 Deformation of hook ends after the three-point bending tests

After sandblasting, the inclination of straight part of the hook was measured and recorded. Most of the reinforcement bars were observed to have a 180-degrees-bent hook as in their original configuration, indicating that they were only slightly deformed. However, two reinforcement bars in Beam 1 were visibly deformed, namely 1 TO and 1 BO. Their deformation was larger than other reinforcement bars, as illustrated in Figure 4.8 that the hook ends were visibly upwarped. The DIC measurements and the crack pattern and positions of longitudinal reinforcement bars of the Beam 1 were illustrated in Figure 4.9. Two bending cracks in the middle were observed. One of the cracks was found near where the hook was located. With this in mind, through overlap of position of the cracks and hook ends, it could be inferred that the reinforcement bars that were completely yielded, were anchored by the hooks and thus all the yield force was carried by the hooks. The hooks were under the tensile state and bent upward against concrete, and the reinforcement bars were subjected to tension and slipped.

(a) Beam 1 reinforcement bar BO 1of2 **(b)** Beam 1 reinforcement bar TO 1of2

Figure 4.8: Large deformation of hooks

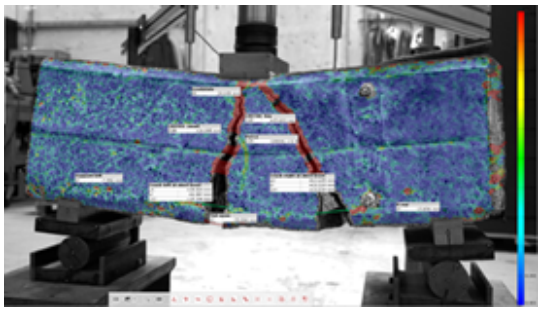

(a) Beam 1 crack pattern by DIC measurement

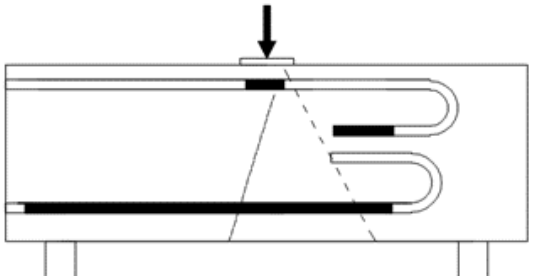

(b) Beam 1 crack pattern and yield penetration illustrated in AutoCAD

Figure 4.9: Crack patterns of beam 1

4.2 Corrosion level

After the three-point bending tests, the reinforcement bars in the beams were extracted, sandblasted and cleaned, and the geometry of all studied bars was obtained by 3D scanning. The corrosion level was evaluated by MATLAB codes, see Appendix A.1. It is important to note that the corrosion level was not evaluated for the yielded zone, since the yielding caused the decrease of cross section, which corrosion also did. Thus, it was difficult to distinguish these two different kinds of area loss. Therefore, a distinction was made between yielded zone and unyielded zone for each reinforcement bar. In the unyielded zone, both the average corrosion level and peak corrosion level were calculated.

In order to visually display the corrosion level of each type of reinforcement bar, the peak corrosion level compared to the average corrosion level is illustrated in Figure 4.10. As mentioned in Section 3.2.1, all beams except Beam 18H were placed upside down during the tests relative to their original placements on the bridge. Further, for the beams with two pairs of hooks, only the tensile reinforcement bars were saved after the tests, which were in fact the top-cast bars originally. Therefore, considering the different problems to be analyzed, in the later sections the original position of the reinforcement bar will be consistently indicated by capital T and B, and the position of the reinforcement bar in the beam in the experiments will be indicated by small t and b. In Figure 4.10, the black diagonal line corresponds to y = x, which means a uniform level of corrosion for the entire bar. This did not occur; instead, it could be observed that all results were distributed above the diagonal line. Thus, the value of the peak corrosion level was larger than that of the average corrosion level, which was reasonable. On the whole, it was reasonable that for all of the reinforcement bars, the peak corrosion level increased with the average corrosion level. Between the two different types of beams, taking the beams with one pair of hooks as example, the corrosion level was much scattered for both top-cast and bottom-cast bars, and no relation between corrosion level and casting position could be found. Moreover, Figure 4.10 showed also that the average corrosion level varied between 0% and 2%, while the peak corrosion level reached 5.5%. In fact, the main corrosion types and corrosion distribution could be intuitively observed in software

GOM Inspect, as shown in Figure 4.11 and Figure 4.12. The surface of the entire reinforcement bars had pitting corrosion, or alternating areas of severe and minor corrosion areas.

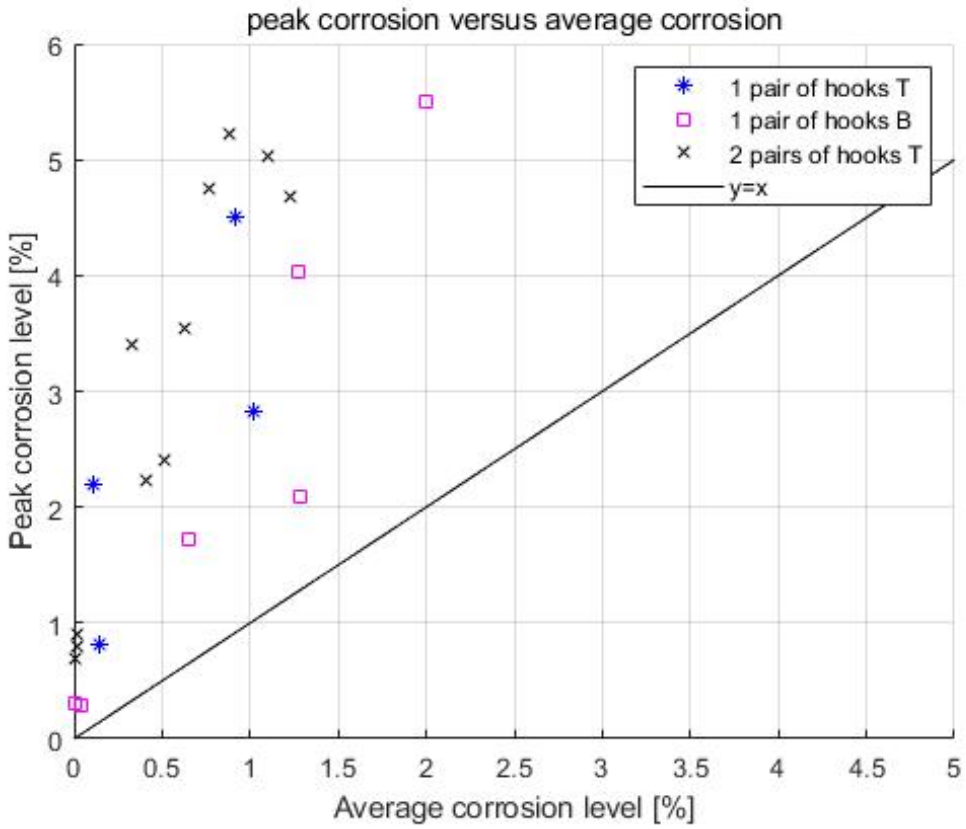

Figure 4.10: Peak corrosion level versus average corrosion level of the bars; for two types of beams

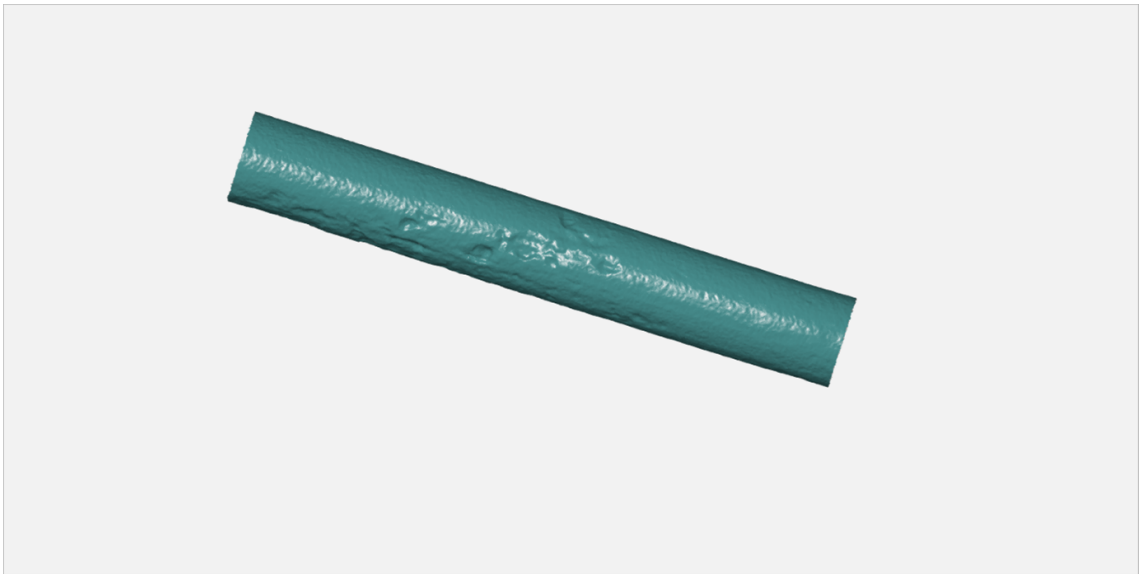

Figure 4.11: Bar 10D TO, example of pitting corrosion

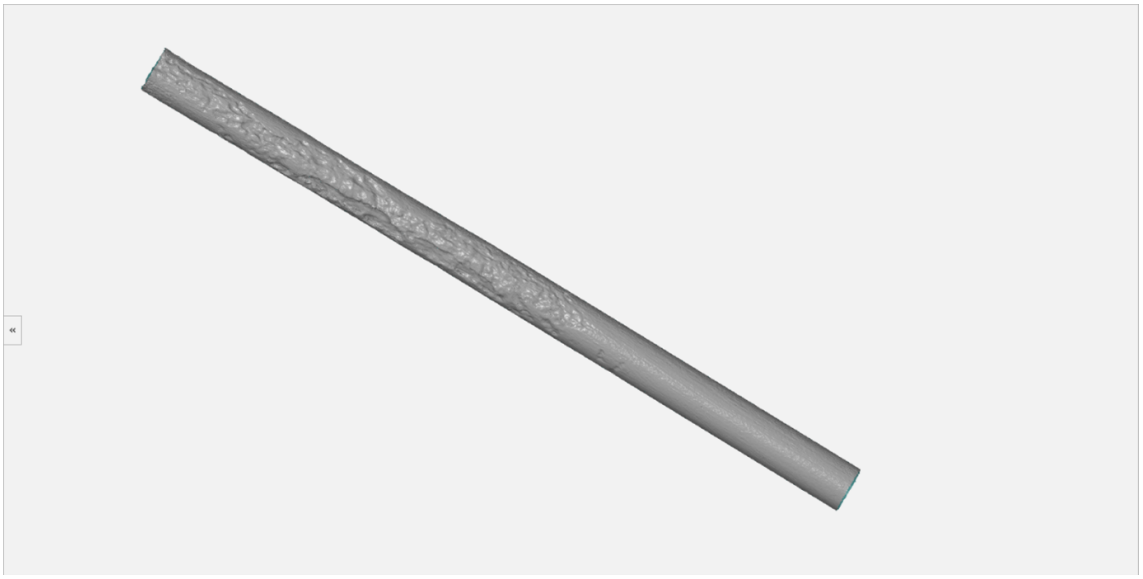

Figure 4.12: The straight part of bar 13G TO CR, example of alternating areas of severe and minor corrosion

4.3 The average bond stress in the yielded zone

After the three-point bending tests, the beams failed in shear or bending owing to the different numbers of reinforcement bars inside the beams. Most of the reinforcement bars underwent various degrees of yielding. The yielding resulted in a reduction of the cross-sectional geometry. The reduced cross-section in yielded zone means that the bond capacity also decreased in the yielded zone. As the connection between concrete and reinforcement bars was reduced, the interlocking mechanism between them was weakened. For the study of the bond stress in the yield penetration, a uniformly distributed bond stress was assumed along the yield penetration of the reinforcement bars. The evaluation was carried out according to the description in the Section 3.5.1. The average bond stress in the yield penetration was investigated to better understand the impact of the yielding on bond, see Appendix C. In addition, the calculation and analysis of the bond stress in the yield penetration also provided useful information on the forces that were applied at the time of anchorage failure.

Reinforcement bar 13G TO CR is described here as an example. The cross-sectional area and perimeter were plotted along the bar length in Figure 4.13 in order to evaluate the yielded zone in the reinforcement bar. Within the marked area in same figure, the yield penetration was captured due to the decrease of both area and perimeter. In order to visualize the yielding in the reinforcement bar, the geometry of Beam 13G and the corresponding position of cracks obtained from the DIC measurements are illustrated in Figure 4.14. As the figure illustrates, the yielded zone located in the middle of the beam and the crack in concrete passed through the yielded zone.

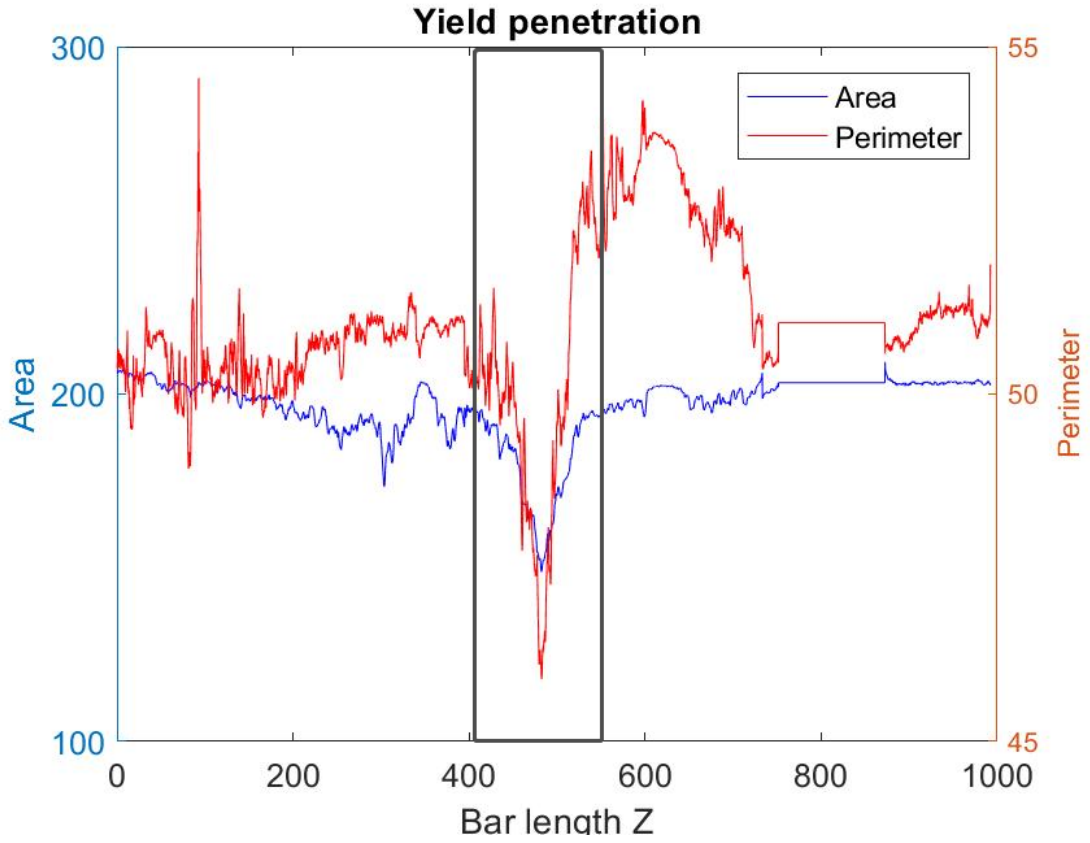

Figure 4.13: Yield penetration of bar 13G TO CR

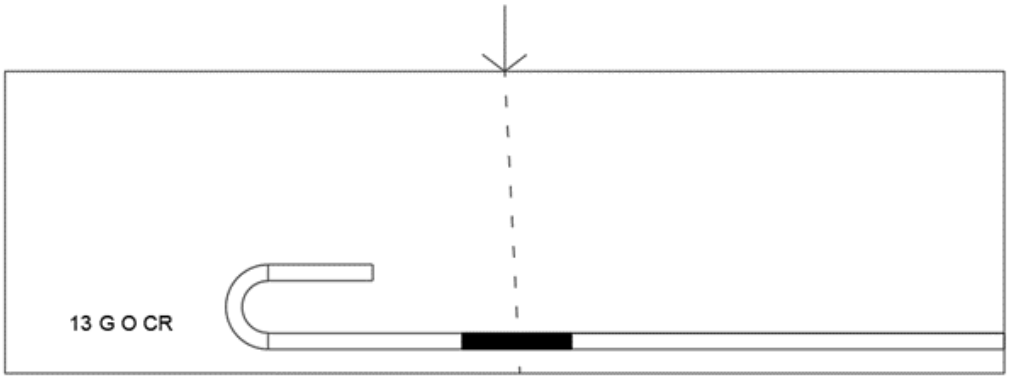

Figure 4.14: Position of yielded zone of bar 13G TO CR

Since the yielding had an impact on bond stress, the yield penetration was an important factor for evaluated bond stress in yielded zone. Figure 4.15 showed the relationship between the average bond stress in the yielded zone and the corresponding yield penetration. The impact of reinforcement bars position during the test on bond stress was also investigated. Since the position of the neutral axis of each beam was different, the top and bottom reinforcement bars were subjected to different degrees of strain. Therefore, the top and bottom reinforcement bars were

considered individually in Figure 4.15. Beam 10D was a special case since the top concrete was broken and part of the bar had been exposed to the air before the test. Negative bond stress was obtained by calculation for the reinforcement bars in Beam 10D using the nominal height of the beam. The negative values could be a result of the uncertainties in the properties and geometry of the materials used in the formulas, and those negative values were therefore assumed to be 0, shown as the points on the x-axis. The bond stress in the yielded zone varied between 0 MPa and 4.5 MPa. The average bond stress was found to be equal to be 1.8 MPa with a standard deviation of 1.3 MPa.

On the whole, the yield penetration of the reinforcement bars of the different types of beams spanned a wide range. One interesting result was that the yield penetration of reinforcement bars in the beams with two pairs of hooks was generally shorter than the beams with one pair of hooks. This is likely due to the presence of one more pair of hooks both in the top and the bottom layers. Thus, each reinforcement bar needed to contribute less than a bar in beams with one pair of hooks to carry the same applied load.

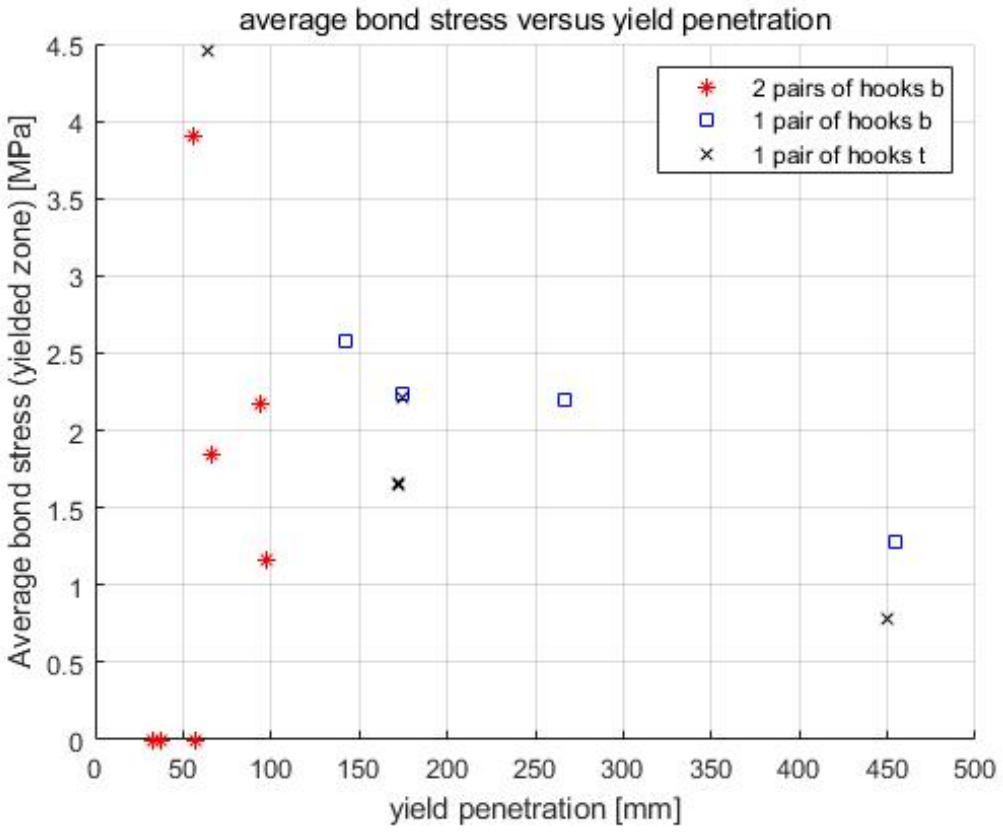

Figure 4.15: Average bond stress in the yielded zone versus yield penetration; for two types of beams.

4.4 Force anchored by the hooks

It was of interest to estimate the force anchored by the hooks and possible effects of corrosion and casting positions on it. The force anchored by the hooks was expressed in term of a linear relation with assumed bond stress in Section 4.4.1. In Section 4.4.2 and 4.4.3, the forces anchored by the hooks were determined assuming a fixed value of the bond stress in the unyielded zone of 1 MPa, to investigate the impact of corrosion and casting positions .

4.4.1 Force anchored by the hooks during the tests

The force anchored by the hooks was evaluated as described in chapter 3, Eq. 3.8. In order to find contribution of the hooks during the tests, assumptions were made about the bond stress in the unyielded zone.

In Model Code 2010 (CEB-FIP (2013))[6], the bond strength for hot-rolled plain reinforcement bars is for "good conditions" given as $0.3\sqrt{f}_{cm}$, f_{cm} being the concrete compressive strength. For "other" bond conditions, there is a reduction factor of 0.5. For the studied specimens, these expressions correspond to peak bond stress of 2 MPa for good bond conditions and 1 MPa for all other bond conditions. From previous research (Robuschi et al., 2020)[19], the average bond strength of reinforcement bars without damage in the anchorage region was found equal to 7.6 MPa, with a deviation of 3 MPa. Thus, the bond stress in the unyielded zone was assumed to vary between 1 MPa and 12 MPa. With this assumption, an estimation of the hook stress was obtained, as the force anchored by the hooks was the difference between the yield force and the force from the bond in the unyielded straight zone.

Figure 4.16 showed that the force anchored by the hooks varied linearly with the assumed bond stress. As the assumed bond stress increased, the force anchored by the hooks decreased. In both types of the beams, the force anchored by the hooks behaved similarly. The range of variation in force magnitude with the assumed bond stress was similar. Reinforcement bars 1 BI and 19 BO exhibited larger force anchored by the hooks with a wider range of variation of the assumed bond stress than the other reinforcement bars. The special feature of reinforcement bars 1 BO and 19 BO was that their straight parts of the bars were yielded along their entire lengths. Due to the area decreased in the yield penetration, the connection between reinforcement bars and concrete was absent. Therefore, the hooks were carrying the yield force. As mentioned earlier, the hook end of reinforcement bar 1 BO was deformed visibly which could be seen from Figure 4.16a.

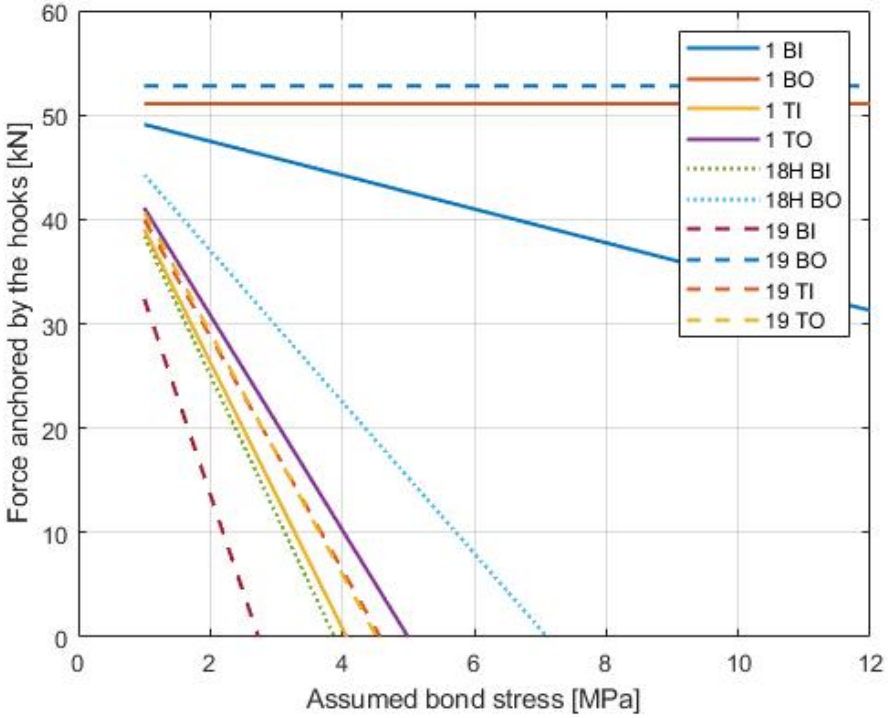

(a) Force anchored by the hooks versus assumed bond stress; for the beams with one pair of hooks

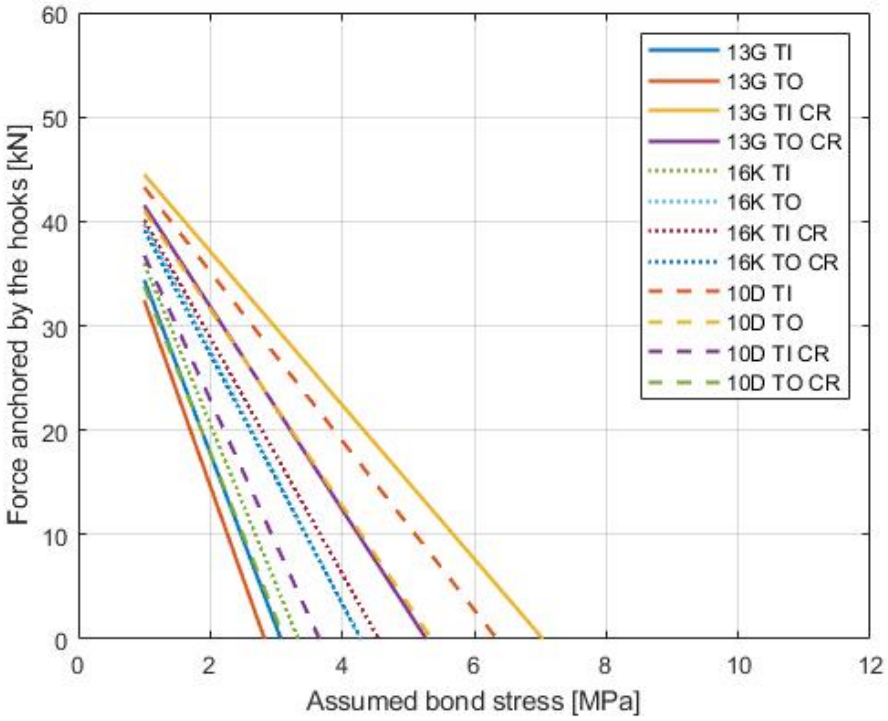

(b) Force anchored by the hooks versus assumed bond stress; for the beams with two pairs of hooks

Figure 4.16: Force anchored by the hooks versus assumed bond stress; for two types of beams

4.4.2 The impact of corrosion

Studying the impact of the corrosion level on the force anchored by the hooks is an important task. The corrosion level was evaluated as described in Section 4.2. The force anchored by the hooks varied depending on the assmued bond stress in the unyielded zone. To investigate the effect of corrosion on the force anchored by the hooks, an assumed value of the bond stress in the unyielded zone was used. The assumed bond stress was 1 MPa for top-cast bars and 2 MPa for bottom-cast bars. These values were assumed based on Model Code 2010[6]. Additionally, from a previous study (Yu et al., 2021)[24], top-cast bars were observed to generally have a lower maximum bond stress for unyielded zone than bottom-cast bars when uncorroded. The calculated force anchored by the hooks with the assumed bond stress was subsequently explored in relation to the corrosion level, as shown in Figure 4.17.

The relationship between the force anchored by the hooks and the corrosion level for reinforcement bars in different types of beams could be observed separately in Figure 4.17. As shown in these two figures, the range of variation in the corrosion level in the two types of beams was about the same, which has been covered in Section 4.2. In comparison, the end hooks of the reinforcement bars in the beams with one pair of hooks were more loaded during the tests and more utilized. The points in the Figure 4.17 were much scattered, and no clear trend between force anchored by the hooks and corrosion level could be identified.

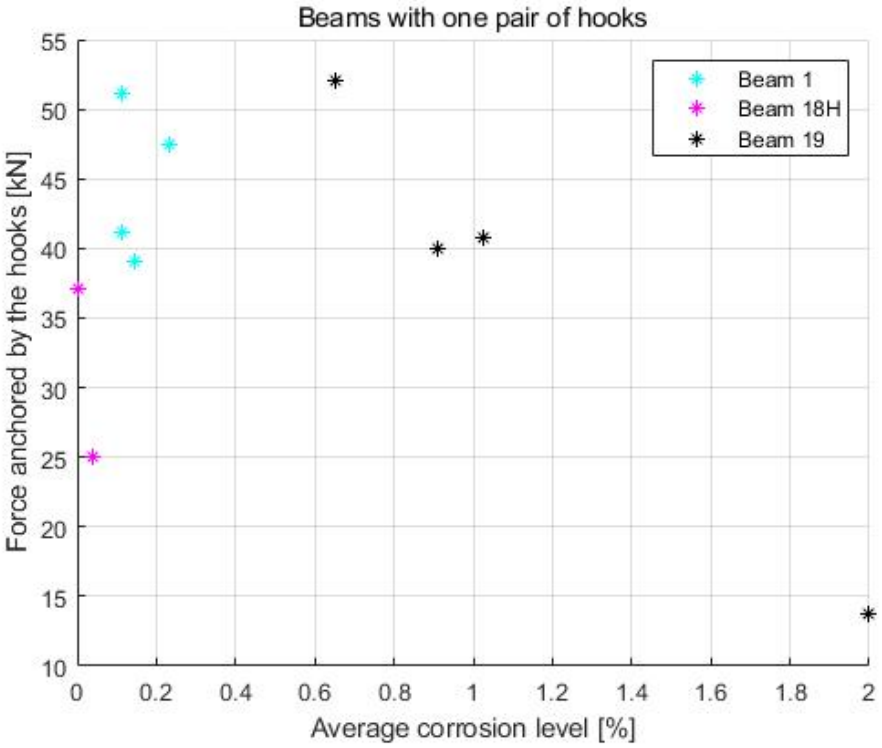

(a) Force anchored by the hooks versus average corrosion level; for beams with one pair of hooks

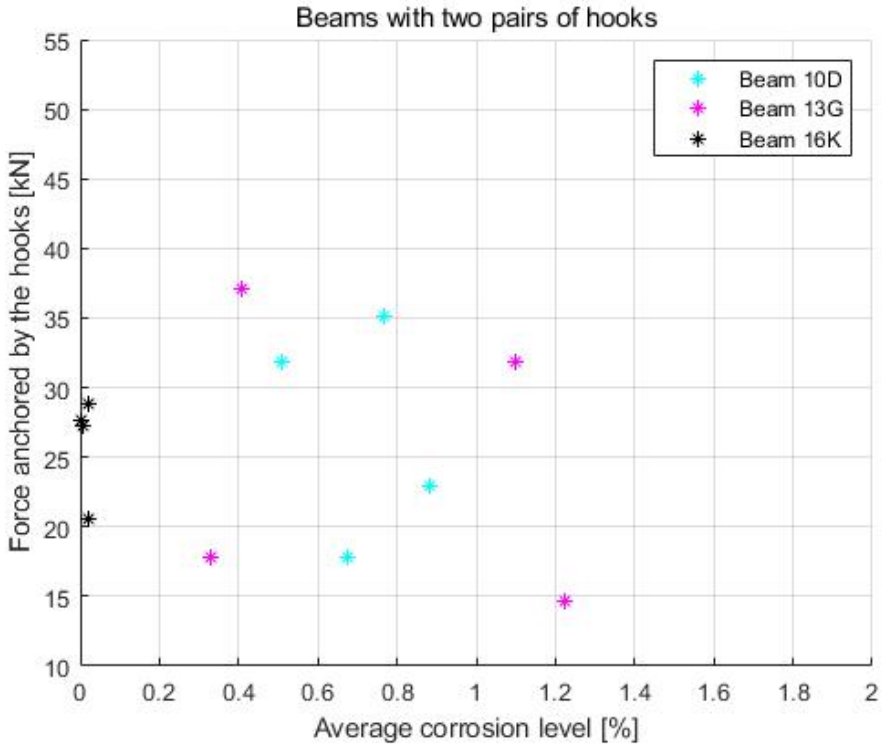

(b) Force anchored by the hooks versus average corrosion level; for beams with two pairs of hooks

Figure 4.17: Force anchored by the hooks versus average corrosion level; for two types of beams

4.4.3 The impact of casting positions

The Gullspång bridge was built for more than eighty years ago. As mentioned in Section 3.1.2, there was no vibration during the casting process. The casting process without the vibration of the concrete resulted in a difference in the density of the concrete at the top and bottom of the beam, with the density at the bottom being slightly greater due to settlement. Attributed to the concrete density, the casting position was regarded as a potential factor affecting the bond of plain reinforcement bars. Investigating whether the casting position had an impact on the force anchored by the hooks was as well one of the important tasks in this thesis.

As shown in Figure 4.18, the casting positions of the reinforcement bars appeared to influence the force anchored by the hooks. The hooks of the bottom-cast bars carried larger force than those of top-cast bars.

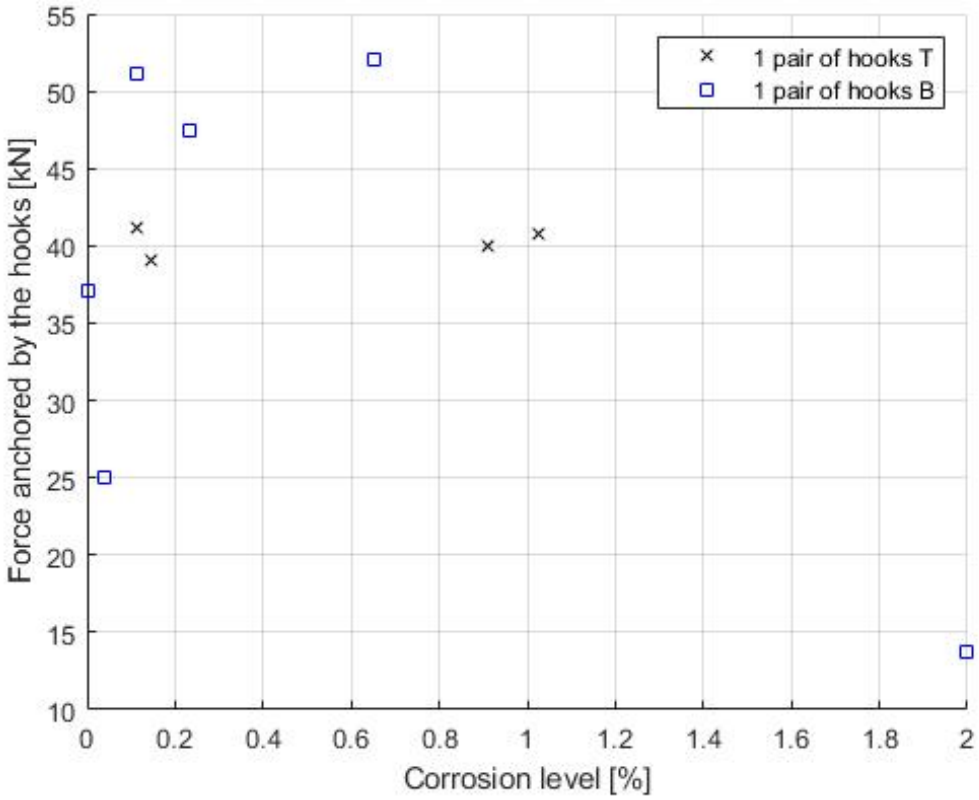

Figure 4.18: Force anchored by the hooks versus the casting positions; for beams with one pair of hooks

4.5 Comparison of anchorage strength calculated by design provisions

The relation between the force anchored by the hooks and the assumed bond stress was evaluated in Section 4.4.1. Based on the assumed bond stress, the force anchored

by the hooks was determined for each reinforcement bar. By comparing the forces anchored by the hooks in the experiments with the design strength of the hooks, the differences between them could be evaluated.

Two formulas in different codes were introduced in Section 3.6 to evaluate design strength of the hooks. The code results of the design anchorage strength for the hooks and the calculated forces anchored by the hooks in the experiments are shown in Table 4.2.

Reinforcement bar		Force anchored by the hooks [kN]		
		Marques and Jirsa	BBK04	From experiment
Beams with one pair of hooks	1 TI	65.3	49.5	39.1
	1 TO	65.0	49.2	41.1
	1 BI	61.3	48.7	49.1
	1 BO	64.6	49.0	51.1
	18H BI	65.3	49.5	38.4
	18H BO	65.7	49.8	44.3
	19 TI	64.5	48.9	40.0
	19 TO	65.1	49.3	40.7
	19 BI	64.6	49.0	32.4
	19 BO	65.8	49.9	52.8
Beams with two pairs of hooks	10D TI	64.2	48.7	43.3
	10D TO	63.7	48.3	41.2
	10D TI CR	64.2	48.6	36.8
	10D TO CR	62.8	47.5	33.8
	13G TI	63.5	48.1	34.4
	13G TO	62.8	47.5	32.5
	13G TI CR	65.1	49.4	44.5
	13G TO CR	64.2	48.6	41.6
	16K TI	64.8	49.2	36.0
	16K TO	65.1	49.4	39.8
	16K TI CR	64.7	49.1	40.2
	16K O CR	64.9	49.2	39.2

Table 4.2: Theoretical design strength of hook for each bar by Marques and Jirsa formula and the formula in Swedish Handbook BBK 04. The third column is the experimentally obtained anchorage force by assuming bond stress in the unyielded zone equal to 1 MPa.

The Swedish formula showed a more conservative result. The American formula showed a higher anchorage strength. Through comparison between the yield force and the design strength of the hooks, the design strength of the hooks calculated by BBK 04 indicated that the force carried by the hooks was smaller, but close to the yield force. Therefore, the yielding at the hook section would theoretically be triggered after anchorage failure. However, the yielding at the hook section was observed on some bars, but the anchorage failure was not. With this in mind, the design strength of the hooks calculated by formula of Marques and Jirsa was closer

to the actual situation.

In Figure 4.19, for one example, the calculated force anchored by the hook of reinforcement bar 10D TI was lower than the design hook strength obtained by Marques and Jirsa's formula and by formula in BBK 04.

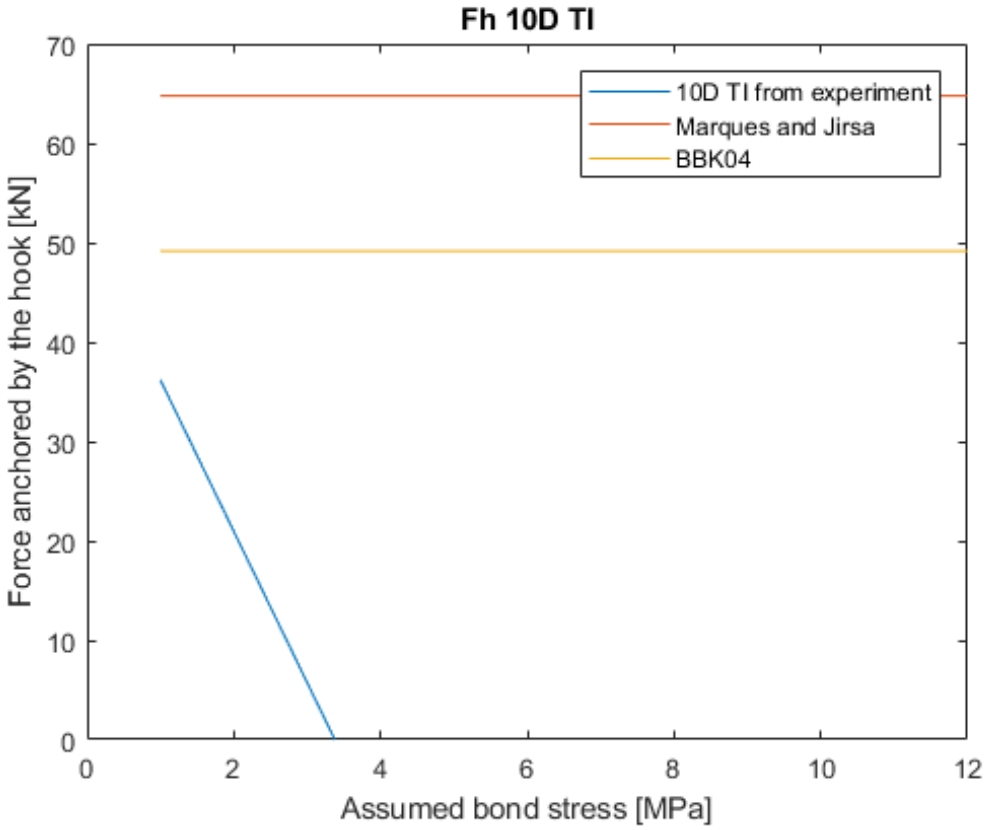

Figure 4.19: Force anchored by the hook versus the assumed bond stress; for top inner reinforcement bar in Beam 10D

Most of the relationship between the assumed bond stress and the anchorage strength of the hooks in the beams with one pair of hooks intersected with the results calculated by the formula in BBK 04 which means that if the bond stress was smaller than that at intersection point, the design anchorage strength of the hook by BBK 04 would be smaller than the force anchored by the hooks in the experiments. However, it was still less than the results obtained by Marques and Jirsa formula. Since there was a combination of anchorage by bond and by the hook in the beams, the contribution from the bond would more or less relieve a part of the force in the hook. The force calculated by the formula of Marques and Jirsa was in fact larger than the one evaluated from experiments for all reinforcement bars, even when it was assumed that the whole force was carried by the hooks (assuming the bond stress equal to zero). The bond stress of reinforcement bars 1 BO, 18H BO, and 19 BO were negligible due to the severe yielding of the bars, as shown in Figure 4.20 and Figure 4.21. Therefore, the force anchored by the hooks in the experiments was

equal to the yield force itself. As shown in Figure 4.20, reinforcement 1 BO was a unique case. The hook was partially yielded. Thus, the contribution of the bond from the straight part was negligible.

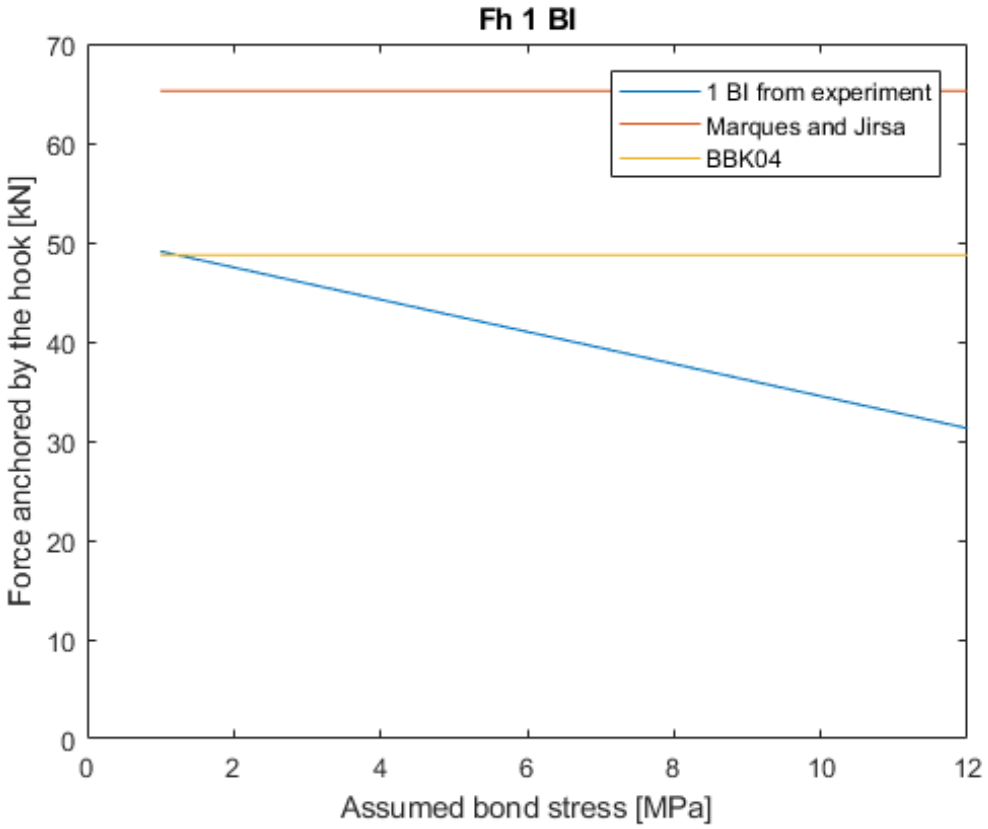

Figure 4.20: Force anchored by the hook versus assumed bond stress; for bottom inner reinforcement bar in Beam 1. Result of BBK 04 and calculated relation intersected at 1.14 MPa bond stress.

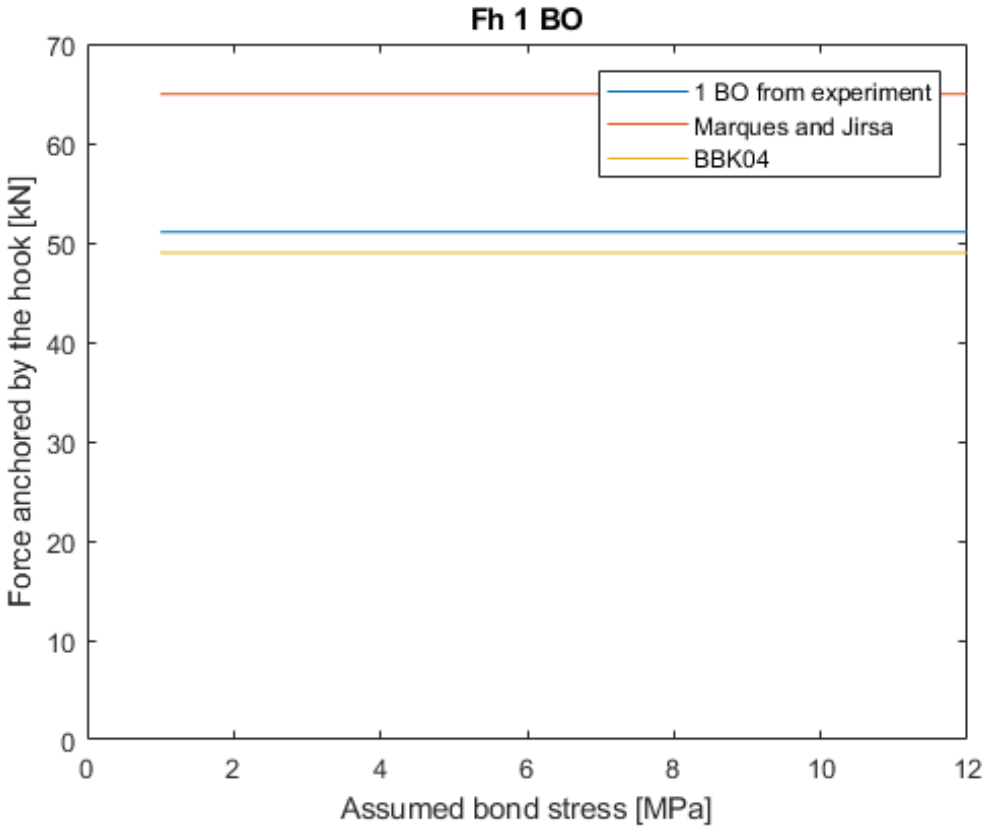

Figure 4.21: Force anchored by the hook versus assumed bond stress; for bottom outer reinforcement bar in Beam 1. Due to the large yield penetration, the effect of assumed bond stress was very small.

5

Conclusion and recommendations for further studies

This chapter answers the research questions, summarizes, and reflects on the research. Further, the suggestions for future research are also made.

5.1 Conclusion

This thesis was based on three-point bending tests which were conducted on edge beams from Gullspång bridge. The aim was to acquire knowledge on the structural behavior of end hook anchorage in naturally corroded reinforced concrete structures with plain reinforcement bars. This was done with a series of data processing and data analysis by utilizing different engineering softwares. The data had been collected by DIC measurements and thus contributed to gain a better understanding of structural behavior of the beams.

From this study, the following was observed:

- The failure of the beams with one pair of hooks was due to the bending moment, while the major cracks were positioned in the middle of the span. The failure of the beams with two pairs of hooks was due to the shear force, while the major cracks were positioned in vicinity of the right support.
- The beams with one pair of hooks only displayed bending cracks and failed in bending.
- The beams with two pairs of hooks displayed both bending and shear cracks, and failed in shear.
- The beams with one pair of hooks showed a more ductile behavior than the beams with two pairs of hooks. However, the beams with two pairs of hooks showed a larger load-carrying capacity.
- None of the hooks failed during the tests.
- Of twenty-two reinforcement bars involved in the experiments, the bending deformation of the end hooks of eighteen reinforcement bars was relatively minor, and only four of the bars with end hooks were observed to have significant deformation. Only the hooks of reinforcement bars 1 BO and 19 BO carried the yield force, with the hook of 1 BO being visibly deformed.

- Pitting corrosion was the main type of corrosion.

From this study, the following conclusions can be drawn:

- Compared to the beams with one pair of hooks, the beams with two pairs of hooks could carry larger applied load because they had two more reinforcement bars both at the top and the bottom layers.
- The corrosion level of the reinforcement bars presented scattered results, with the average corrosion level ranging from 0-2%. The scattering results might be due to the stochastic nature of the natural corrosion process.
- Nine bars from the beams with one pair of hooks and seven bars from the beams with two pairs of hooks were observed to yield. The bond stress in the yielded zone varied mainly between 0 MPa and 4.5 MPa. The yield penetration of reinforcement bars in the beams with one pairs of hooks was generally longer than the beams with two pairs of hooks. Thus, the reinforcement bars in the beams with one pair of hooks were more utilized than the beams with two pairs of the hooks.
- The range of variation in the magnitude of the force anchored by the hooks was very close in both types of beams. But in further comparison, the hooks in the beams with one pair of hooks managed to carry the yield force in some cases, while for the beams with two pair of hooks, the shear failure limited the deformation capacity of the beams.
- At the assumed bond stress 1 MPa in the unyielded zone, the force anchored by the hooks during the tests for most of the reinforcement bars was less than the design anchorage strength according to the codes. The calculated force anchored by the hooks during the tests was on average 84% and 64% of the code results according to the BBK04 formula and Marques and Jirsa formula respectively. The formula of BBK04 was more conservative. The formula of Marques and Jirsa was more close to the actual situation.
- None of the reinforcement bars was observed to have anchorage failure, while the hooks were yielded in some cases. The anchorage strength was thus larger than the yield strength, in agreement with the codes.

5.2 Recommendations for further studies

The following is suggested for further research:

- Adequate beams could be selected to further investigate the relationship between the corrosion level of reinforcement bars and the force anchored by the hooks.
- The shear contribution of hooks in concrete is interesting to investigate further. For future study, more tests on beams with two pairs of hooks was recommended to detect the hooks effect on shear capacity.
- Plain reinforcement bars with end-hooks could be analyzed using FE modeling.

References

[1] Ali Ajaam and Matthew O Reilly. "ANCHORAGE STRENGTH OF REINFORCING BARS By". In: 125 (2017).

[2] Brian Bell and Network Rail. "European railway bridge demography". In: *European FP* 6 (2004).

[3] Boverket. "Boverkets handbok om betongkonstruktioner, BBK 04". In: *Bbk_04* (2004), p. 273.

[4] J. Cairns, Y. Du, and D. Law. "Residual bond strength of corroded plain round bars". In: *Magazine of Concrete Research* 58.4 (2006), pp. 221–231. ISSN: 00249831. DOI: 10.1680/macr.2006.58.4.221.

[5] John Cairns and Lisa Feldman. "Strength of laps and anchorages of plain surface bars". In: *Structural Concrete* 19.6 (2018), pp. 1782–1791. ISSN: 17517648. DOI: 10.1002/suco.201700242.

[6] CEB-FIP (2013). *fib Model Code for Concrete Structures 2010.* ISBN: 9783433030615.

[7] Giovanni Fabbrocino, GM Verderame, and G Manfredi. "Experimental behaviour of straight and hooked smooth bars in existing RC buildings". In: *Proceedings of 12th European Conference on Earthquake Engineering, London, UK*. 2002.

[8] Giovanni Fabbrocino et al. "Experimental response and behavioral modelling of anchored smooth bars in existing RC frames". In: *Bond in Concrete - from research to standards* (2002).

[9] Giovanni Fabbrocino et al. "Structural models of critical regions in old-type r.c. frames with smooth rebars". In: *Engineering Structures* 26.14 (2004), pp. 2137–2148. ISSN: 01410296. DOI: 10.1016/j.engstruct.2004.07.018.

[10] Congqi Fang et al. "Bond behaviour of corroded reinforcing steel bars in concrete". In: *Cement and concrete research* 36.10 (2006), pp. 1931–1938.

[11] Congqi Fang et al. "Corrosion influence on bond in reinforced concrete". In: *Cement and concrete research* 34.11 (2004), pp. 2159–2167.

[12] Congqi Fang et al. "Effect of corrosion on bond in reinforced concrete under cyclic loading". In: *Cement and Concrete Research* 36.3 (2006), pp. 548–555.

[13] Ignasi Fernandez, Karin Lundgren, and Kamyab Zandi. "Evaluation of corrosion level of naturally corroded bars using different cleaning methods, computed tomography, and 3D optical scanning". In: *Materials and Structures/-Materiaux et Constructions* 51.3 (2018), pp. 1–13. ISSN: 13595997. DOI: 10.1617/s11527-018-1206-z. URL: https://doi.org/10.1617/s11527-018-1206-z.

[14] "H E U R O P E a N N I O N". In: 1.2005 (2011).

[15] K. Lundgren. “Bond between ribbed bars and concrete. Part 1: Modified model”. In: *Magazine of Concrete Research* 57.7 (2005), pp. 371–382. ISSN: 00249831. DOI: 10.1680/macr.2005.57.7.371.

[16] K. Lundgren. “Bond between ribbed bars and concrete. Part 2: The effect of corrosion”. In: *Magazine of Concrete Research* 57.7 (2005), pp. 383–395. ISSN: 00249831. DOI: 10.1680/macr.2005.57.7.383.

[17] K. Lundgren. “Effect of corrosion on the bond between steel and concrete: An overview”. In: *Magazine of Concrete Research* 59.6 (2007), pp. 447–461. ISSN: 00249831. DOI: 10.1680/macr.2007.59.6.447.

[18] Jesper Olsson and Samanta Robuschi. “Provningsmetoder/ Genomförande”. In: 1002 (2018).

[19] Samanta Robuschi et al. “Anchorage of naturally corroded, plain reinforcement bars in flexural members”. In: *Materials and Structures/Materiaux et Constructions* 53.2 (2020). ISSN: 13595997. DOI: 10.1617/s11527-020-01471-2. URL: https://doi.org/10.1617/s11527-020-01471-2.

[20] Irina Sæther. “Bond deterioration of corroded steel bars in concrete”. In: *Structure and Infrastructure Engineering* 7.6 (2011), pp. 415–429. ISSN: 15732479. DOI: 10.1080/15732470802674836.

[21] Sarah J Williamson and Leslie A Clark. “Effect of corrosion and load on reinforcement bond strength”. In: *Structural engineering international* 12.2 (2002), pp. 117–122.

[22] Yuan-Zhou Wu et al. “Degradation model of bond performance between deteriorated concrete and corroded deformed steel bars”. In: *Construction and Building Materials* 119 (2016), pp. 89–95.

[23] Hakan Yalciner, Ozgur Eren, and Serhan Sensoy. “An experimental study on the bond strength between reinforcement bars and concrete as a function of concrete cover, strength and corrosion level”. In: *Cement and Concrete Research* 42.5 (2012), pp. 643–655.

[24] Xiaotong Yu et al. “Numerical assessment of bond-slip relationships for naturally corroded plain reinforcement bars in concrete beams”. In: *Engineering Structures* 239.April (2021), p. 112309. ISSN: 18737323. DOI: 10.1016/j.engstruct.2021.112309. URL: https://doi.org/10.1016/j.engstruct.2021.112309.

A

Appendix

A.1 Corrosion level and yield penetration

```
% The main corrosion analysis document
% Analysis of the corrosion level of plain bars

% Function that loads the .txt data containing the point
    cloud

% Insert the point cloud file as txt in the current
    directory. Substitute
% bar1 with the name of your file.

ScanFile = '1 BO 2of2.asc';


sd = getData_scanFile(ScanFile); % X Y Z and rho and theta
    in Polar coordinate

% Outputs a variable with the cohordinates of the points,
    both in a XYZ
% plan and in polar cohordinates (theta, rho)

% This is to remove noise along the length of the bar
[bar] = fromScan_filterAlongLength(sd, ScanFile);

%Get geometrical and corrosion info
[bar] = fromScan_createFit(bar);

[bar] = extract_polysection_data(bar);

save('1 BO 2of2.mat','bar')

%% plot

Z = bar.mesh.Z;
```

```
for i = 1:length(Z)
    area(i) = bar.mesh.geometry(i).area;
    perimeter(i) = bar.mesh.geometry(i).perimeter;
end
[AX,H1,H2] = plotyy(Z,area,Z,perimeter)

xlabel('bar length Z')
set(gca,'FontSize',12);
set(get(gca,'xlabel'),'string','Bar length Z');
set(get(AX(1),'Ylabel'),'string','Area');
set(get(AX(2),'Ylabel'),'string','Perimeter');
set(H1,'color','b');
set(H2,'color','r');
title('Yielding penetration');
legend('Area','Perimeter');

figure
An_orig = zeros(length(area),1);
for j = 1:length(An_orig)
    An_orig(j) = 16^2*pi()/4;
end
plot(Z,area,Z,An_orig)
```

```
function [bar] = fromScan_createFit(bar)
% This function takes input 'bar' as class 'rebar'
% Operation extracts [filtered] scan data and conducts a transformation
% process on the cloud point scatter to best-fit align with 1) the global
% i,j,k coordinate system and also with the long-axis of the scanned rebar
% aligned with the global 'z' axis.

% Note:
% Alignment is currently defined by a best-fit axis designed to track
% the centroid x,y positions of individual "slices" along the rebar. As the
% centroid x,y positions are relative to the poly_shape area, this best-fit
% process is not 'exact' for any single section.


    % Scan data
    filter_condition = bar.scan.filter_condition;
    X = bar.scan.X(filter_condition);
```

```
18      Y = bar.scan.Y(filter_condition);
19      Z = bar.scan.Z(filter_condition);
20      theta = bar.scan.theta(filter_condition);
21      rho = bar.scan.rho(filter_condition);
22
23  %     % Check plot
24  %      figure;
25  %      hold on;
26  %      scatter3(bar.scan.X(bar.scan.filter_condition),bar.
        scan.Y(bar.scan.filter_condition),bar.scan.Z(bar.scan.
        filter_condition),'.');
27  %      scatter3(bar.scan.X(~bar.scan.filter_condition),bar.
        scan.Y(~bar.scan.filter_condition),bar.scan.Z(~bar.scan.
        filter_condition),'.');
28
29      % Set 'Z' to origin
30      Z = Z - min(Z);
31
32      % Establish preliminary geometry
33      % Creates 3D mesh with interpolate
34      % Compacts poly_shape data into 'geometry'
35      [geometry,zz,~,~] = create_meshgrid_polyshape(Z,theta,
            rho);
36
37      % Collect spread of x,y centroid to re-orient the cloud
            point data
38      xbar = [geometry.xbar]';
39      ybar = [geometry.ybar]';
40      centroid_scatter = [xbar,ybar,zz'];
41
42      % Fit a 1st order (in x and y) plane to the x,y centroid
            scatter
43      % Plane equation: z = d+ax+by
44      f = fit([centroid_scatter(:,1),centroid_scatter(:,2)],
            centroid_scatter(:,3), 'poly11' );
45      c = 1;
46      d = f.p00;
47      a = f.p10;
48      b = f.p01;
49      plane_eq = @(x,y) d + a*x + b*y;
50
51      % Project x,y centroid scatter onto the best-fit plane
52      % Plane equation d = ax+by+cz, to project points xyz
            onto the plane
53      % https://www.mathworks.com/matlabcentral/answers/
            uploaded_files/124894/projection.m
```

```
54      a = -a;
55      b = -b;
56      c = -(-c);
57      d = -(-d);
58
59      M = [1 0 0 -a; 0 1 0 -b; 0 0 1 -c; a b c 0];
60      point_array = [centroid_scatter,ones(size(
            centroid_scatter,1),1) .* d];
61      proj_points = M \ point_array';
62      proj_points = proj_points(1:3,:)';
63
64      % Define the coordinate system of the best-fit plane (
            with basis of global axes)
65      % Goal is to define the plane local coordinate system on
             which lay the
66      % x,y centroid scatter.
67      % Then to transform all points on the "Frame" (key word
            for this
68      % operation) to the i,j,k global coordinate system so as
             to yield a
69      % scatter in 2D (because points are projected onto the
            plane as 2D in space)
70
71      % Two points on plane
72      Q0 = [0, 0, plane_eq(0,0)]; % Intersect w/ z-axis
73      Q1 = [15, 15, plane_eq(15,15)]; % Arbitrary, selected "x
            ,y = 15"
74
75      u1 = Q1-Q0; % in-plane vector
76      u3 = [a, b, c]; % normal-to-plane vector
77      u2 = cross(u1,u3); % resulting vector from cross-product
78
79      u1 = u1 / norm(u1);
80      u2 = u2 / norm(u2);
81      u3 = u3 / norm(u3);
82
83      % Establish the transformation matrix for points based
            on "frame transformations"
84      % https://www.uio.no/studier/emner/matnat/ifi/nedlagte-
            emner/INF3320/h03/undervisningsmateriale/lecture3.pdf
85      M = [u1,0; u2,0; u3,0; Q0,1];
86      point_array = [proj_points,ones(size(centroid_scatter,1)
            ,1)];
87      trsf_points = M' \ point_array';
88      trsf_points = trsf_points(1:3,:)';
89
```

```
90      % Having transformed the projected x,y centroid scatter
            from the space
91      % plane to the i,j,k global coordinates... results
            should be 'roughly'
92      % 2D scatter.
93      % Fit this data with a linear regression to find the
            best-fit trend
94      xx = trsf_points(:,1);
95      yy = trsf_points(:,2);
96      p = polyfit(xx,yy,1);
97      f1 = polyval(p,trsf_points(:,1));
98
99      % Collect start and end points of this best-fit line
100     line_eq = @(x) p(1)*x + p(2);
101     idx1 = 1;
102     idx2 = length(f1);
103     centroid_best_fit(1,:) = [trsf_points(idx1,1),line_eq(
            trsf_points(idx1,1)),trsf_points(idx1,3)];
104     centroid_best_fit(2,:) = [trsf_points(idx2,1),line_eq(
            trsf_points(idx2,1)),trsf_points(idx2,3)];
105
106     % Reverse transform (two) points defining the best-fit
            relationship
107     % between projected x,y centroid scatter. This results
            in a linear
108     % best-fit of 3D scatter data on the space plane
109     point_array = [centroid_best_fit,ones(size(
            centroid_best_fit,1),1)];
110     centroid_best_fit = M' * point_array';
111     centroid_best_fit = centroid_best_fit(1:3,:)';
112
113 %     figure;
114 %     plot(f, [centroid_scatter(:,1),centroid_scatter(:,2)],
    centroid_scatter(:,3));
115 %     hold on;
116 %     pause(1)
117 %     scatter3(proj_points(:,1),proj_points(:,2),proj_points
    (:,3),'r')
118 %     plot3(centroid_best_fit(:,1),centroid_best_fit(:,2),
    centroid_best_fit(:,3),'k','Marker','*','LineWidth',2)
119 %     xlabel('X')
120 %     ylabel('Y')
121 %     zlabel('Z')
122
123     %%
124     % Now for the more complicated math operations
```

```
125     %%
126
127     % Thus far we have created a best-fit, linear trend line
            for 3D scatter
128     % 1) We need to move this line so that it passes through
            the origin
129     % 2) We need to rotate the best-fit line onto the xz
            plane. This will yield the angle to
130     % construct a rotational transformation of the point
            cloud data
131     % 3) We need to rotate the best-fit line to align with
            the x-axis. This will yield another angle to
132     % construct a rotational transformation of the point
            cloud data
133
134     % [#1] Translate to origin
135     % Shift best-fit line and point cloud data by the
            position of the first
136     % coordinate of the best-fit line (so that best-fit line
            is moved to the global origin: [0,0,0])
137
138     new_centroid_best_fit = centroid_best_fit - repmat(
            centroid_best_fit(1,:),2,1);
139     vector = new_centroid_best_fit(2,:) -
            new_centroid_best_fit(1,:);
140     new_points = [X,Y,Z] - repmat(centroid_best_fit(1,:),
            length(X),1);
141
142     % For record keeping...
143     pullout_angle = acos(dot(vector,[0,0,1])/(norm(vector)))
            ;
144
145     % [#2] Rotate to XZ plane (rotation is about z-axis)
146     % Project the best-fit vector to the xy plane and find
            the angle to the
147     % 'x' axis defined by i = [1,0,0]
148
149     v_xy = [vector(1),vector(2),0];
150     ang_to_xz = acos(dot(v_xy,[1,0,0])/(norm(v_xy)));
151
152     % Angle management. Differs based on y-coordinate of
            projected xy
153     % vector. This was hand-calced for all (4) quadrants.
            Goal to get angle
154     % sign resulting into rotation to (+) 'x' axis
            consistently.
```

```
155     switch sign(v_xy(2))
156         case 1
157             ang = -ang_to_xz;
158         case -1
159             ang = ang_to_xz;
160         otherwise
161             error('Something went wrong with vector v_xy.');
162     end
163
164     Rz = [cos(ang) -sin(ang) 0 0;
165           sin(ang) cos(ang) 0 0;
166           0 0 1 0;
167           0 0 0 1];
168
169     rotated_to_xz = Rz * [new_centroid_best_fit,ones(2,1)]';
170     vector = rotated_to_xz(1:3,:)';
171
172     rotated_to_xz = Rz * [new_points,ones(length(X),1)]';
173     new_points = rotated_to_xz(1:3,:)';
174
175     % [#3] Rotate to Z axis (rotation is about y-axis)
176     % Take the rotated xz plane vector (originally the
            projected best-fit on the xy plane)
177     % and calculate the angle to the 'z' axis defined by k =
            [0,0,1].
178     % Purpose is that this vector describes the best-fit
            centroid data.
179     % This operation will align the centroid on the global '
            Z' axis...
180     % centering the data.
181
182     v_xz = vector(2,:);
183     ang_to_zaxis = acos(dot(v_xz,[0,0,1])/(norm(v_xz)));
184
185     % Angle management. Differs based on y-coordinate of
            projected xy
186     % vector. This was hand-calced for all (4) quadrants.
            Goal to get angle
187     % sign resulting into rotation to (+) 'x' axis
            consistently.
188     switch sign(v_xz(1))
189         case 1
190             ang = -ang_to_zaxis;
191         case -1
192             ang = ang_to_zaxis;
193         otherwise
```

```
194             error('Something went wrong with vector v_xz.');
195     end
196
197     Ry = [cos(ang) 0 sin(ang) 0;
198           0 1 0 0;
199           -sin(ang) 0 cos(ang) 0;
200           0 0 0 1];
201
202     aligned_to_z = Ry * [vector,ones(2,1)]';
203     vector = aligned_to_z(1:3,:)';
204
205     aligned_to_z = Ry * [new_points,ones(length(X),1)]';
206     new_points = aligned_to_z(1:3,:)';
207
208     X = new_points(:,1);
209     Y = new_points(:,2);
210     Z = new_points(:,3);
211     [theta,rho] = cart2pol(X,Y);
212
213     % Set 'Z' to origin
214     Z = Z - min(Z);
215
216     % Establish secondary geometry
217     % Creates 3D mesh with interpolate
218     % Compacts poly_shape data into 'geometry'
219     [geometry,zz,TT,RR] = create_meshgrid_polyshape(Z,theta,
            rho);
220
221     %
222     % Hard-code in a filter against 'bad data'
223     % Based on diviation from circular
224     % |
225     % |
226     % v
227
228     A = [geometry.area];
229     P = [geometry.perimeter];
230
231     d_fromA = sqrt((4/pi) .* A);
232     d_fromP = P ./ pi;
233     circ = d_fromA ./ d_fromP;
234     condition = circ > 0.8 & circ < 1.20;
235
236     % ^
237     % |
238     % |
```

```
239     % Hard-code in a filter against 'bad data'
240     % Based on diviation from circular
241     %
242
243     % Add all data to 'bar' class
244     bar.mesh.Z = zz(condition);
245     bar.mesh.theta = TT(:,condition);
246     bar.mesh.rho = RR(:,condition);
247     bar.mesh.geometry = geometry(condition);
248
249     % Add all data to 'bar' class
250     bar.rotated.X = X;
251     bar.rotated.Y = Y;
252     bar.rotated.Z = Z;
253     bar.rotated.theta = theta;
254     bar.rotated.rho = rho;
255     bar.rotated.angle_pullout_vs_zaxis = abs(pullout_angle)
          * 180/pi; % angle in [deg]
256 end
```

```
1  function [sd] = getData_scanFile(scanFile)
2  % This function acts to strip 3D scan data as acquired from
       experimental testing
3  % 'scan' file is to be input as '.txt' file in current
       directory
4
5      % Gather scan data and sort
6      % Make sure to orient local and global coordinate axes
           in
7      % program -> export .txt file
8      xyz = load(scanFile);
9      X = xyz(:,1);   % points to top of cross-section
10     Y = xyz(:,2);   % arbitrary
11     Z = xyz(:,3);   % long axis
12
13     % Sort/re-order
14     [~,idx] = sort(Z);
15     X = X(idx);
16     Y = Y(idx);
17     Z = Z(idx);
18     [theta,rho] = cart2pol(X,Y);
19
20     % Add all data to 'rebar' class
21     sd.X = X;
22     sd.Y = Y;
23     sd.Z = Z;
```

```
    sd.theta = theta;
    sd.rho = rho;
end
```

```
function hfig = tightfig(hfig)
% tightfig: Alters a figure so that it has the minimum size necessary to
% enclose all axes in the figure without excess space around them.
%
% Note that tightfig will expand the figure to completely encompass all
% axes if necessary. If any 3D axes are present which have been zoomed,
% tightfig will produce an error, as these cannot easily be dealt with.
%
% Input
%
% hfig - handle to figure, if not supplied, the current figure will be used
%   instead.
%
%


    if nargin == 0
        hfig = gcf;
    end

    % There can be an issue with tightfig when the user has been modifying
    % the contnts manually, the code below is an attempt to resolve this,
    % but it has not yet been satisfactorily fixed
%     origwindowstyle = get(hfig, 'WindowStyle');
    set(hfig, 'WindowStyle', 'normal');

    % 1 point is 0.3528 mm for future use

    % get all the axes handles note this will also fetch legends and
    % colorbars as well
    hax = findall(hfig, 'type', 'axes');
    % TODO: fix for modern matlab, colorbars and legends are no longer axes
    hcbar = findall(hfig, 'type', 'colorbar');
```

```
33      hleg = findall(hfig, 'type', 'legend');
34
35      % get the original axes units, so we can change and
            reset these again
36      % later
37      origaxunits = get(hax, 'Units');
38
39      % change the axes units to cm
40      set(hax, 'Units', 'centimeters');
41
42      pos = [];
43      ti = [];
44
45      % get various position parameters of the axes
46      if numel(hax) > 1
47  %         fsize = cell2mat(get(hax, 'FontSize'));
48          ti = cell2mat(get(hax,'TightInset'));
49          pos = [pos; cell2mat(get(hax, 'Position')) ];
50      else
51  %         fsize = get(hax, 'FontSize');
52          ti = get(hax,'TightInset');
53          pos = [pos; get(hax, 'Position') ];
54      end
55
56      if ~isempty (hcbar)
57
58          set(hcbar, 'Units', 'centimeters');
59
60          % colorbars do not have tightinset property
61          for cbind = 1:numel(hcbar)
62              %         fsize = cell2mat(get(hax, 'FontSize'))
                    ;
63              [cbarpos, cbarti] = colorbarpos (hcbar);
64
65              pos = [pos; cbarpos];
66              ti = [ti; cbarti];
67          end
68      end
69
70      if ~isempty (hleg)
71
72          set(hleg, 'Units', 'centimeters');
73
74          % legends do not have tightinset property
75          if numel(hleg) > 1
76              %         fsize = cell2mat(get(hax, 'FontSize'))
```

```
                ;
77              pos = [pos; cell2mat(get(hleg, 'Position')) ];
78          else
79              %           fsize = get(hax, 'FontSize');
80              pos = [pos; get(hleg, 'Position') ];
81          end
82          ti = [ti; repmat([0,0,0,0], numel(hleg), 1); ];
83      end
84
85      % ensure very tiny border so outer box always appears
86      ti(ti < 0.1) = 0.15;
87
88      % we will check if any 3d axes are zoomed, to do this we
            will check if
89      % they are not being viewed in any of the 2d directions
90      views2d = [0,90; 0,0; 90,0];
91
92      for i = 1:numel(hax)
93
94          set(hax(i), 'LooseInset', ti(i,:));
95  %         set(hax(i), 'LooseInset', [0,0,0,0]);
96
97          % get the current viewing angle of the axes
98          [az,el] = view(hax(i));
99
100         % determine if the axes are zoomed
101         iszoomed = strcmp(get(hax(i), 'CameraViewAngleMode')
                , 'manual');
102
103         % test if we are viewing in 2d mode or a 3d view
104         is2d = all(bsxfun(@eq, [az,el], views2d), 2);
105
106         if iszoomed && ~any(is2d)
107             error('TIGHTFIG:haszoomed3d', 'Cannot make
                    figures containing zoomed 3D axes tight.')
108         end
109
110     end
111
112     % we will move all the axes down and to the left by the
            amount
113     % necessary to just show the bottom and leftmost axes
            and labels etc.
114     moveleft = min(pos(:,1) - ti(:,1));
115
116     movedown = min(pos(:,2) - ti(:,2));
```

```
117
118     % we will also alter the height and width of the figure
            to just
119     % encompass the topmost and rightmost axes and lables
120     figwidth = max(pos(:,1) + pos(:,3) + ti(:,3) - moveleft)
            ;
121
122     figheight = max(pos(:,2) + pos(:,4) + ti(:,4) - movedown
            );
123
124     % move all the axes
125     for i = 1:numel(hax)
126
127         set(hax(i), 'Position', [pos(i,1:2) - [moveleft,
                movedown], pos(i,3:4)]);
128
129     end
130
131     for i = 1:numel(hcbar)
132
133         set(hcbar(i), 'Position', [pos(i+numel(hax),1:2) - [
                moveleft,movedown], pos(i+numel(hax),3:4)]);
134
135     end
136
137     for i = 1:numel(hleg)
138
139         set(hleg(i), 'Position', [pos(i+numel(hax)+numel(
                hcbar),1:2) - [moveleft,movedown], pos(i+numel(
                hax)+numel(hcbar),3:4)]);
140
141     end
142
143     origfigunits = get(hfig, 'Units');
144
145     set(hfig, 'Units', 'centimeters');
146
147     % change the size of the figure
148     figpos = get(hfig, 'Position');
149
150     set(hfig, 'Position', [figpos(1), figpos(2), figwidth,
            figheight]);
151
152     % change the size of the paper
153     set(hfig, 'PaperUnits','centimeters');
154     set(hfig, 'PaperSize', [figwidth, figheight]);
```

```
155     set(hfig, 'PaperPositionMode', 'manual');
156     set(hfig, 'PaperPosition',[0 0 figwidth figheight]);
157 
158     % reset to original units for axes and figure
159     if ~iscell(origaxunits)
160         origaxunits = {origaxunits};
161     end
162 
163     for i = 1:numel(hax)
164         set(hax(i), 'Units', origaxunits{i});
165     end
166 
167     set(hfig, 'Units', origfigunits);
168 
169 %       set(hfig, 'WindowStyle', origwindowstyle);
170 
171 end
172 
173 
174 function [pos, ti] = colorbarpos (hcbar)
175 
176     % 1 point is 0.3528 mm
177 
178     pos = hcbar.Position;
179     ti = [0,0,0,0];
180 
181     if ~isempty (strfind (hcbar.Location, 'outside'))
182 
183         if strcmp (hcbar.AxisLocation, 'out')
184 
185             tlabels = hcbar.TickLabels;
186 
187             fsize = hcbar.FontSize;
188 
189             switch hcbar.Location
190 
191                 case 'northoutside'
192 
193                     % make exta space a little more than the
                            font size/height
194                     ticklablespace_cm = 1.1 * (0.3528/10) *
                        fsize;
195 
196                     ti(4) = ti(4) + ticklablespace_cm;
197 
198                 case 'eastoutside'
```

```
199
200                         maxlabellen = max ( cellfun (@numel,
                                tlabels, 'UniformOutput', true) );
201
202                         % 0.62 factor is arbitrary and added
                                because we don't
203                         % know the width of every character in
                                the label, the
204                         % fsize refers to the height of the font
205                         ticklablespace_cm = (0.3528/10) * fsize
                                * maxlabellen * 0.62;
206
207                         ti(3) = ti(3) + ticklablespace_cm;
208
209                     case 'southoutside'
210
211                         % make exta space a little more than the
                                font size/height
212                         ticklablespace_cm = 1.1 * (0.3528/10) *
                                fsize;
213
214                         ti(2) = ti(2) + ticklablespace_cm;
215
216                     case 'westoutside'
217
218                         maxlabellen = max ( cellfun (@numel,
                                tlabels, 'UniformOutput', true) );
219
220                         % 0.62 factor is arbitrary and added
                                because we don't
221                         % know the width of every character in
                                the label, the
222                         % fsize refers to the height of the font
223                         ticklablespace_cm = (0.3528/10) * fsize
                                * maxlabellen * 0.62;
224
225                         ti(1) = ti(1) + ticklablespace_cm;
226
227                 end
228
229             end
230
231         end
232
233 end
```

```
function [bar] = fromScan_filterAlongLength(sd, ScanFile)
% This function takes input 'bar' as class 'rebar'
% Operation extracts stored scan data and asks the user to
    subjectively filter the cloud point scatter.
% This is performed through use of a GUI.
% 'Filtering' takes the form of a stored binary array with 0
    s and 1s assigned for each data point.
% THIS function assumes 1s at every index, and filtering
    sets which data should be turned from 1 to 0.
% RE-EXECUTION of this function will reset previous
    filtering
% A .pdf file is saved per 'bar' for record keeping.

    % No execution without scan data

    % Inputs
    xlim = [0,500];
    ylim = [-5,20];
    color_scan = [0, 0.4470, 0.7410];
    color_trim = [0.6350, 0.0780, 0.1840];

    % Scan data
    Z = sd.Z;
    rho  = sd.rho;

    bar.scan = sd;

    % Filter scan data (Manual inspection)
    fig = figure('Units','Inches','Position',[1,1,16,8]);
    ax = gca;
    hold on;

    % Add widgets
    c(1) = uicontrol(fig,'Style','slider',...
                     'Tag', 'Move Left',...
                     'Callback', @plot_line,...
                     'Max', max(Z) + 0.1*(max(Z)+min(Z)),...
                     'Value', 0.25*(max(Z)+min(Z)),...
                     'Min', min(Z) - 0.1*(max(Z)+min(Z)),...
                     'SliderStep', [1/200, 1/50], ...
                     'Units', 'Inches',...
                     'Position', [1.0 1.0 2 0.2]);

    c(2) = uicontrol(fig,'Style','text',...
                     'String', 'Horizontal Limit - [Left]'
                        ,...
```

```
42                      'FontWeight', 'Bold',...
43                      'BackgroundColor', 'w',...
44                      'Units', 'Inches',...
45                      'Position', [1.0 1.25 2.0 0.2]);
46
47      c(3) = uicontrol(fig,'Style','slider',...
48                      'Tag', 'Move Right',...
49                      'Callback', @plot_line,...
50                      'Max', max(Z) + 0.1*(max(Z)+min(Z)),...
51                      'Value', 0.75*(max(Z)+min(Z)),...
52                      'Min', min(Z) - 0.1*(max(Z)+min(Z)),...
53                      'SliderStep', [1/200, 1/50], ...
54                      'Units', 'Inches',...
55                      'Position', [1.0 1.75 2 0.2]);
56
57      c(4) = uicontrol(fig,'Style','text',...
58                      'String', 'Horizontal Limit - [Right]'
                            ,...
59                      'FontWeight', 'Bold',...
60                      'BackgroundColor', 'w',...
61                      'Units', 'Inches',...
62                      'Position', [1.0 2.0 2 0.2]);
63
64      c(5) = uicontrol(fig,'Style','slider',...
65                      'Tag', 'Move Down',...
66                      'Callback', @plot_line,...
67                      'Max', max(rho) + 0.5*(max(rho)+min(rho
                            )),...
68                      'Value', 0.25*(max(rho)+min(rho)),...
69                      'Min', min(rho) - 0.5*(max(rho)+min(rho
                            )),...
70                      'SliderStep', [1/200, 1/50], ...
71                      'Units', 'Inches',...
72                      'Position', [3.5 1.0 2 0.2]);
73
74      c(6) = uicontrol(fig,'Style','text',...
75                      'String', 'Vertical Limit - [Bottom]'
                            ,...
76                      'FontWeight', 'Bold',...
77                      'BackgroundColor', 'w',...
78                      'Units', 'Inches',...
79                      'Position', [3.5 1.25 2 0.2]);
80
81      c(7) = uicontrol(fig,'Style','slider',...
82                      'Tag', 'Move Up',...
83                      'Callback', @plot_line,...
```

```
84                      'Max', max(rho) + 0.5*(max(rho)+min(rho
                            )),...
85                      'Value', 0.75*(max(rho)+min(rho)),...
86                      'Min', min(rho) - 0.5*(max(rho)+min(rho
                            )),...
87                      'SliderStep', [1/200, 1/50], ...
88                      'Units', 'Inches',...
89                      'Position', [3.50 1.75 2 0.2]);
90
91      c(8) = uicontrol(fig,'Style','text',...
92                      'String', 'Vertical Limit - [Top]',...
93                      'FontWeight', 'Bold',...
94                      'BackgroundColor', 'w',...
95                      'Units', 'Inches',...
96                      'Position', [3.50 2.0 2 0.2]);
97
98      c(9) = uicontrol(fig,'Style','pushbutton',...
99                      'String', 'Done',...
100                     'Callback', @plot_done,...
101                     'FontWeight', 'Bold',...
102                     'ForegroundColor', 'k',...
103                     'Units', 'Inches',...
104                     'Position', [6 1 0.75 0.4]);
105
106     % Plot reference text
107     name = strsplit(ScanFile,'.');
108     bar.ID = name;
109     text(20,19,'For match reference:');
110     text(20,18,['Rebar ID: ',name{1}]);
111
112     % Plot boundary lines
113     val_hL = c(1).Value;
114     val_hR = c(3).Value;
115     val_vB = c(5).Value;
116     val_vT = c(7).Value;
117
118     condition_zz = Z <= val_hL | Z >= val_hR;
119     condition_rr = rho <= val_vB | rho >= val_vT;
120     condition = condition_zz | condition_rr;
121
122     plot([val_hL,val_hL],ylim,'k','LineWidth',1,'Tag','
            Horizontal Limit - [Left]');
123     plot([val_hR,val_hR],ylim,'k','LineWidth',1,'Tag','
            Horizontal Limit - [Right]');
124     plot(xlim,[val_vB,val_vB],'k','LineWidth',1,'Tag','
            Vertical Limit - [Bottom]');
```

```
125     plot(xlim,[val_vT,val_vT],'k','LineWidth',1,'Tag','
            Vertical Limit - [Top]');
126
127     % Plot point cloud
128     ss(1) = scatter(Z(~condition),rho(~condition),'.');
129     ss(1).MarkerEdgeColor = color_scan;
130     ss(1).Tag = 'Point Cloud';
131
132     % Plot filtered
133     ss(2) = scatter(Z(condition),rho(condition),'.');
134     ss(2).MarkerEdgeColor = color_trim;
135     ss(2).Tag = 'Filtered Points';
136
137     % Adjustments
138     set(ax,'XLim',xlim);
139     set(ax,'YLim',ylim);
140     set(ax.XLabel,'String','Bar Length [mm]');
141     set(ax.YLabel,'String','Bar Radius, \rho [mm]');
142     tightfig(fig);
143
144     % Pack in main fig information for transfer
145     fig.UserData = condition;
146     [c.UserData] = deal({Z,rho});
147
148     % This wait control gives time and control to GUI
149     uiwait(fig);
150
151     % Extract information from GUI
152     condition = fig.UserData;
153
154     % Flip to 'keep' rather than 'remove'
155     condition = ~condition;
156
157 %     % Check plot
158 %     figure;
159 %     hold on;
160 %     scatter(Z(condition),rho(condition),'.','
        MarkerEdgeColor',color_scan);
161 %     scatter(Z(~condition),rho(~condition),'.','
        MarkerEdgeColor',color_trim);
162
163     % Add filter condition to 'rebar' class
164     bar.scan.filter_condition = condition;
165
166     % The goal is to keep the raw data, but also to have
            logic in place so
```

```
167     % that we only analyze points within the 'filtered' zone
            . This is done
168     % with binary indexing to which [1] = "yes, keep" and
            [0] = "no, filter
169     % out". BUT keep all data, for record keeping and memory
            and reuse, whatever.
170
171     close(fig)
172 end
173
174 % Slider call-back
175 function plot_line(source,~)
176
177     fig = source.Parent;
178     val = source.Value;
179     tag = source.Tag;
180     ax = fig.CurrentAxes;
181
182     Z = source.UserData{1};
183     rho = source.UserData{2};
184
185     line_hL = findobj(fig,'Tag','Horizontal Limit - [Left]')
            ;
186     line_hR = findobj(fig,'Tag','Horizontal Limit - [Right]'
            );
187     line_vB = findobj(fig,'Tag','Vertical Limit - [Bottom]')
            ;
188     line_vT = findobj(fig,'Tag','Vertical Limit - [Top]');
189
190     move_left = findobj(fig,'Tag','Move Left');
191     move_right = findobj(fig,'Tag','Move Right');
192     move_down = findobj(fig,'Tag','Move Down');
193     move_up = findobj(fig,'Tag','Move Up');
194
195     h1 = findobj(fig,'Tag','Point Cloud');
196     h2 = findobj(fig,'Tag','Filtered Points');
197
198     switch tag
199         case 'Move Left'
200
201             val_hL = val;
202             val_hR = move_right.Value;
203             val_vB = move_down.Value;
204             val_vT = move_up.Value;
205
206         case 'Move Right'
```

```
207             val_hL = move_left.Value;
208             val_hR = val;
209             val_vB = move_down.Value;
210             val_vT = move_up.Value;
211
212         case 'Move Down'
213             val_hL = move_left.Value;
214             val_hR = move_right.Value;
215             val_vB = val;
216             val_vT = move_up.Value;
217
218         case 'Move Up'
219             val_hL = move_left.Value;
220             val_hR = move_right.Value;
221             val_vB = move_down.Value;
222             val_vT = val;
223
224         otherwise
225             error(['Unacceptable slider tag: ',source.Tag])
226     end
227
228     % Re-draw lines
229     xx = ax.XLim;
230     yy = ax.YLim;
231
232     line_hL.XData = [val_hL,val_hL];
233     line_hL.YData = yy;
234
235     line_hR.XData = [val_hR,val_hR];
236     line_hR.YData = yy;
237
238     line_vB.XData = xx;
239     line_vB.YData = [val_vB,val_vB];
240
241     line_vT.XData = xx;
242     line_vT.YData = [val_vT,val_vT];
243
244     % Impose filter within lines
245     condition_zz = Z <= val_hL | Z >= val_hR;
246     condition_rr = rho <= val_vB | rho >= val_vT;
247     condition = condition_zz | condition_rr;
248
249     % Plot
250     h1.XData = Z(~condition);
251     h1.YData = rho(~condition);
252
```

```
253     % Plot Filtered
254     h2.XData = Z(condition);
255     h2.YData = rho(condition);
256
257     % Store conditioning
258     fig.UserData = condition;
259 end
260
261 % Button call-back
262 function plot_done(source,~)
263     fig = source.Parent;
264     uiresume(fig)
265 end
```

```
1  function [bar] = extract_polysection_data(bar)
2  % This function takes scanned bars.
3  % Goal is to determine nominal area and perimeter based on
       the scan mesh -> circularity assessment.
4  % This is done in two ways
5  % 1) Cross-sections along individual bars are compared to an
       idealized circular condition.
6  % If found, the poly-section area/perimeters are averaged
       and assigned as An,Pn
7  % 2) If no cross-sections meet circularity requirements, the
       average of
8  % 'good' bars are assigned as An/Pn. An Pn are defined from
       previous
9  % studies.
10
11
12          % Base assumption
13          bar.assumed.dn_drawings = 16; % from drawings [mm]
14          bar.assumed.flag_if_avg = 0; % if =1, then following
                data is with respect to averaging, (not original
               )
15          bar.assumed.An = []; %
16          bar.assumed.Pn = []; %
17          bar.assumed.An_std = []; %
18          bar.assumed.Pn_std = []; %
19          bar.assumed.A_circular = []; %
20          bar.assumed.P_circular = []; %
21
22          % Mesh data
23          A = [bar.mesh.geometry.area];
24          P = [bar.mesh.geometry.perimeter];
25
```

```
26          d_fromA = sqrt((4/pi) .* A);
27          d_fromP = P ./ pi;
28          circ = abs(d_fromA ./ d_fromP);
29
30          %
31          % Hard-code in a filter against 'bad data'
32          % Based on diviation from circular
33          % |
34          % |
35          % v
36
37          allow_diff = 0.01;
38          condition = abs(1-circ) <= allow_diff;
39
40          % ^
41          % |
42          % |
43          % Hard-code in a filter against 'bad data'
44          % Based on diviation from circular
45          %
46
47          good_circ = circ(condition);
48          [~,idx] = sort(good_circ,'descend');
49
50          if sum(condition) > 0
51              A_use = A(idx);
52              P_use = P(idx);
53
54              An_avg = mean(A_use);
55              Pn_avg = mean(P_use);
56
57              bar.assumed.An = An_avg;
58              bar.assumed.Pn = Pn_avg;
59              bar.assumed.An_std = std(A_use);
60              bar.assumed.Pn_std = std(P_use);
61              bar.assumed.A_circular = A_use;
62              bar.assumed.P_circular = P_use;
63          end
64
65          An_global = 16^2*pi/4;
66          An_std = 0.97;
67          Pn_global = 2*pi*16;
68          Pn_std = 0.39;
69
70
71          if isempty(bar.assumed.An) || isempty(bar.assumed.Pn
```

```
            )
72              bar.assumed.flag_if_avg = 1;
73              bar.assumed.An = An_global;
74              bar.assumed.An_std = An_std;
75              bar.assumed.Pn = Pn_global;
76              bar.assumed.Pn_std = Pn_std;
77          end
78
79      % Gives mean and peak corrosion (in %).
80      An = bar.assumed.An;
81      % Peak corrosion
82
83      corrosion_peak = ((An - min([bar.mesh.geometry.area])) ./
            An) .* 100;
84      corrosion_peak = max(corrosion_peak,0);
85      bar.corrosion.peak = corrosion_peak;
86
87      corrosion_mean = ((An - mean([bar.mesh.geometry.area]))
            ./ An) .* 100;
88
89      corrosion_mean = max(corrosion_mean,0);
90      bar.corrosion.mean = corrosion_mean;
91
92  end
```

```
1   function [geometry,zz,TT,RR] = create_meshgrid_polyshape(Z,
        theta,rho)
2   % Helper function to build a mesh interpolation based on
        rebar
3   % scan data. This function accepts Z, theta, rho info and
        establishes
4   % a mesh and poly-section geometry.
5   % NOTE: This is blatant plagiarism from Natxo, Carlos,
        Samanta previous work.
6
7       % Assumption
8       scan_resolution = 0.2; % scan setting [mm]
9       angle = 360; % [deg]
10
11      % Set meshgrid for interpolate function
12      nz = ceil((max(Z)-min(Z))/scan_resolution);
13      nt = angle;
14
15      zz = linspace(min(Z),max(Z),nz);
16      tt = linspace(-pi,pi,2*nt);
17      [ZZ,TT] = meshgrid(zz,tt);
```

```
18
19      F = scatteredInterpolant(Z,theta,rho);
20      RR = F(ZZ,TT);
21
22      % Trim ends (plotting)
23      ZZ = ZZ(:,2:end-1);
24      TT = TT(:,2:end-1);
25      RR = RR(:,2:end-1);
26      zz = zz(2:end-1);
27
28      % Consider individual section 'strips' as polyshape
29      for i = 1:length(zz)
30          [xx,yy] = pol2cart(tt',RR(:,i));
31          poly_section = polyshape(xx,yy,'Simplify',false);
32          [xbar,ybar] = centroid(poly_section);
33
34          % Polyshape functions
35          geometry(i).shape = poly_section;
36          geometry(i).xbar = xbar;
37          geometry(i).ybar = ybar;
38          geometry(i).area = area(poly_section);
39          geometry(i).perimeter = perimeter(poly_section);
40      end
41  end
```

A.2 Calculation of correlation coefficient

```
1       % Anchorage force (BBK) versus bond strength and the
            correlation coefficient
2       % Anchorage force BBK
3   F_h1BIBBK = 49.453;
4   F_h1BOBBK = 49.219;
5   F_h1TIBBK = 48.727;
6   F_h1TOBBK = 48.980;
7   F_h18HIBBK = 49.501;
8   F_h18HOBBK = 49.817;
9   F_h19BIBBK = 48.872;
10  F_h19BOBBK = 49.325;
11  F_h19TIBBK = 48.980;
12  F_h19TOBBK = 49.884;
13  F_h10DIBBK = 48.679;
14  F_h10DOBBK = 48.274;
15  F_h10DICRBBK = 48.641;
16  F_h10DOCRBBK = 47.460;
17  F_h13GIBBK = 48.084;
```

```
F_h13GOBBK = 47.476;
F_h13GICRBBK = 49.414;
F_h13GOCRBBK = 48.643;
F_h16KIBBK = 49.157;
F_h16KOBBK = 49.436;
F_h16KICRBBK = 49.063;
F_h16KOCRBBK = 49.238;
F_h1BBK = [F_h1BIBBK F_h1BOBBK F_h1TIBBK F_h1TOBBK];
F_h18BBK = [F_h18HIBBK F_h18HOBBK];
F_h19BBK = [F_h19BOBBK F_h19BIBBK F_h19TIBBK F_h19TOBBK];
F_h10BBK = [F_h10DIBBK F_h10DOBBK F_h10DICRBBK F_h10DOCRBBK
    ];
F_h13BBK = [F_h13GIBBK F_h13GOBBK F_h13GICRBBK F_h13GOCRBBK
    ];
F_h16BBK = [F_h16KIBBK F_h16KOBBK F_h16KICRBBK F_h16KOCRBBK
    ];
F_hBBK = [F_h1BBK F_h18BBK F_h19BBK F_h10BBK F_h13BBK
    F_h16BBK];

% Anchorage force Experiments
F_h1BI = 49.1;
F_h1BO = 51.1;
F_h1TI = 39.1;
F_h1TO = 41.1;
F_h18HI = 38.4;
F_h18HO = 44.3;
F_h19BI = 42.4;
F_h19BO = 52.8;
F_h19TI = 40;
F_h19TO = 40.7;
F_h10DI = 43.3;
F_h10DO = 41.2;
F_h10DICR = 36.8;
F_h10DOCR = 33.8;
F_h13GI = 34.4;
F_h13GO = 32.5;
F_h13GICR = 44.5;
F_h13GOCR = 41.6;
F_h16KI = 36;
F_h16KO = 39.8;
F_h16KICR = 40.2;
F_h16KOCR = 39.2;
F_h1 = [F_h1BI F_h1BO F_h1TI F_h1TO];
F_h18 = [F_h18HI F_h18HO];
F_h19 = [F_h19BO F_h19BI F_h19TI F_h19TO];
F_h10 = [F_h10DI F_h10DO F_h10DICR F_h10DOCR];
```

```
F_h13 = [F_h13GI F_h13GO F_h13GICR F_h13GOCR];
F_h16 = [F_h16KI F_h16KO F_h16KICR F_h16KOCR];
F_h = [F_h1 F_h18 F_h19 F_h10 F_h13 F_h16];

% Difference in value
F_h1BIBBKdiff = -0.363;
F_h1BOBBKdiff = -2.1;
F_h1TIBBKdiff = 10.393;
F_h1TOBBKdiff = 8.099;
F_h18HIBBKdiff = 11.091;
F_h18HOBBKdiff = 5.527;
F_h19BIBBKdiff = 16.57;
F_h19BOBBKdiff = -2.896;
F_h19TIBBKdiff = 8.902;
F_h19TOBBKdiff = 8.625;
F_h10DIBBKdiff = 5.409;
F_h10DOBBKdiff = 7.064;
F_h10DICRBBKdiff = 11.861;
F_h10DOCRBBKdiff = 13.65;
F_h13GIBBKdiff = 13.694;
F_h13GOBBKdiff = 15.016;
F_h13GICRBBKdiff = 4.914;
F_h13GOCRBBKdiff = 7.093;
F_h16KIBBKdiff = 13.157;
F_h16KOBBKdiff = 9.676;
F_h16KICRBBKdiff = 8.903;
F_h16KOCRBBKdiff = 10.078;
F_h1BBKdiff = [F_h1BIBBKdiff F_h1BOBBKdiff F_h1TIBBKdiff
    F_h1TOBBKdiff];
F_h18BBKdiff = [F_h18HIBBKdiff F_h18HOBBKdiff];
F_h19BBKdiff = [F_h19BOBBKdiff F_h19BIBBKdiff F_h19TIBBKdiff
     F_h19TOBBKdiff];
F_h10BBKdiff = [F_h10DIBBKdiff F_h10DOBBKdiff
    F_h10DICRBBKdiff F_h10DOCRBBKdiff];
F_h13BBKdiff = [F_h13GIBBKdiff F_h13GOBBKdiff
    F_h13GICRBBKdiff F_h13GOCRBBKdiff];
F_h16BBKdiff = [F_h16KIBBKdiff F_h16KOBBKdiff
    F_h16KICRBBKdiff F_h16KOCRBBKdiff];
F_hBBKdiff = [F_h1BBKdiff F_h18BBKdiff F_h19BBKdiff
    F_h10BBKdiff F_h13BBKdiff F_h16BBKdiff];

% Difference in percentage
F_h1BIBBKdiffp = -0.7;
F_h1BOBBKdiffp = -4.1;
F_h1TIBBKdiffp = 26.6;
F_h1TOBBKdiffp = 19.7;
```

```
100 F_h18HIBBKdiffp = 28.8;
101 F_h18HOBBKdiffp = 12.5;
102 F_h19BIBBKdiffp = 51.1;
103 F_h19BOBBKdiffp = -5.5;
104 F_h19TIBBKdiffp = 22.3;
105 F_h19TOBBKdiffp = 21.2;
106 F_h10DIBBKdiffp = 12.5;
107 F_h10DOBBKdiffp = 17.1;
108 F_h10DICRBBKdiffp = 32.3;
109 F_h10DOCRBBKdiffp = 40.4;
110 F_h13GIBBKdiffp = 39.8;
111 F_h13GOBBKdiffp = 46.3;
112 F_h13GICRBBKdiffp = 11;
113 F_h13GOCRBBKdiffp = 17.1;
114 F_h16KIBBKdiffp = 36.6;
115 F_h16KOBBKdiffp = 24.3;
116 F_h16KICRBBKdiffp = 22.2;
117 F_h16KOCRBBKdiffp = 25.7;
118 F_h1BBKdiffp = [F_h1BIBBKdiffp F_h1BOBBKdiffp F_h1TIBBKdiffp
        F_h1TOBBKdiffp];
119 F_h18BBKdiffp = [F_h18HIBBKdiffp F_h18HOBBKdiffp];
120 F_h19BBKdiffp = [F_h19BOBBKdiffp F_h19BIBBKdiffp
        F_h19TIBBKdiffp F_h19TOBBKdiffp];
121 F_h10BBKdiffp = [F_h10DIBBKdiffp F_h10DOBBKdiffp
        F_h10DICRBBKdiffp F_h10DOCRBBKdiffp];
122 F_h13BBKdiffp = [F_h13GIBBKdiffp F_h13GOBBKdiffp
        F_h13GICRBBKdiffp F_h13GOCRBBKdiffp];
123 F_h16BBKdiffp = [F_h16KIBBKdiffp F_h16KOBBKdiffp
        F_h16KICRBBKdiffp F_h16KOCRBBKdiffp];
124 F_hBBKdiffp = [F_h1BBKdiffp F_h18BBKdiffp F_h19BBKdiffp
        F_h10BBKdiffp F_h13BBKdiffp F_h16BBKdiffp];
125
126 % Corrosion level
127 C_1BIBBK = 1.997;
128 C_1BOBBK = 0.65;
129 C_1TIBBK = 0.912;
130 C_1TOBBK = 1.025;
131 C_18HIBBK = 0.037;
132 C_18HOBBK = 0.003;
133 C_19BIBBK = 1.288;
134 C_19BOBBK = 1.275;
135 C_19TIBBK = 0.145;
136 C_19TOBBK = 0.113;
137 C_10DIBBK = 0.766;
138 C_10DOBBK = 0.509;
139 C_10DICRBBK = 0.883;
```

```
C_10DOCRBBK = 0.633;
C_13GIBBK = 0.329;
C_13GOBBK = 1.224;
C_13GICRBBK = 0.41;
C_13GOCRBBK = 1.099;
C_16KIBBK = 0.023;
C_16KOBBK = 0.003;
C_16KICRBBK = 0.022;
C_16KOCRBBK = 0.005;
C_1 = [C_1BIBBK C_1BOBBK C_1TIBBK C_1TOBBK];
C_18 = [C_18HIBBK C_18HOBBK];
C_19 = [C_19BIBBK C_19BOBBK C_19TIBBK C_19TOBBK];
C_10 = [C_10DIBBK C_10DOBBK C_10DICRBBK C_10DOCRBBK];
C_13 = [C_13GIBBK C_13GOBBK C_13GICRBBK C_13GOCRBBK];
C_16 = [C_16KIBBK C_16KOBBK C_16KICRBBK C_16KOCRBBK];
C = [C_1 C_18 C_19 C_10 C_13 C_16];
figure(1)
scatter(C(1:4),F_hBBKdiffp(1:4),'r*')
hold on
scatter(C(5:6),F_hBBKdiffp(5:6),'bs')
scatter(C(7:10),F_hBBKdiffp(7:10),'kx')
scatter(C(11:14),F_hBBKdiffp(11:14),'gp')
scatter(C(15:18),F_hBBKdiffp(15:18),'m^')
scatter(C(19:22),F_hBBKdiffp(19:22))

Co_diff1 = corrcoef(C(1:4),F_hBBKdiffp(1:4))
Co_diff2 = corrcoef(C(5:6),F_hBBKdiffp(5:6))
Co_diff3 = corrcoef(C(7:10),F_hBBKdiffp(7:10))
Co_diff4 = corrcoef(C(11:14),F_hBBKdiffp(11:14))
Co_diff5 = corrcoef(C(15:18),F_hBBKdiffp(15:18))
Co_diff6 = corrcoef(C(19:22),F_hBBKdiffp(19:22))

Co1bbk = corrcoef(C(1:4),F_hBBK(1:4))
Co2bbk = corrcoef(C(5:6),F_hBBK(5:6))
Co3bbk = corrcoef(C(7:10),F_hBBK(7:10))
Co4bbk = corrcoef(C(11:14),F_hBBK(11:14))
Co5bbk = corrcoef(C(15:18),F_hBBK(15:18))
Co6bbk = corrcoef(C(19:22),F_hBBK(19:22))

Co1 = corrcoef(C(1:4),F_h(1:4))
Co2 = corrcoef(C(5:6),F_h(5:6))
Co3 = corrcoef(C(7:10),F_h(7:10))
Co4 = corrcoef(C(11:14),F_h(11:14))
Co5 = corrcoef(C(15:18),F_h(15:18))
Co6 = corrcoef(C(19:22),F_h(19:22))

```

```
186 title('Fh difference in percentage versus corrosion level')
187 legend('Beam 1','Beam 18','Beam 19','Beam 10','Beam 13','
    Beam 16')
188 xlabel('Corrosion level [%]')
189 ylabel('Difference between two anchorage force[%]')
190 grid on
```

```
  %% bond anchored force for end hooks
% Average corrosion level
%% Beam 1
clc
clear all
close all

L_uy1BI = 32; L_uy1BO = 0; L_uy1TI = 249; L_uy1TO = 200; % mm
L_uy1 = [L_uy1BI L_uy1BO L_uy1TI L_uy1TO];
P_n1BI = 50.63; P_n1BO = 50.85; P_n1TI = 51.14; P_n1TO = 51.43; % mm
P_n1 = [P_n1BI P_n1BO P_n1TI P_n1TO];
F_y1BI = 50.715; F_y1BO = 51.083; F_y1TI = 51.794; F_y1TO = 51.408; % kN
F_y1 = [F_y1BI F_y1BO F_y1TI F_y1TO];
%%
tau_bond = linspace(1,12,100)';
F_u1 = zeros(length(L_uy1), length(tau_bond));
for i = 1:length(L_uy1)
F_u1(i,:) = tau_bond * (L_uy1(i) .* P_n1(i)) /1000;
F_h1(i,:) = F_y1(i) - F_u1(i,:);
end
figure(1)
plot(tau_bond, F_h1)
title('Beam 1')
legend('1 BI','1 BO','1 TI','1 TO')
xlabel('Assumed bond strength [MPa]')
ylabel('Anchored force [kN]')
axis([0 12 0 60])

for i = 1:length(F_h1)
    F_h1MJ(i,1) = 65.265;
    F_h1MJ(i,2) = 64.956;
    F_h1MJ(i,3) = 61.307;
    F_h1MJ(i,4) = 64.641;
end
for i = 1:length(F_h1)
    F_h1BBK(i,1) = 48.727;
    F_h1BBK(i,2) = 48.980;
    F_h1BBK(i,3) = 49.453;
    F_h1BBK(i,4) = 49.219;
end
%%
figure(2)
```

```
43 plot(tau_bond, F_h1(1,:)', tau_bond, F_h1MJ(:,1), tau_bond,
       F_h1BBK(:,1))
44 title('Fh 1 BI')
45 legend('1 BI','Marques and Jirsa','BBK04')
46 xlabel('Assumed bond strength [MPa]')
47 ylabel('Anchored force [kN]')
48 axis([0 12 0 70])
49 %%
50 figure(3)
51 plot(tau_bond, F_h1(2,:)', tau_bond, F_h1MJ(:,2), tau_bond,
       F_h1BBK(:,2))
52 title('Fh 1 BO')
53 legend('1 BO','Marques and Jirsa','BBK04')
54 xlabel('Assumed bond strength [MPa]')
55 ylabel('Anchored force [kN]')
56 axis([0 12 0 70])
57
58 figure(4)
59 plot(tau_bond, F_h1(3,:)', tau_bond, F_h1MJ(:,3), tau_bond,
       F_h1BBK(:,3))
60 title('Fh 1 TI')
61 legend('1 TI','Marques and Jirsa','BBK04')
62 xlabel('Assumed bond strength [MPa]')
63 ylabel('Anchored force [kN]')
64 axis([0 12 0 70])
65
66 figure(5)
67 plot(tau_bond, F_h1(4,:)', tau_bond, F_h1MJ(:,4), tau_bond,
       F_h1BBK(:,4))
68 title('Fh 1 TO')
69 legend('1 TO','Marques and Jirsa','BBK04')
70 xlabel('Assumed bond strength [MPa]')
71 ylabel('Anchored force [kN]')
72 axis([0 12 0 70])
73
74 %% Beam 18H
75 L_uy18I = 261; L_uy18O = 142; % mm
76 L_uy18 = [L_uy18I L_uy18O];
77 P_n18I = 51.05; P_n18O = 51.1; % mm
78 P_n18 = [P_n18I P_n18O];
79 F_y18I = 51.733; F_y18O = 51.547; % kN
80 F_y18 = [F_y18I F_y18O];
81
82 F_u18 = zeros(length(L_uy18), length(tau_bond));
83 for i = 1:length(L_uy18)
84 F_u18(i,:) = tau_bond * (L_uy18(i) .* P_n18(i) /1000);
```

```
F_h18(i,:) = F_y18(i) - F_u18(i,:);
end
figure(6)
plot(tau_bond, F_h18)
title('Beam 18H')
legend('18H I','18H O')
xlabel('Assumed bond strength [MPa]')
ylabel('Anchored force [kN]')
axis([0 12 0 60])

for i = 1:length(F_h18)
    F_h18MJ(i,1) = 65.328;
    F_h18MJ(i,2) = 65.745;
end
for i = 1:length(F_h18)
    F_h18BBK(i,1) = 49.501;
    F_h18BBK(i,2) = 49.817;
end
figure(7)
plot(tau_bond, F_h18(1,:)', tau_bond, F_h18MJ(:,1), tau_bond
    , F_h18BBK(:,1))
title('Fh 18H I')
legend('18H I','Marques and Jirsa','BBK04')
xlabel('Assumed bond strength [MPa]')
ylabel('Anchored force [kN]')
axis([0 12 0 70])
figure(8)
plot(tau_bond, F_h1(2,:)', tau_bond, F_h1MJ(:,2), tau_bond,
   F_h1BBK(:,2))
title('Fh 18H O')
legend('18H O','Marques and Jirsa','BBK04')
xlabel('Assumed bond strength [MPa]')
ylabel('Anchored force [kN]')
axis([0 12 0 70])

%% Beam 19
L_uy19BI = 367; L_uy19BO = 0; L_uy19TI = 219; L_uy19TO =
    226; % mm
L_uy19 = [L_uy19BI L_uy19BO L_uy19TI L_uy19TO];
P_n19BI = 51.06; P_n19BO = 51.48; P_n19TI = 51; P_n19TO =
    51.13; % mm
P_n19 = [P_n19BI P_n19BO P_n19TI P_n19TO];
F_y19BI = 51.153; F_y19BO = 52.784; F_y19TI = 51.136;
    F_y19TO = 52.26; % kN
F_y19 = [F_y19BI F_y19BO F_y19TI F_y19TO];

```

```
126 F_u19 = zeros(length(L_uy19), length(tau_bond));
127 for i = 1:length(L_uy19)
128 F_u19(i,:) = tau_bond * (L_uy19(i) .* P_n19(i)) /1000;
129 F_h19(i,:) = F_y19(i) - F_u19(i,:);
130 end
131 figure(9)
132 plot(tau_bond, F_h19)
133 title('Beam 19')
134 legend('19 BI','19 BO','19 TI','19 TO')
135 xlabel('Assumed bond strength [MPa]')
136 ylabel('Anchored force [kN]')
137 axis([0 12 0 60])
138
139 for i = 1:length(F_h19)
140     F_h19MJ(i,1) = 64.498;
141     F_h19MJ(i,2) = 65.096;
142     F_h19MJ(i,3) = 64.641;
143     F_h19MJ(i,4) = 65.834;
144 end
145 for i = 1:length(F_h19)
146     F_h19BBK(i,1) = 48.872;
147     F_h19BBK(i,2) = 49.884;
148     F_h19BBK(i,3) = 48.980;
149     F_h19BBK(i,4) = 49.325;
150 end
151 figure(10)
152 plot(tau_bond, F_h19(1,:)', tau_bond, F_h19MJ(:,1), tau_bond
    , F_h19BBK(:,1))
153 title('Fh 19 BI')
154 legend('19 BI','Marques and Jirsa','BBK04')
155 xlabel('Assumed bond strength [MPa]')
156 ylabel('Anchored force [kN]')
157 axis([0 12 0 70])
158
159 figure(11)
160 plot(tau_bond, F_h19(2,:)', tau_bond, F_h19MJ(:,2), tau_bond
    , F_h19BBK(:,2))
161 title('Fh 19 BO')
162 legend('19 BO','Marques and Jirsa','BBK04')
163 xlabel('Assumed bond strength [MPa]')
164 ylabel('Anchored force [kN]')
165 axis([0 12 0 70])
166
167 figure(12)
168 plot(tau_bond, F_h19(3,:)', tau_bond, F_h19MJ(:,3), tau_bond
    , F_h19BBK(:,3))
```

```
169 title('Fh 19 TI')
170 legend('19 TI','Marques and Jirsa','BBK04')
171 xlabel('Assumed bond strength [MPa]')
172 ylabel('Anchored force [kN]')
173 axis([0 12 0 70])
174
175 figure(13)
176 plot(tau_bond, F_h19(4,:)', tau_bond, F_h19MJ(:,4), tau_bond
    , F_h19BBK(:,4))
177 title('Fh 19 TO')
178 legend('19 TO','Marques and Jirsa','BBK04')
179 xlabel('Assumed bond strength [MPa]')
180 ylabel('Anchored force [kN]')
181 axis([0 12 0 70])
182
183 %%
184 figure(14)
185 plot(tau_bond, F_h1, '-', tau_bond, F_h18, ':', tau_bond,
    F_h19, '--')
186 title('Beam 1 18H 19')
187 legend('1 BI','1 BO','1 TI','1 TO','18H I','18H O','19 BI','
    19 BO','19 TI','19 TO')
188 xlabel('Assumed bond strength [MPa]')
189 ylabel('Anchored force [kN]')
190 axis([0 12 0 60])
```

```
  % bond anchored force for spliced beams
   clear all
close all
clc

%% 13G
Fy_gicr = 51.66; Fy_gocr = 50.854; %kN
lu_gicr = 125; lu_gocr = 193; %mm
Pn_gicr = 50.79; Pn_gocr = 50.38; %mm

x1 = linspace (1,12,100);
y_gicr = Fy_gicr - x1*lu_gicr*Pn_gicr*10e-4;
y_gocr = Fy_gocr - x1*lu_gocr*Pn_gocr*10e-4;

figure(1)
plot(x1,y_gicr,x1,y_gocr);
title('Beam 13G')
xlabel('Assumed bond strength [MPa]')
ylabel('Anchored force [kN]')
legend('13 GICR','13 GOCR')
axis([0 12 0 60])


for i = 1:length(y_gicr)
    F_h13MJ(i,1) = 65.072;
    F_h13MJ(i,2) = 64.175;

end
for i = 1:length(y_gicr)
    F_h13BBK(i,1) = 49.414;
    F_h13BBK(i,2) = 48.643;
end
figure(2)
plot(x1, y_gicr, x1, F_h13MJ(:,1), x1, F_h13BBK(:,1))
title('Fh 13G I CR TO')
xlabel('Assumed bond strength [MPa]')
ylabel('Anchored force [kN]')
legend('13G I CR','Marques and Jirsa','BBK04')
axis([0 12 0 70])

figure(3)
plot(x1, y_gocr, x1, F_h13MJ(:,2), x1, F_h13BBK(:,2))
title('Fh 13G O CR')
xlabel('Assumed bond strength [MPa]')
ylabel('Anchored force [kN]')
```

```
46 legend('13G O CR','Marques and Jirsa','BBK04')
47 axis([0 12 0 70])
48
49
50 %% 16K
51 Fy_ki = 51.39; Fy_ko = 51.839; %kN
52 lu_ki = 300; lu_ko = 384; %mm
53 Pn_ki = 50.73; Pn_ko = 51; %mm
54
55 x2 = linspace(1,12,100);
56 y_ki = Fy_ki-x2*lu_ki*Pn_ki*10e-4;
57 y_ko = Fy_ko-x2*lu_ko*Pn_ko*10e-4;
58
59 figure(4)
60 plot(x2,y_ki,x2,y_ko);
61 title('Beam 16K')
62 xlabel('Assumed bond strength [MPa]')
63 ylabel('Anchored force [kN]')
64 legend('16 KI','16 KO')
65 axis([0 12 0 60])
66
67 for i = 1:length(y_ki)
68     F_h16MJ(i,1) = 64.781;
69     F_h16MJ(i,2) = 65.149;
70
71 end
72 for i = 1:length(y_ki)
73     F_h16BBK(i,1) = 49.157;
74     F_h16BBK(i,2) = 48.436;
75 end
76 figure(5)
77 plot(x2, y_ki, x2, F_h16MJ(:,1), x2, F_h16BBK(:,1))
78 title('Fh 16K I')
79 xlabel('Assumed bond strength [MPa]')
80 ylabel('Anchored force [kN]')
81 legend('16K I','Marques and Jirsa','BBK04')
82 axis([0 12 0 70])
83
84 figure(6)
85 plot(x2, y_ko, x2, F_h16MJ(:,2), x2, F_h16BBK(:,2))
86 title('Fh 16K O')
87 xlabel('Assumed bond strength [MPa]')
88 ylabel('Anchored force [kN]')
89 legend('16K O','Marques and Jirsa','BBK04')
90 axis([0 12 0 70])
91
```

```
92
93 %% 10D
94 Fy_di = 50.891; Fy_do = 50.468; Fy_docr = 49.548; %kN
95 lu_di = 160; lu_do = 210; lu_docr = 350; %mm
96 Pn_di = 50.59; Pn_do = 50.40; Pn_docr = 49.81; %mm
97
98 x3 = linspace(1,12,100);
99 y_di = Fy_di-x3*lu_di*Pn_di*10e-4;
100 y_do = Fy_do-x3*lu_do*Pn_do*10e-4;
101 y_docr = Fy_docr-x3*lu_docr*Pn_docr*10e-4;
102
103 figure(7)
104 plot(x3,y_di,x3,y_do,x3,y_docr);
105 title('Beam 10D')
106 xlabel('Assumed bond strength [MPa]')
107 ylabel('Anchored force [kN]')
108 legend('10 DI','10 DO','10 DOCR')
109 axis([0 12 0 60])
110
111 for i = 1:length(y_ki)
112     F_h10MJ(i,1) = 64.781;
113     F_h10MJ(i,2) = 65.149;
114
115 end
116 for i = 1:length(y_ki)
117     F_h10BBK(i,1) = 49.157;
118     F_h10BBK(i,2) = 48.436;
119 end
120 figure(8)
121 plot(x3, y_ki, x3, F_h10MJ(:,1), x3, F_h10BBK(:,1))
122 title('Fh 10D I')
123 xlabel('Assumed bond strength [MPa]')
124 ylabel('Anchored force [kN]')
125 legend('10D I','Marques and Jirsa','BBK04')
126 axis([0 12 0 70])
127
128
129 figure(9)
130 plot(x3, y_ko, x3, F_h10MJ(:,2), x3, F_h10BBK(:,2))
131 title('Fh 10D O')
132 xlabel('Assumed bond strength [MPa]')
133 ylabel('Anchored force [kN]')
134 legend('10D O','Marques and Jirsa','BBK04')
135 axis([0 12 0 70])
136
137 figure(10)
```

```
138 plot(x3, y_ko, x3, F_h10MJ(:,2), x3, F_h10BBK(:,2))
139 title('Fh 10D O CR')
140 xlabel('Assumed bond strength [MPa]')
141 ylabel('Anchored force [kN]')
142 legend('10D O CR','Marques and Jirsa','BBK04')
143 axis([0 12 0 70])
144
145
146 %%
147 figure(11)
148 plot(x1,y_gicr,'-',x1,y_gocr,'-',x2,y_ki,':',x2,y_ko,':',x3,
      y_di,'--',x3,y_do,'--',x3,y_docr,'--','LineWidth',1.5)
149 title('Beam 10D 13G 16K')
150 legend('13G I CR','13G O CR','16K I','16K O','10D I','10D O'
      ,'10D O CR')
151 xlabel('Assumed bond strength [MPa]')
152 ylabel('Anchored force [kN]')
153 axis([0 12 0 60])
154 grid on
```

A.3 Source code in MATLAB file for figures

```
% Average corrosion versus peak corrosion
clc
clear all
close all

%%
x = linspace (0,5,100);
y = x;

%% End-hook Top cast
C_a19ti = 0.912; C_a19to = 1.025; C_p19ti = 4.501; C_p19to = 2.817;
C_a1ti = 0.145; C_a1to = 0.113; C_p1ti = 0.819; C_p1to = 2.204;
C_aet = [C_a19ti C_a19to C_a1ti C_a1to];
C_pet = [C_p19ti C_p19to C_p1ti C_p1to];
%% End-hook bottom cast
C_a19bi = 1.997; C_a19bo = 0.650; C_p19bi = 5.509; C_p19bo = 1.725;
C_a18hi = 0.037; C_a18ho = 0.003; C_p18hi = 0.294; C_p18ho = 0.307;
C_a1bi = 1.288; C_a1bo = 1.275; C_p1bi = 2.086; C_p1bo = 4.030;
C_aeb = [C_a19bi C_a19bo C_a18hi C_a18ho C_a1bi C_a1bo];
C_peb = [C_p19bi C_p19bo C_p18hi C_p18ho C_p1bi C_p1bo];

%% Spliced top cast
C_a16ki = 0.023; C_a16ko = 0.003; C_a16kicr = 0.022; C_a16kocr = 0.005;
C_p16ki = 0.799; C_p16ko = 0.683; C_p16kicr = 0.900; C_p16kocr = 0.697;
C_a13gi = 0.329; C_a13go = 1.224; C_a13gicr = 0.410; C_a13gocr = 1.099;
C_p13gi = 3.400; C_p13go = 4.672; C_p13gicr = 2.233; C_p13gocr = 5.028;
C_a10di = 0.766; C_a10do = 0.509; C_a10dicr = 0.883; C_a10docr = 0.633;
C_p10di = 4.758; C_p10do = 2.407; C_p10dicr = 5.214; C_p10docr = 3.540;
C_ast = [C_a16ki C_a16ko C_a16kicr C_a16kocr C_a13gi C_a13go C_a13gicr C_a13gocr C_a10di C_a10do C_a10dicr C_a10docr ];
C_pst = [C_p16ki C_p16ko C_p16kicr C_p16kocr C_p13gi C_p13go C_p13gicr C_p13gocr C_p10di C_p10do C_p10dicr C_p10docr
```

```
    ];

%% figures
figure(1)
scatter(C_aet,C_pet,'r*');
hold on
scatter(C_aeb,C_peb,'gs');
scatter(C_ast,C_pst,'kx');
plot(x,y,'k')
% title('Spliced Top Cast')
xlabel('Average corrosion level [%]')
ylabel('Peak corrosion level [%]')
legend('1 pair of hooks T','1 pair of hooks B','2 pairs of
    hooks T','y=x') %'End-hook Bottom Cast','Spliced Top Cast
    '
grid on
hold off
```

```
% Average bond stress versus yielded length
clc
clear all
close all

%% Spliced beam
B_10di = 0; B_10do = 0; B_10docr = 0;
B_13gicr = 1.87; B_13gocr= 1.981;
B_16ki = 1.526; B_16ko = 1.169;
L_10di = 45.08; L_10do = 42.41; L_10docr = 57.22;
L_13gicr = 111; L_13gocr = 113.68;
L_16ki = 80.5; L_16ko = 97;
L_spliced = [L_10di L_10do L_10docr L_13gicr L_13gocr L_16ki
    L_16ko];
B_spliced = [B_10di B_10do B_10docr B_13gicr B_13gocr B_16ki
    B_16ko];

%% End-hook beams
B_1bi = 2.192; B_1bo = 1.278; B_1ti = 4.457;
B_18i = 1.647; B_18o = 1.666;
B_19bi = 2.212; B_19bo = 0.786; B_19ti = 2.238; B_19to =
   2.581;
L_1bi = 267; L_1bo = 455; L_1ti = 64;
L_18i = 172; L_18o = 172;
L_19bi = 174; L_19bo = 450; L_19ti = 174; L_19to = 142;
L_eht = [L_1ti L_19ti L_19to];
B_eht = [B_1ti B_19ti B_19to];
L_ehb = [L_1bi L_1bo L_18i L_18o L_19bi L_19bo];
B_ehb = [B_1bi B_1bo B_18i B_18o B_19bi B_19bo];

figure(1)
scatter(L_spliced,B_spliced,'r*')
hold on
scatter(L_ehb,B_ehb,'bs')
scatter(L_eht,B_eht,'kx')
xlabel('Yielded length [mm]')
ylabel('Average bond stress (yield zone) [MPa]')
legend('2 pairs of hooks B','1 pair of hooks B','1 pair of
   hooks T')
grid on
hold off
```

```
%Force anchored by the hooks vs. average corrosion level for two pairs of hooks and 1 pair of hooks
clc
clear all
close all

%% End-hook beam
F_1bo = 51.08; F_1bi = 47.4747; F_1to = 41.12; F_1ti = 39.06;
F_18hi = 25.0849; F_18ho = 37.0346;
F_19to = 40.7; F_19ti = 39.97;F_19bo = 52,78; F_19bi = 13.675;
C_1bo = 0.113; C_1bi = 0.235; C_1to = 0.113; C_1ti = 0.145;
C_18hi = 0.037; C_18ho = 0.003;
C_19to = 1.025; C_19ti = 0.912; C_19bo = 0.650; C_19bi = 1.997;

F_1 = [F_1bo F_1bi F_1to F_1ti];
F_18 = [F_18hi F_18ho];
F_19 = [F_19to F_19ti F_19bo F_19bi];
C_1 = [C_1bo C_1bi C_1to C_1ti];
C_18 = [C_18hi C_18ho];
C_19 = [C_19to C_19ti C_19bo C_19bi];

F_e1b = [F_1bi F_1bo]; F_e18b = [F_18hi F_18ho]; F_e19b = [F_19bi F_19bo];
C_e1b = [C_1bi C_1bo]; C_e18b = [C_18hi C_18ho]; C_e19b = [C_19bi C_19bo];
F_e1t = [F_1to F_1ti]; F_e19t = [F_19to F_19ti];
C_e1t = [C_1to C_1ti]; C_e19t = [C_19to C_19ti];

F_et = [F_1to F_1ti F_19to F_19ti];
C_et = [C_1to C_1ti C_19to C_19ti];
F_eb = [F_1bi F_1bo F_18hi F_18ho F_19bi F_19bo];
C_eb = [C_1bi C_1bo C_18hi C_18ho C_19bi C_19bo];

%% Spliced beam
F_10di = 35.174; F_10do = 31.782; F_10dicr = 22.918; F_10docr = 17.871;
F_13gi = 17.781; F_13go = 14.659; F_13gicr = 37.13; F_13gocr = 31.825;
F_16ki = 20.574; F_16ko = 27.623; F_16kicr = 28.859;F_16kocr = 27.233;
C_10di = 0.766; C_10do = 0.509; C_10dicr = 0.883;C_10docr = 0.677;
```

```
C_13gi = 0.329; C_13go = 1.224; C_13gicr = 0.41; C_13gocr = 1.099;
C_16ki = 0.023; C_16ko = 0.003; C_16kicr = 0.022; C_16kocr = 0.005;

F_10 = [F_10di F_10do F_10dicr F_10docr];
F_13 = [F_13gi F_13go F_13gicr F_13gocr];
F_16 = [F_16ki F_16ko F_16kicr F_16kocr];
C_10 = [C_10di C_10do C_10dicr C_10docr];
C_13 = [C_13gi C_13go C_13gicr C_13gocr];
C_16 = [C_16ki C_16ko C_16kicr C_16kocr];

F_st = [F_10di F_10do F_10dicr F_10docr F_13gi F_13go F_13gicr F_13gocr F_16ki F_16ko F_16kicr F_16kocr];
C_st = [C_10di C_10do C_10dicr C_10docr C_13gi C_13go C_13gicr C_13gocr C_16ki C_16ko C_16kicr C_16kocr];

F_10i = [F_10di F_10dicr]; C_10i = [C_10di C_10dicr]; F_10o = [F_10do F_10docr]; C_10o = [C_10do C_10docr];
F_13i = [F_13gi F_13gicr]; C_13i = [C_13gi C_13gicr]; F_13o = [F_13go F_13gocr]; C_13o = [C_13go C_13gocr];
F_16i = [F_16ki F_16kicr]; C_16i = [C_16ki C_16kicr]; F_16o = [F_16ko F_16kocr]; C_16o = [C_16ko C_16kocr];


figure(1);
scatter(C_10,F_10,'r*');
hold on
scatter(C_13,F_13,'g*')
scatter(C_16,F_16,'b*')
title('Two pairs of hooks')
xlabel('Average corrosion level [%]')
ylabel('Force anchored by the hooks [kN]')
legend('Beam 10D','Beam 13G','Beam 16K')
grid on
hold off

figure(2);
scatter(C_1,F_1,'r*')
hold on
scatter(C_18,F_18,'g*')
scatter(C_19,F_19,'b*')
title('One pair of hooks')
xlabel('Average corrosion level [%]')
ylabel('Force anchored by the hooks [kN]')
legend('Beam 1','Beam 18H','Beam 19')
```

```
75 grid on
76 hold off
```

```
% Bond stress (yield zone) vs. corrosion level
clc
clear all
close all

%% Spliced beam
B_10di = 0; B_10do = 0; B_10docr = 0;
B_13gicr = 2.174; B_13gocr= 3.909;
B_16ki = 1.839; B_16ko = 1.157;
L_10di = 32.63; L_10do = 36.87; L_10docr = 57.22;
L_13gicr = 93.68; L_13gocr = 55.5;
L_16ki = 66.5; L_16ko = 97;
L_spliced = [L_10di L_10do L_10docr L_13gicr L_13gocr L_16ki
    L_16ko];
B_spliced = [B_10di B_10do B_10docr B_13gicr B_13gocr B_16ki
    B_16ko];

C_10di = 0.766; C_10do = 0.509; C_10dicr = 0.883;C_10docr =
    0.677;
C_13gi = 0.329; C_13go = 1.224; C_13gicr = 0.41; C_13gocr =
    1.099;
C_16ki = 0.023; C_16ko = 0.003; C_16kicr = 0.022; C_16kocr =
    0.005;
C_10 = [C_10di C_10do C_10dicr C_10docr];
C_13 = [C_13gi C_13go C_13gicr C_13gocr];
C_16 = [C_16ki C_16ko C_16kicr C_16kocr];
C_spliced = [C_10di C_10do C_10docr C_13gicr C_13gocr C_16ki
    C_16ko];

%% End-hook beams
B_1bi = 2.192; B_1bo = 1.278; B_1ti = 4.457;  %beam1 as it
    is
B_18ti = 1.647; B_18to = 1.666;                %beam18
    upside down during test
B_19ti = 2.212; B_19to = 0.786; B_19bi = 2.238; B_19bo =
    2.581;       %beam19 upsidedown during test
L_1bi = 267; L_1bo = 455; L_1ti = 64;
L_18ti = 172; L_18to = 172;
L_19ti = 174; L_19to = 450; L_19bi = 174; L_19bo = 142;
L_eht = [L_1ti L_18ti L_18to L_19ti L_19to];    %top during
    the test
B_eht = [B_1ti B_18ti B_18to B_19ti B_19to];
L_ehb = [L_1bi L_1bo L_19bi L_19bo]; %bottom during the test
B_ehb = [B_1bi B_1bo B_19bi B_19bo];

```

```
C_1bo = 0.113; C_1bi = 0.235; C_1to = 0.113; C_1ti = 0.145;
C_18ti = 0.037; C_18to = 0.003;
C_19to = 1.025; C_19ti = 0.912; C_19bo = 0.650; C_19bi =
    1.997;
C_1 = [C_1bo C_1bi C_1to C_1ti];
C_18 = [C_18ti C_18to];
C_19 = [C_19to C_19ti C_19bo C_19bi];
C_ehb = [C_1bi C_1bo C_19bi C_19bo];
C_eht = [C_1ti C_18ti C_18to C_19ti C_19to];


figure(1)
scatter(C_spliced,B_spliced,'r*')
hold on
scatter(C_ehb,B_ehb,'bs')
scatter(C_eht,B_eht,'kx')
title('Bond stress versus corrosion level')
xlabel('Average corrosion level [%]')
ylabel('Average bond stress (yield zone) [MPa]')
legend('2 pairs of hooks B','1 pair of hooks B','1 pair of
    hooks T')
grid on
hold off
```

```
%Casting position
clc
clear all
close all

%% End-hook beam
F_1bo = 51.08; F_1bi = 47.4747; F_1to = 41.12; F_1ti = 39.06;
F_18hi = 25.0849; F_18ho = 37.0346;
F_19to = 40.7; F_19ti = 39.97;F_19bo = 52,78; F_19bi = 13.675;
C_1bo = 0.113; C_1bi = 0.235; C_1to = 0.113; C_1ti = 0.145;
C_18hi = 0.037; C_18ho = 0.003;
C_19to = 1.025; C_19ti = 0.912; C_19bo = 0.650; C_19bi = 1.997;

F_1 = [F_1bo F_1bi F_1to F_1ti];
F_18 = [F_18hi F_18ho];
F_19 = [F_19to F_19ti F_19bo F_19bi];
C_1 = [C_1bo C_1bi C_1to C_1ti];
C_18 = [C_18hi C_18ho];
C_19 = [C_19to C_19ti C_19bo C_19bi];

F_e1b = [F_1bi F_1bo]; F_e18b = [F_18hi F_18ho]; F_e19b = [F_19bi F_19bo];
C_e1b = [C_1bi C_1bo]; C_e18b = [C_18hi C_18ho]; C_e19b = [C_19bi C_19bo];
F_e1t = [F_1to F_1ti]; F_e19t = [F_19to F_19ti];
C_e1t = [C_1to C_1ti]; C_e19t = [C_19to C_19ti];

F_et = [F_1to F_1ti F_19to F_19ti];
C_et = [C_1to C_1ti C_19to C_19ti];
F_eb = [F_1bi F_1bo F_18hi F_18ho F_19bi F_19bo];
C_eb = [C_1bi C_1bo C_18hi C_18ho C_19bi C_19bo];

%% Spliced beam
F_10di = 35.174; F_10do = 31.782; F_10dicr = 22.918; F_10docr = 17.871;
F_13gi = 17.781; F_13go = 14.659; F_13gicr = 37.13; F_13gocr = 31.825;
F_16ki = 20.574; F_16ko = 27.623; F_16kicr = 28.859;F_16kocr = 27.233;
C_10di = 0.766; C_10do = 0.509; C_10dicr = 0.883;C_10docr = 0.677;
C_13gi = 0.329; C_13go = 1.224; C_13gicr = 0.41; C_13gocr =
```

```
    1.099;
C_16ki = 0.023; C_16ko = 0.003; C_16kicr = 0.022; C_16kocr =
    0.005;

F_10 = [F_10di F_10do F_10dicr F_10docr];
F_13 = [F_13gi F_13go F_13gicr F_13gocr];
F_16 = [F_16ki F_16ko F_16kicr F_16kocr];
C_10 = [C_10di C_10do C_10dicr C_10docr];
C_13 = [C_13gi C_13go C_13gicr C_13gocr];
C_16 = [C_16ki C_16ko C_16kicr C_16kocr];

F_st = [F_10di F_10do F_10dicr F_10docr F_13gi F_13go
    F_13gicr F_13gocr F_16ki F_16ko F_16kicr F_16kocr];
C_st = [C_10di C_10do C_10dicr C_10docr C_13gi C_13go
    C_13gicr C_13gocr C_16ki C_16ko C_16kicr C_16kocr];

F_10i = [F_10di F_10dicr]; C_10i = [C_10di C_10dicr]; F_10o
    = [F_10do F_10docr]; C_10o = [C_10do C_10docr];
F_13i = [F_13gi F_13gicr]; C_13i = [C_13gi C_13gicr]; F_13o
    = [F_13go F_13gocr]; C_13o = [C_13go C_13gocr];
F_16i = [F_16ki F_16kicr]; C_16i = [C_16ki C_16kicr]; F_16o
    = [F_16ko F_16kocr]; C_16o = [C_16ko C_16kocr];

figure(1)
scatter(C_st,F_st,'r*')
hold on
scatter(C_et,F_et,'kx')
scatter(C_eb,F_eb,'bs')
% title('The impact from casting position')
xlabel('Corrosion level [%]')
ylabel('Force anchored by the hooks [kN]')
legend('2 pairs of hooks T','1 pair of hooks T','1 pair of
    hooks B')
grid on
hold off
```

B

Appendix

B.1 Corrosion data in Excel

Beam nr.	Beam label	peak [%]	mean [%]	Length	GOM length	L_uy	Z	An	An.ave	An.original	Pn	Pn.ave	Pn.original	bending length (mm)	Ave. for entire bar [%]	Peak for entire bar [%]	Discussion	Notes	
19	BI 1of2 hook	0.47	0.10	86.00			0-90	203.96			50.82								
19	BI 1of2 straight	2.12	0.05	357.00		952.00	-	203.10	203.19	203.75	50.86	50.86	51.06	134.00	1.997%	5.509%			
19	BI 2of2	11.86	5.00	375.00			75-end	203.10			50.86						Used global area	YES	
19	BO 1of2 hook	0.74	0.00	116.00			-	208.93			51.38								
19	BO 1of2 straight bottom	3.35	1.99	15.00			-	203.34			50.55						Corrosion and yielding, used global area		
19	BO 1of2 straight top	7.82	3.06	157.00		523.00	40-end	203.34	206.94	209.46	50.55	51.10	51.48	119.00	0.650%	1.725%	Corrosion and yielding, used global area		
19	BO 2of2	1.17	0.39	288.00			0-290	205.56			51.02							YES	
19	B O 1of2 bending1	4.99	3.40	21.00			-	206.70			50.97								
19	B O 1of2 bending2	11.00	4.84	19.00			-	206.74			50.97							straight-21-19-14-uncrossion-hook	
19	B O 1of2 bending3	11.83	4.57	14.00			-	206.74			50.97								
19	TI 1of2 hook	1.52	0.04	117.00			-	203.00			50.83								
19	TI 1of2 straight	6.10	1.45	265.00			150-end	203.34			50.55								
19	TI 2of2	6.16	0.08	400.00		515.00	0-400	192.25	202.74	202.92	49.33	50.55	51.00	133.00	0.912%	4.501%	Very small area, maybe entire bar is yielded, not included in corrosion	NO	
19	T I 1of2 bending1	5.00	2.36	25.00			-	200.86			50.24								
19	T I 1of2 bending2	7.31	0.00	30.00			-	200.86			50.24							straight-18 uncorrosion-25-30-20-25-13uncorrosion-hook	
19	T I 1of2 bending3	7.71	1.10	20.00			-	200.86			50.24								
19	T I 1of2 bending4	1.01	0.00	25.00			-	200.86			50.24								
19	TO 1of2 hook	0.17	0.00	60.00			30-90	204.65			50.73								
19	TO 1of2 straight left	0.80	0.01	125.00			120-end	204.08			50.82						Yielding		
19	TO 1of2 straight middle	1.51	0.01	20.00		421.00	-	203.66	204.62	207.38	50.60	51.30	51.13	126.00	1.025%	2.817%			
19	TO 1of2 straight right	0.90	0.00	75.00			-	206.07			50.96								
19	TO 2of2	2.51	0.11	15.00			410-425	203.91			50.65						Corrosion and yielding, used global area	NO	
19	TO 1of2 bending1	33.62	16.32	28.00			-	204.15			84.58							hook-28-uncorrosion-straight	
18H	O 1of2 hook	0.23	0.01	90.00			0-90	206.95			51.05								
18H	O 1of2 straight	0.64	0.00	140.00		359.00	230-end	206.48	206.66	206.93	51.07	51.06	51.10	129.00	0.003%	0.307%	Corrosion and yielding		
18H	O 2of2	9.65	6.28	445.00			20-460	206.48			51.07						Corrosion and yielding, small area maybe yielded, not include in corrosionused global	NO	
18H	I 1of2 hook	0.46	0.01	90.00			-	205.83			50.98								
18H	I 1of2 straight	0.09	0.00	75.00		328.75	110-end	205.43	205.35	206.19	50.95	50.93	51.05	122.00	0.037%	0.294%	Corrosion and yielding		
18H	I 2of2 top	1.16	0.27	41.75			45-end	204.78			50.81						Corrosion and yielding		
18H	I 2of2 middle	25.56	15.87	155.00			-	205.43			50.95						Corrosion and yielding, not include in corrosion,used global area	YES	
18H	I 2of2 bottom	65.26	27.31	153.00			-	205.43			50.95						Corrosion and yielding, not include in corrosion,used global area		
16K	CR 1of2 hook	0.64	0.01	111.00			-	202.95			50.77								
16K	CR 1of2 straight	1.53	0.00	283.00	609.00	839.00	-	203.50	203.54	204.24	50.78	50.77	50.79	135.00	0.022%	0.900%			
16K	CR 2of2	0.69	0.00	310.00			-	203.73			50.76							NO	
16K	CR 1of2 bending1	3.71	1.75	10.00			-	205.12			50.77							hook-10corrosion-125uncorrosion-straight	
16K	I 1of2 hook left	0.85	0.29	18.00			0-45	204.53			50.82								
16K	I 1of2 hook right	0.36	0.05	295.00	694.00	883.00	105-120	204.77	203.93	204.04	50.84	50.73	50.82	130.00	0.023%	0.799%			
16K	I 1of2 straight	1.25	0.00	300.00			90-end	203.15			50.64						Corrosion and yielding		
16K	I 2of2	1.49	0.00	140.00			160-end	203.77			50.69						Corrosion and yielding	NO	
16K	O 1of3 hook	0.37	0.01	76.00			-	203.62			50.93								
16K	O 1of3 straight	0.99	0.00	235.00			30-end	205.53			51.09								
16K	O 2of3	1.18	0.00	140.00	669.00	646.30	0-140	204.62	205.09	205.95	50.81	51.00	51.21	133.00	0.003%	0.683%		NO	
16K	O 3of3 bottom left	0.87	0.13	9.30			0-10	205.08			51.22							YES	
16K	O 3of3 bottom right	0.14	0.00	53.00			30-85	206.49			51.16								
16K	O 3of3 top	1.37	0.05	90.00			-	198.18			50.29						Yielded, ave. Area 10mm2 smaller than bottom		
16K	O CR 1of2 hook	0.44	0.00	115.00			-	205.11			50.94								
16K	O CR 1of2 straight	0.97	0.00	310.00		767.00	-	203.91	204.27	202.70	50.77	50.81	50.95	132.00	0.005%	0.697%			
16K	O CR 2of2	8.13	0.02	210.00			0-230	204.15			50.80							NO	
16K	O CR 1of2 bending1	1.36	0.00	27.00			-	205.68			50.84							straight-27corrosion-105uncorrosion-hook	
13G	I 1of3 hook	1.59	0.66	88.00			-	204.98			50.75								
13G	I 1of3 straight	6.98	0.13	260.00			-	201.69			50.34								
13G	I 2of3 left	4.93	1.53	76.00			0-75	202.54			50.45						Used global area for p = 50.55	0,001	NO
13G	I 2of3 right	6.79	0.67	154.00		783.50	130-end	197.36	199.48	202.36	49.80	50.40	50.71	135.00	0.329%	3.40%	Used global area for p = 49.8 not included	0,005	
13G	I 3of3 bottom left	1.05	0.06	5.00			0-10	203.10			50.73							0,001	
13G	I 3of3 bottom right	0.97	0.08	121.00			30-end	195.11			49.67							0,005	
13G	I 3of3 top left	2.14	0.44	90.00			0-85	191.40			49.83							0,002	YES
13G	I 3of3 top right	1.98	0.02	8.50			116-end	192.95			49.40							0,005	
13G	I CR 1of2 hook	0.48	0.02	103.00			-	204.52			50.80							0,005	
13G	I CR 1of2 straight left	12.85	5.37	60.50			0-65	204.15			50.65						Left part yielding or corrosion? Used global area p = 50.2	0,01	
13G	I CR 1of2 straight right	4.73	0.69	180.00	707.00	609.00	140-end	204.15	205.00	205.79	50.65	50.79	50.90	140.00	0.410%	2.233%	Used global area p = 50.2	0,005	
13G	I CR 2of2 left	3.84	1.11	111.00			60-170	204.15			50.65								NO
13G	I CR 2of2 right	0.44	0.00	75.00			330-end	208.94			51.33						Weired area, maybe yielding along entire length	0,001	
13G	O 1of3 hook	0.79	0.00	107.00			0-120	200.81			50.38							0,00191	
13G	O 1of3 straight left	1.74	0.41	56.00			25-80	199.36			50.33							0,005	
13G	O 1of3 straight right	4.71	0.17	120.00			160-end	197.15			50.02							0,005	
13G	O 2of3 left	9.15	5.97	71.00			0-70	198.94			50.00						Used global area for p = 50	0,001	

						953.80			196.96	199.44		49.93	50.10	136.00	1.224%	4.672%			NO
13G	O 2of3 right	12.95	3.67	137.00			110-end	198.94			50.00						Used global area for p = 50	0,001	
13G	O 3of3 bottom	3.63	1.03	205.00			-	191.68			49.41							0,0015	
13G	O 3of3 top 1 left	1.37	0.24	13.00			0-12	199.43			50.10							0,005	NO
13G	O 3of3 top 1 right	0.64	0.00	8.80			28-36	203.23			50.59							0,00111	
13G	O 3of3 top 2	2.92	0.06	100.00			-	196.56			49.93							0,003	
13G	O 1of3 bending1	10.76	0.14	21.00			-	199.58			50.08							straight-15 uncorrosion-21- 100 uncorrosion -hook	
13G	O CR 1of2 hook	0.50	0.05	104.00			0-105	203.28			50.70							0,003	
13G	O CR 1of2 straight left	10.17	5.62	60.00			0-60	201.50			50.32						Used global area for p = 50,32 yielding	0,005	
13G	O CR 1of2 straight right	5.18	1.61	210.00	707.00	774.00	130-end	201.50	201.80	203.46	50.32	50.38	50.67	139.00	1.099%	5.028%	Used global area for p = 50,32	0,005	
13G	O CR 2of2 left	5.27	1.42	21.00			30-50	201.50			50.32						Used global area for p = 50,32	0,005	NO
13G	O CR 2of2 right	8.70	1.62	300.00			100-end	201.50			50.32						Used global area for p = 50,32	0,005	
13G	O CR 1of2 bending1	1.72	0.62	18.00			-	202.14			50.40							straight-18corrosion-121uncorrosion-hook	
1	B I 1of2 hook	1.46	0.44	160.00			-	202.14			50.40						Used global area for p = 50.4		
1	B I 1of2 straight bottom	1.47	0.54	126.00			-	194.20			49.40						Used global area for p = 49.4		
1	B I 1of2 straight top left	1.65	0.00	72.00			-	192.77			49.35						yielding		
1	B I 1of2 straight top right	1.62	0.00	139.00		297.00	-	198.21	202.14	203.74	50.00	50.40	50.63	137.00	1.288%	2.086%			
1	B I 2of2 left part	3.85	3.85	285.00			-	194.20			49.40						Used global area for p = 49.4		
1	B I 2of2 right part-left	2.30	0.00	113.00			-	196.84			49.86								NO
1	B I 2of2 right part-right	4.68	0.00	33.00			-	194.84			49.72						yielding		
1	B O 1of2 hook	0.93	0.24	135.00			90-110	203.19			50.90								
1	B O 1of2 straight bottom	3.29	1.33	135.00		265.00	0-end	191.85	203.19	203.93	49.10	50.90	50.85	130.00	1.275%	4.030%	Used global area for p = 49.1		
1	B O 1of2 straight top	3.37	0.00	265.00			0-200	193.09			49.44						yielding		
1	B O 2of2	6.35	1.94	450.00			0-end	195.77			49.60						Used global area for p = 49.6		NO
1	T I 1of2 hook left	30.84	21.50	105.00			-	181.22			48.79						Yielding		
1	T I 1of2 hook right	2.48	0.53	60.00			-	205.77			50.85						Used global area for p = 50.85		
1	T I 1of2 straight left	1.90	0.00	75.00		859.00	0-75	199.22	205.15	205.53	50.21	50.85	51.14	134.00	0.145%	0.819%	Yielding		
1	T I 1of2 straight right	1.03	0.22	290.00			75-315	205.77			50.85						Used global area for p = 50.85		
1	T I 2of2 left	0.69	0.08	375.00			-	205.77			50.85						Used global area for p = 50.85		YES
1	T I 2of2 right	2.17	0.46	35.00			-	202.73			50.72						Yielding		
1	T O 1of2 hook	0.65	0.02	150.00			-	204.34			50.87						Yielding		
1	T O 1of2 straight	4.46	0.06	245.00		943.00	-	204.15	204.18	204.29	50.65	50.69	51.43	135.00	0.113%	2.204%	Used global area for p = 50.65		
1	T O 2of2	2.15	0.21	413.00			-	204.15			50.65						Used global area for p = 50.65		NO
10	D I 1of2 hook	0.91	0.00	86.00			-	200.00			50.34								
10	D I 1of2 straight	11.80	1.93	280.00			0-end	200.06			50.14						Used global area for p = 50.14		
10	D I 2of2	1.38	0.00	380.00	670.00	871.00	0-end	203.63	201.95	203.82	50.99	50.59	50.69	125.00	0.766%	4.758%			NO
10	D I 1of2 bending1	5.34	3.56	20.00			-	203.29			50.49							straight-20corrosion-23corrosion-82uncorrsion-hook	
10	D I 1of2 bending2	5.75	2.35	23.00			-	203.26			50.49								
10	D I CR 1of2 hook left	0.80	0.00	60.00			-	203.93			50.74								
10	D I CR 1of2 hook right	0.58	0.00	46.00			-	203.78			50.69								
10	D I CR 1of2 straight	8.47	1.90	327.00			0-end	202.47			50.67								NO
10	D I CR 2of2 left	2.67	0.74	175.00			0-175	202.54			50.84						Corrosion		
10	D I CR 2of2 middle	3.12	0.16	50.00		913.00	175-225	194.72	201.79	203.90	49.70	50.62	50.70	140.00	0.883%	5.214%	Corrosion and yielding		
10	D I CR 2of2 right	1.96	0.00	165.00			225-390	197.87			50.28						Corrosion		
10	D I CR 1of2 bending1	12.34	0.98	27.00			-	202.78			50.48							straight-27-21-25-67uncorrosion-hook	
10	D I CR 1of2 bending2	5.58	0.27	21.00			-	202.78			50.48								
10	D I CR 1of2 bending3	27.00	0.95	25.00			-	202.78			50.48								NO
10	D O 1of2 hook	2.61	0.58	105.00			0-end	201.34			50.30						Used global area for p = 50.3		
10	D O 1of2 straight left	5.56	5.56	50.00			0-50	199.80			50.36						Corrosion		
10	D O 1of2 straight middle	11.01	3.92	50.00	702.00	885.00	50-100	191.02	200.27	200.92	49.66	50.40	50.41	135.00	0.509%	2.407%	Corrosion and yielding		
10	D O 1of2 straight right	2.58	0.00	210.00			100-310	200.19			50.50						Corrosion		
10	D O 2of2	2.69	0.29	385.00			0-end	200.09			50.38								NO
10	D O CR 1of2 hook	2.55	0.09	115.00			0-end	197.72			50.73								
10	D O CR 1of2 straight left	6.26	0.85	25.00			0-25	179.62			48.33								
10	D O CR 1of2 straight right	4.73	0.44	350.00	820.00	######	25-375	195.77	196.89	197.42	49.60	49.83	49.95	133.00	0.633%	3.540%	Corrosion Used global area for p = 49.6		
10	D O CR 2of2	24.02	1.09	441.00			0-230	197.36			49.80								
10	D O CR 1of2 bending1	6.53	0.51	26.00			-	200.30			49.61							straight-26corrosion-107uncorrosion-hook	
Beam nr.	Beam label	peak [%]	mean [%]	Length	straight only	L_uy	Z	An	An.ave	An.ori	Pn	Pn.ave	Pn.ori	bending length (mm)	Ave. for entire bar [%]	Peak for entire bar [%]	Discussion	Notes	

C

Appendix

C.1 Beam **1**

Beam 1

$b := 250mm$ $h := 300mm$ $f_y := 252MPa$

$F_1 := 100kN$ $F_2 := 180kN$ $F_3 := 203kN$

$L := 88.5cm$

$$R_1 := \frac{F_1}{2} = 50 \cdot kN$$

$$R_2 := \frac{F_2}{2} = 90 \cdot kN$$

$$R_3 := \frac{F_3}{2} = 101.5 \cdot kN$$

$V_1(x) := R_1$

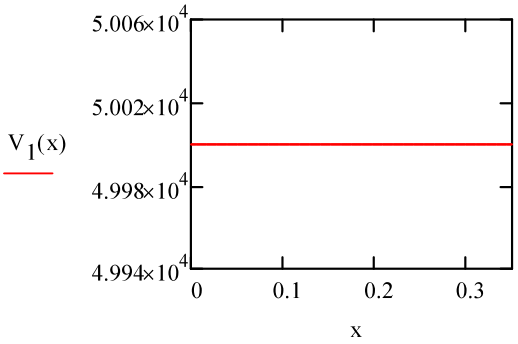

$V_2(x) := R_2$

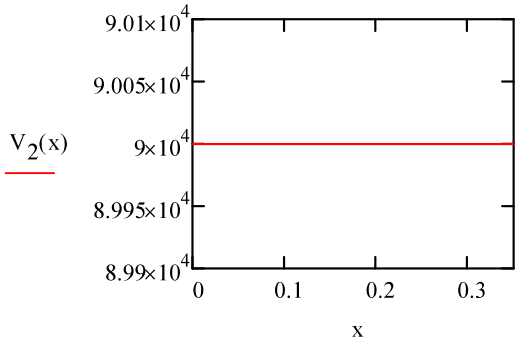

$V_3(x) := R_3$

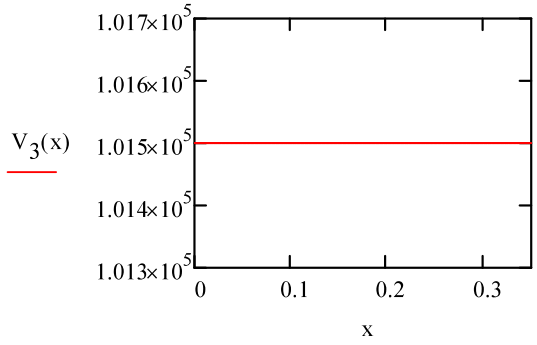

$$M_1(x) := \frac{(F_1)\cdot x}{2}$$

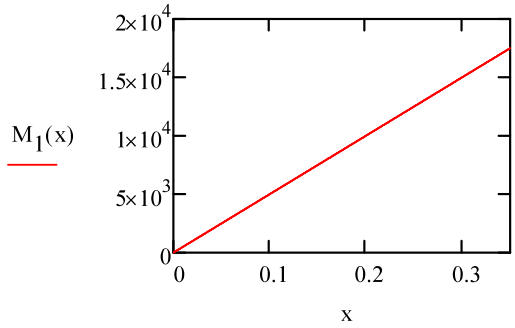

$$M_2(x) := \frac{(F_2)\cdot x}{2}$$

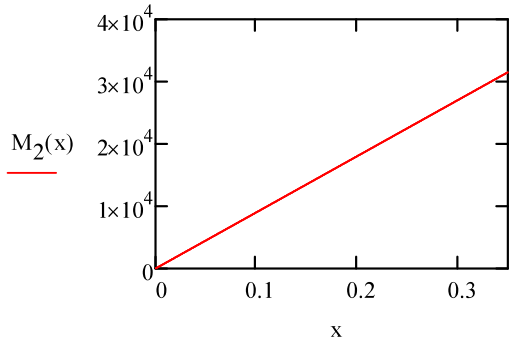

$$M_3(x) := \frac{(F_3)\cdot x}{2}$$

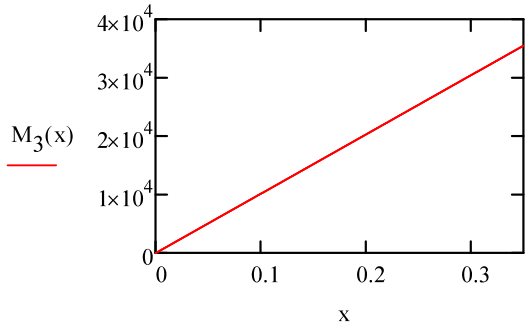

$\alpha := 0.81$ $\beta := 0.416$ $\alpha_{cc} := 1$ $f_{ck} := 45.55\text{MPa}$

$E_s := 200\text{GPa}$ $\varepsilon_{cu} := 3.5\cdot 10^{-3}$

$d_{BI} := 54.5\text{mm}$ $d_{BO} := 56.5\text{mm}$ $d_{TI} := 34\text{mm}$ $d_{TO} := 34\text{mm}$

$d_B := \frac{d_{BI} + d_{BO}}{2} = 55.5\cdot\text{mm}$ $d_T := \frac{d_{TI} + d_{TO}}{2} = 34\cdot\text{mm}$

$d := 300\text{mm} - \frac{(54.5 + 56.5)\text{mm}}{2} = 0.244\,\text{m}$

$P_{n.BI} := 50.63\text{mm}$ $P_{n.BO} := 50.85\text{mm}$ $P_{n.TI} := 51.14\text{mm}$ $P_{n.TO} := 51.43\text{mm}$

Length (unyielded zone):

$L_{uy.BI.left} := 78\text{mm}$ $L_{uy.BO.left} := 58\text{mm}$

$L_{uy.TI.left} := 387\text{mm}$ $L_{uy.TO.left} := 413\text{mm}$

$L_{uy.BI.right} := 217\text{mm}$ $L_{uy.BO.right} := 0\text{mm}$

$L_{uy.TI.right} := 249\text{mm}$ $L_{uy.TO.right} := 245\text{mm}$

Length (yielded zone):

$L_{y.BI} := 267\text{mm}$ $L_{y.BO} := 455\text{mm}$ $L_{y.TI} := 64\text{mm}$ $L_{y.TO} := 46\text{mm}$

$$d := 300\text{mm} - \frac{(41.5 + 71)\text{mm}}{2} = 0.244\,\text{m}$$

$A_{n.BI} := 203.74\text{mm}^2$ $\quad F_{y.BI} := A_{n.BI} \cdot f_y = 51.342 \cdot \text{kN}$

$A_{n.BO} := 203.93\text{mm}^2$ $\quad F_{y.BO} := A_{n.BO} \cdot f_y = 51.39 \cdot \text{kN}$

$A_{n.TI} := 205.53\text{mm}^2$ $\quad F_{y.TI} := A_{n.TI} \cdot f_y = 51.794 \cdot \text{kN}$

$A_{n.TO} := 204.29\text{mm}^2$ $\quad F_{y.TO} := A_{n.TO} \cdot f_y = 51.481 \cdot \text{kN}$

Mid-span:

$V_{mid.1} := V_1(35\text{cm}) = 50 \cdot \text{kN}$ $\quad M_{mid.1} := M_1(35\text{cm}) = 17.5 \cdot \text{kN} \cdot \text{m}$

$V_{mid.2} := V_2(35\text{cm}) = 90 \cdot \text{kN}$ $\quad M_{mid.2} := M_2(35\text{cm}) = 31.5 \cdot \text{kN} \cdot \text{m}$

$V_{mid.3} := V_3(35\text{cm}) = 101.5 \cdot \text{kN}$ $\quad M_{mid.3} := M_3(35\text{cm}) = 35.525 \cdot \text{kN} \cdot \text{m}$

$$F_{t.mid.1} := \frac{M_{mid.1}}{0.9 \cdot d \cdot 2} = 39.886 \cdot \text{kN}$$

$$F_{t.mid.2} := \frac{M_{mid.2}}{0.9 \cdot d \cdot 2} = 71.795 \cdot \text{kN}$$

$$F_{t.mid.3} := \frac{M_{mid.3}}{0.9 \cdot d \cdot 2} = 80.969 \cdot \text{kN}$$

Assume that neutral axis is between top and bottom reinforcement layers

$$x := \frac{\left(F_{y.BI} + F_{y.BO} - F_{y.TI} - F_{y.TO}\right)}{b \cdot \alpha \cdot f_{ck}} = -0.059 \cdot \text{mm} \qquad x > d_T = 0$$

Assume that neutral axis is above the top reinforcement layer

$$x := \frac{\left(F_{y.BI} + F_{y.BO} + F_{y.TI} + F_{y.TO}\right)}{b \cdot \alpha \cdot f_{ck}} = 22.334 \cdot \text{mm} \qquad x < d_T = 1$$

Compare to DIC => acceptable

$$\varepsilon_{sy} := \frac{f_y}{E_s} = 1.26 \times 10^{-3}$$

$$\varepsilon_{cu}\cdot\frac{d_T - x}{x} = 1.828\times 10^{-3}$$

$$\varepsilon_{cu}\cdot\frac{h - d_B - x}{x} = 0.035$$

$$F_c := f_{ck}\cdot\alpha\cdot b\cdot x = 206.007\cdot kN$$

$$d_m := h - d_B = 0.244\,m$$

$$M_{Rd} := f_{ck}\cdot\alpha\cdot b\cdot x\cdot\left(d_m - \beta\cdot x\right) - \left(F_{y.BI} + F_{y.BO}\right)\cdot\left(d_m - d_T\right) = 26.83\cdot kN\cdot m$$

Moment capacity of beam 1 $\quad P_y := \frac{M_{Rd}\cdot 2}{35cm} = 153.312\cdot kN$

$$\frac{x}{d_m} = 0.091$$

Bond stress right:

$$\tau_{y.BI.right} := \frac{F_{t.mid.3} - F_{y.BI}}{L_{y.BI}\cdot P_{n.BI}} = 2.192\cdot MPa \qquad \tau_{y.BO.right} := \frac{F_{t.mid.3} - F_{y.BO}}{L_{y.BO}\cdot P_{n.BO}} = 1.278\cdot MPa$$

$$\tau_{y.TI.right} := \frac{F_{t.mid.3} - F_{y.TI}}{\left(L_{y.TI}\cdot P_{n.TI}\right)} = 8.914\cdot MPa$$

There was no yielding phenomenon for TO

Hook length:

Angles were greater than 150 deg, which means that the hook belong to standard hook accroding to EC

$\phi := 16mm$ According to the EC, the hook length should to be longer than 5*ϕ

$$L_{develop.min} := 5\cdot\phi = 80\cdot mm$$

$L_{develop.TI} := 165mm$ $\qquad L_{develop.TO} := 150mm$

$L_{develop.BI} := 135mm$ $\qquad L_{develop.BO} := 160mm$

The hook part of TI was corroded and yielded, the remaining unyielded part was 62 mm.

The unyielded straight parts near the hook were shorter than hook length. (BI, BO)

Predicted anchorage strength:

Marques and Jirsa

$\psi := 1 \qquad f_{ck} = 6.606 \times 10^3 \cdot psi \qquad \phi = 0.63 \cdot in$

$f_h := 700(1 - 0.3 \cdot 0.63) \cdot \psi \cdot \sqrt{6.606 \cdot 10^3}\ psi = 318.132 \cdot MPa$ $\qquad f_h = 700(1 - 0.3 d_b)\psi\sqrt{f_c'} \le f_y$

Hook strength:

$F_{H.TI} := f_h \cdot A_{n.TI} = 65.386 \cdot kN$

$F_{H.TO} := f_h \cdot A_{n.TO} = 64.991 \cdot kN$

$F_{H.BI} := f_h \cdot A_{n.BI} = 64.816 \cdot kN$

$F_{H.BO} := f_h \cdot A_{n.BO} = 64.877 \cdot kN$

Residual strength:

$A_{ave.aftercorrosion.BI} := 202.14mm^2 \qquad A_{ave.aftercorrosion.BO} := 203.19mm^2$

$A_{ave.aftercorrosion.TI} := 205.15mm^2 \qquad A_{ave.aftercorrosion.TO} := 204.18mm^2$

$d_{after.BI} := 2\sqrt{\frac{A_{ave.aftercorrosion.BI}}{\pi}} = 0.632 \cdot in$

$f_{h.BI} := 700(1 - 0.3 \cdot 0.632) \cdot \psi \cdot \sqrt{6.606 \cdot 10^3}\ psi = 317.896 \cdot MPa$

$d_{after.BO} := 2\sqrt{\frac{A_{ave.aftercorrosion.BO}}{\pi}} = 0.633 \cdot in$

$f_{h.BO} := 700(1 - 0.3 \cdot 0.633) \cdot \psi \cdot \sqrt{6.606 \cdot 10^3}\ psi = 317.779 \cdot MPa$

$d_{after.TI} := 2\sqrt{\frac{A_{ave.aftercorrosion.TI}}{\pi}} = 0.636 \cdot in$

$f_{h.TI} := 700(1 - 0.3 \cdot 0.636) \cdot \psi \cdot \sqrt{6.606 \cdot 10^3}\ psi = 317.426 \cdot MPa$

$d_{after.TO} := 2\sqrt{\frac{A_{ave.aftercorrosion.TO}}{\pi}} = 0.635 \cdot in$

$f_{h.TO} := 700(1 - 0.3 \cdot 0.635) \cdot \psi \cdot \sqrt{6.606 \cdot 10^3}\ psi = 317.543 \cdot MPa$

$F_{h.BI} := f_h \cdot A_{ave.aftercorrosion.BI} = 64.307 \cdot kN$

$F_{h.BO} := f_h \cdot A_{ave.aftercorrosion.BO} = 64.641 \cdot kN$

$F_{h.TI} := f_h \cdot A_{ave.aftercorrosion.TI} = 65.265 \cdot kN$

$F_{h.TO} := f_h \cdot A_{ave.aftercorrosion.TO} = 64.956 \cdot kN$

$F_{u.BI} := F_{y.BI} - F_{h.BI} = -12.965 \cdot kN$

$F_{u.BO} := F_{y.BO} - F_{h.BO} = -13.251 \cdot kN$

$F_{u.TI} := F_{y.TI} - F_{h.TI} = -13.471 \cdot kN$

$F_{u.TO} := F_{y.TO} - F_{h.TO} = -13.475 \cdot kN$

BBK 04 3.9.1.5a

$f_{cm} := f_{ck} + 8MPa = 53.55 \cdot MPa$

$f_{ctm} := 0.3 \cdot \left(f_{ck} \cdot \frac{1}{MPa} \right)^{\frac{2}{3}} \cdot MPa = 3.826 \cdot MPa$

$f_{ctk.0.05} := 0.7 \cdot f_{ctm} = 2.678 \cdot MPa$

$\xi := 90$ For plain bar

$F_{h.BBK.BI} := A_{ave.aftercorrosion.BI} \cdot \xi \cdot f_{ctk.0.05} = 48.727 \cdot kN$

$F_{h.BBK.BO} := A_{ave.aftercorrosion.BO} \cdot \xi \cdot f_{ctk.0.05} = 48.98 \cdot kN$

$F_{h.BBK.TI} := A_{ave.aftercorrosion.TI} \cdot \xi \cdot f_{ctk.0.05} = 49.453 \cdot kN$

$F_{h.BBK.TO} := A_{ave.aftercorrosion.TO} \cdot \xi \cdot f_{ctk.0.05} = 49.219 \cdot kN$

The equation in ACI 318-77 for use in designing the development length of hooks was based on previous provisions (ACI 318-71, ACI 318-63), which were not supported by the results of the tests by Marques and Jirsa (1975). The procedure in ACI 318-77 separated the contributions of the hook and the straight lead embedment. The tensile stress contributed by the hooked portion of the bar was equal to

$$f_h = \xi \times \sqrt{f_c'} \tag{1.9}$$

where f_h is the tensile stress developed by the hooked portion of the bar, in psi, and f_c' is the concrete compressive strength. The values of ξ were given in a table as a function of the bar size, yield stress, and the casting position. The value of ξ could be increased 30% where transverse reinforcement was provided perpendicular to the plane of the hooked bar. The difference in stress between f_y and f_h was carried by substituting a value of stress equal to $f_y - f_h$ in place of f_y in the basic development length equation for straight reinforcement.

Sperry et al.

$$T_c = 304 f_{cm}^{0.29} \ell_{eh}^{1.1} d_b^{0.5}$$

$N := 0$ $A_{tr} := 0$ $n := 2$ $f_{ck} = 6.606 \times 10^3 \cdot psi$

$d_{after.BI} = 0.632 \cdot in$ $L_{uy.BI.right} = 8.543 \cdot in$

$F_{h.BI.Sperry} := \left[304 \cdot \left(6.606 \times 10^3\right)^{0.29} \cdot 8.543^{1.1} \cdot 0.632^{0.5} \cdot lb\right] \cdot g = 145.872 \cdot kN$

$d_{after.BO} = 0.633 \cdot in$ $L_{uy.BO.right} = 0 \cdot in$

$F_{h.BO.Sperry} := \left[304 \cdot \left(6.606 \times 10^3\right)^{0.29} \cdot 0^{1.1} \cdot 0.633^{0.5} \cdot lb\right] \cdot g = 0 \cdot kN$

$d_{after.TI} = 0.636 \cdot in$ $L_{uy.TI.right} = 9.803 \cdot in$

$F_{h.TI.Sperry} := \left[304 \cdot \left(6.606 \times 10^3\right)^{0.29} \cdot 9.803^{1.1} \cdot 0.636^{0.5} \cdot lb\right] \cdot g = 170.242 \cdot kN$

$d_{after.TO} = 0.635 \cdot in$ $L_{uy.TO.right} = 9.646 \cdot in$

$$F_{h.TO.Sperry} := \left[304 \cdot \left(6.606 \times 10^{3}\right)^{0.29} \cdot 9.646^{1.1} \cdot 0.635^{0.5} \cdot lb\right] \cdot g = 167.113 \cdot kN$$

where T_c is the anchorage strength of hooked bar without confining reinforcement in lb, T_h is the anchorage strength of hooked bar confined by confining reinforcement in lb, f_{cm} is the measured concrete compressive strength in psi, ℓ_{eh} is the embedment length of the hooked bar in in., d_b is the diameter of the hooked bar in in., N is the number of legs of confining reinforcement, A_{tr} is area of a single leg of the confining reinforcement, in in^2, and n is the number of the hooked being confined

C.2 Beam 18H

Beam 18

$b := 250mm$ $h := 300mm$ $f_y := 252MPa$

$F_1 := 167kN$ $F_2 := 192kN$ $F_3 := 199kN$

$L := 88cm$

$R_1 := \frac{F_1}{2} = 83.5 \cdot kN$

$R_2 := \frac{F_2}{2} = 96 \cdot kN$

$R_3 := \frac{F_3}{2} = 99.5 \cdot kN$

$V_1(x) := R_1$

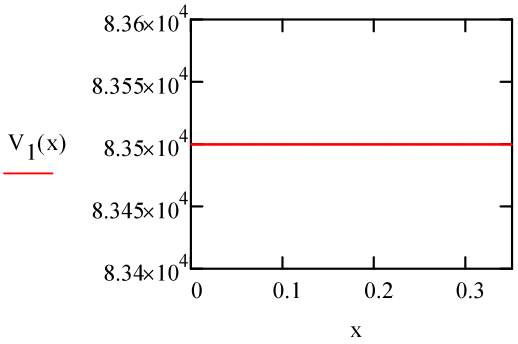

$V_2(x) := R_2$

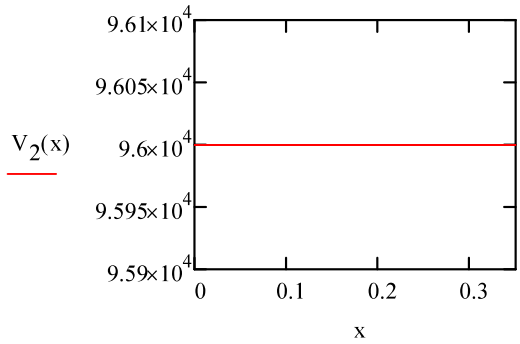

$V_3(x) := R_3$

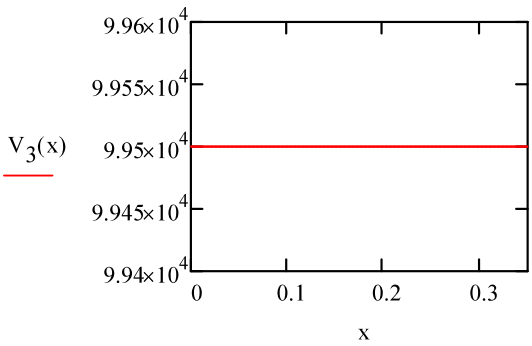

$M_1(x) := \frac{(F_1)\cdot x}{2}$

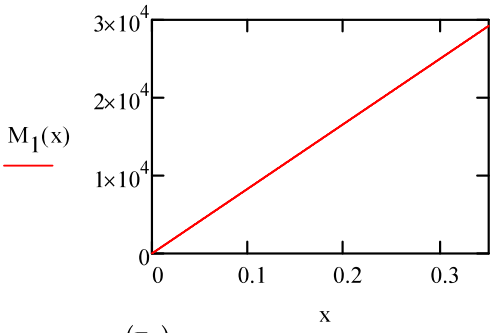

$M_2(x) := \frac{(F_2)\cdot x}{2}$

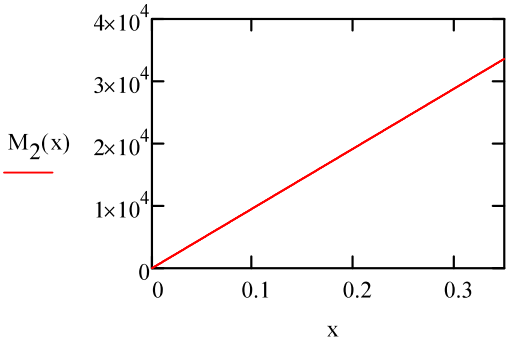

$$M_3(x) := \frac{(F_3)\cdot x}{2}$$

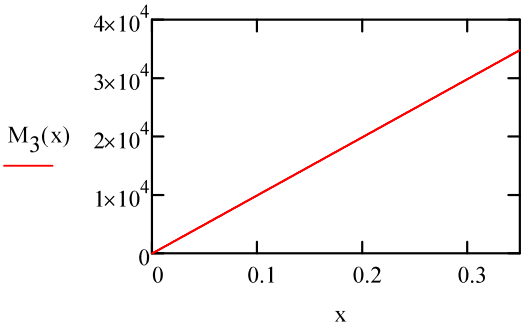

$$d := 300mm - \frac{(19 + 17)mm}{2} = 0.282\,m$$

$P_{n.I} := 51.05mm$ $P_{n.O} := 51.1mm$

$L_{uy.I.left} := 0mm$ $L_{uy.O.left} := 32mm$

$L_{uy.I.right} := 260mm$ $L_{uy.O.right} := 142mm$

$L_{y.I} := 172mm$ $L_{y.O} := 172mm$

$A_{n.I} := 206.93mm^2$ $F_{y.I} := A_{n.I}\cdot f_y = 52.146\cdot kN$

$A_{n.O} := 206.19mm^2$ $F_{y.O} := A_{n.O}\cdot f_y = 51.96\cdot kN$

Mid-span:

$V_{mid.1} := V_1(35cm) = 83.5\cdot kN$ $M_{mid.1} := M_1(35cm) = 29.225\cdot kN\cdot m$ $F_{t.mid.1} := \frac{M_{mid.1}}{0.9\cdot d\cdot 2} = 57.575\cdot kN$

$V_{mid.2} := V_2(35cm) = 96\cdot kN$ $M_{mid.2} := M_2(35cm) = 33.6\cdot kN\cdot m$ $F_{t.mid.2} := \frac{M_{mid.2}}{0.9\cdot d\cdot 2} = 66.194\cdot kN$

$V_{mid.3} := V_3(35cm) = 99.5\cdot kN$ $M_{mid.3} := M_3(35cm) = 34.825\cdot kN\cdot m$ $F_{t.mid.3} := \frac{M_{mid.3}}{0.9\cdot d\cdot 2} = 68.607\cdot kN$

Bond stress right:

$$\tau_{y.I.right} := \frac{F_{t.mid.2} - F_{y.I}}{(L_{y.I}\cdot P_{n.I})} = 1.6\cdot MPa \qquad \tau_{y.O.right} := \frac{F_{t.mid.2} - F_{y.O}}{(L_{y.O}\cdot P_{n.O})} = 1.619\cdot MPa$$

$\alpha := 0.81 \qquad \beta := 0.416 \qquad \alpha_{cc} := 1 \qquad f_{ck} := 45.55\text{MPa}$

$E_s := 200\text{GPa} \qquad \varepsilon_{cu} := 3.5 \cdot 10^{-3}$

$d_{BI} := 17\text{mm} \qquad d_{BO} := 19\text{mm} \qquad d_{TI} := 34\text{mm} \qquad d_{TO} := 34\text{mm}$

$d_B := \frac{d_{BI} + d_{BO}}{2} = 18 \cdot \text{mm} \qquad d_T := \frac{d_{TI} + d_{TO}}{2} = 34 \cdot \text{mm}$

Assume that neutral axis is between top and bottom reinforcement layers

$x := \frac{\left(F_{y.I} + F_{y.O} - F_{y.I} - F_{y.O}\right)}{b \cdot \alpha \cdot f_{ck}} = 0 \cdot \text{mm} \qquad x > d_T = 0$

Assume that neutral axis is above the topreinforcement layer

$x := \frac{\left(F_{y.I} + F_{y.O} + F_{y.I} + F_{y.O}\right)}{b \cdot \alpha \cdot f_{ck}} = 22.573 \cdot \text{mm} \qquad x < d_T = 1$

Compare to DIC above => acceptable

$\varepsilon_{sy} := \frac{f_y}{E_s} = 1.26 \times 10^{-3}$

$\varepsilon_{cu} \cdot \frac{d_T - x}{x} = 1.772 \times 10^{-3}$

$\varepsilon_{cu} \cdot \frac{h - d_B - x}{x} = 0.04$

$F_c := f_{ck} \cdot \alpha \cdot b \cdot x = 208.212 \cdot \text{kN}$

$d_m := h - d_B = 0.282\,\text{m}$

$M_{Rd} := f_{ck} \cdot \alpha \cdot b \cdot x \cdot \left(d_m - \beta \cdot x\right) - \left(F_{y.I} + F_{y.O}\right) \cdot \left(d_m - d_T\right) = 30.942 \cdot \text{kN} \cdot \text{m}$

Moment capacity of beam 19 $\qquad P_y := \frac{M_{Rd} \cdot 2}{35\text{cm}} = 176.813 \cdot \text{kN}$

$\frac{x}{d_m} = 0.08$

Development length:

Angles were greater than 150 deg, which means that the hook belong to standard hook accroding to EC

$\phi := 16mm$ According to the EC, the development length should to be longer than 5*ϕ

$L_{develop.min} := 5 \cdot \phi = 80 \cdot mm$

$L_{develop.I} := 88mm$ $L_{develop.O} := 113mm$

All unyielded straight parts near the hook were longer than development length. (Beam 18H)

Predicted anchorage strength :

Marques and Jirsa $f_h = 700(1-0.3d_b)\psi\sqrt{f_c'} \le f_y$

$\psi := 1$ $f_{ck} = 6.606 \times 10^3 \cdot psi$ $\phi = 0.63 \cdot in$

$f_h := 700(1 - 0.3 \cdot 0.63) \cdot \psi \cdot \sqrt{6.606 \cdot 10^3}\, psi = 318.132 \cdot MPa$

Hook strength:

$F_{H.I} := f_h \cdot A_{n.I} = 65.831 \cdot kN$

$F_{H.O} := f_h \cdot A_{n.O} = 65.596 \cdot kN$

Residual strength:

$A_{ave.aftercorrosion.I} := 205.35mm^2$ $A_{ave.aftercorrosion.O} := 206.66mm^2$

$d_{after.I} := 2\sqrt{\frac{A_{ave.aftercorrosion.I}}{\pi}} = 0.637 \cdot in$

$f_{h.I} := 700(1 - 0.3 \cdot 0.637) \cdot \psi \cdot \sqrt{6.606 \cdot 10^3}\, psi = 317.308 \cdot MPa$

$d_{after.O} := 2\sqrt{\frac{A_{ave.aftercorrosion.O}}{\pi}} = 0.639 \cdot in$

$f_{h.O} := 700(1 - 0.3 \cdot 0.639) \cdot \psi \cdot \sqrt{6.606 \cdot 10^3}\, psi = 317.073 \cdot MPa$

$F_{h.I} := f_h \cdot A_{ave.aftercorrosion.I} = 65.328 \cdot kN$

$F_{h.O} := f_h \cdot A_{ave.aftercorrosion.O} = 65.745 \cdot kN$

$F_{u.I} := F_{y.I} - F_{h.I} = -13.182 \cdot kN$

$F_{u.O} := F_{y.O} - F_{h.O} = -13.785 \cdot kN$

BBK 04 3.9.1.5a

$f_{cm} := f_{ck} + 8MPa = 53.55 \cdot MPa$

$f_{ctm} := 0.3 \cdot \left(f_{ck} \cdot \frac{1}{MPa} \right)^{\frac{2}{3}} \cdot MPa = 3.826 \cdot MPa$

$f_{ctk.0.05} := 0.7 \cdot f_{ctm} = 2.678 \cdot MPa$

$\xi := 90$ For plain bar

$F_{h.BBK.I} := A_{ave.aftercorrosion.I} \cdot \xi \cdot f_{ctk.0.05} = 49.501 \cdot kN$

$F_{h.BBK.O} := A_{ave.aftercorrosion.O} \cdot \xi \cdot f_{ctk.0.05} = 49.817 \cdot kN$

Sperry et al. $T_c = 304 f_{cm}^{0.29} \ell_{eh}^{1.1} d_b^{0.5}$

$N := 0$ $A_{tr} := 0$ $n := 2$ $f_{ck} = 6.606 \times 10^3 \cdot psi$

$d_{after.O} = 0.639 \cdot in$ $L_{uy.O.right} = 5.591 \cdot in$

$F_{h.O.Sperry} := \left[304 \cdot \left(6.606 \times 10^3 \right)^{0.29} \cdot 9.646^{1.1} \cdot 0.635^{0.5} \cdot lb \right] \cdot g = 167.113 \cdot kN$

$d_{after.I} = 0.637 \cdot in$ $L_{uy.I.right} = 10.236 \cdot in$

$F_{h.I.Sperry} := \left[304 \cdot \left(6.606 \times 10^3 \right)^{0.29} \cdot 8.543^{1.1} \cdot 0.632^{0.5} \cdot lb \right] \cdot g = 145.872 \cdot kN$

C.3 Beam 19

Beam 19

$b := 250mm$ $h := 300mm$

$F_1 := 115kN$ $F_2 := 178kN$ $F_3 := 183kN$ $f_y := 252MPa$

$L := 89cm$

$R_1 := \frac{F_1}{2} = 57.5 \cdot kN$

$R_2 := \frac{F_2}{2} = 89 \cdot kN$

$R_3 := \frac{F_3}{2} = 91.5 \cdot kN$

$V_1(x) := R_1$

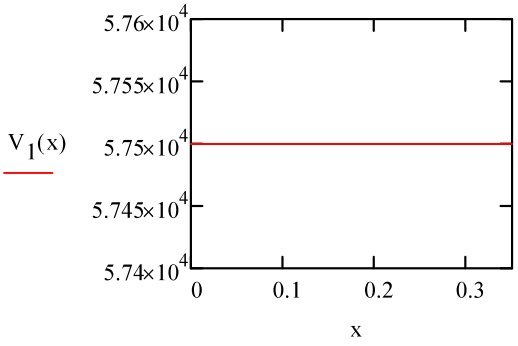

$V_2(x) := R_2$

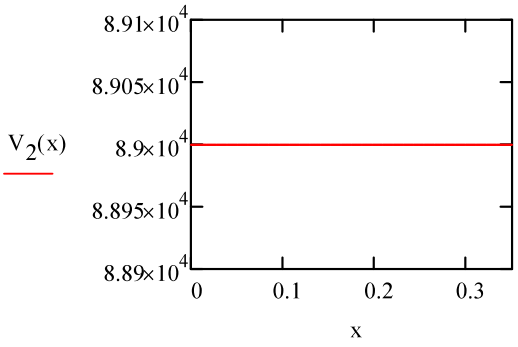

$V_3(x) := R_3$

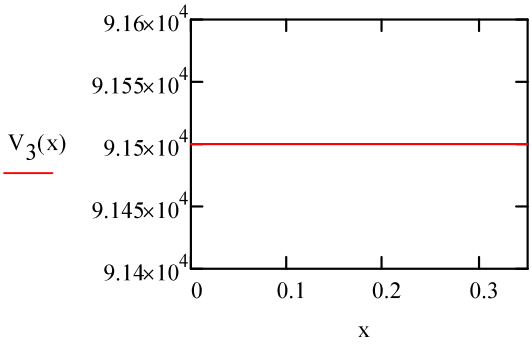

$$M_1(x) := \frac{(F_1)\cdot x}{2}$$

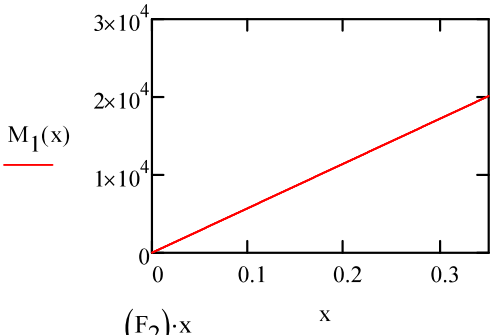

$$M_2(x) := \frac{(F_2)\cdot x}{2}$$

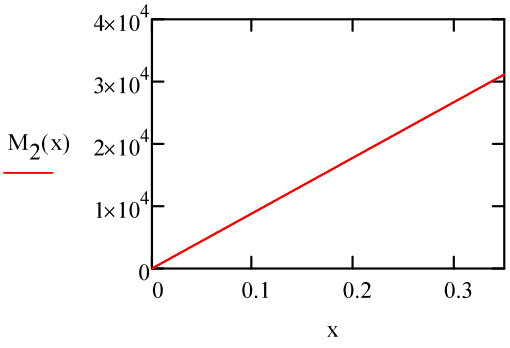

$$M_3(x) := \frac{(F_3)\cdot x}{2}$$

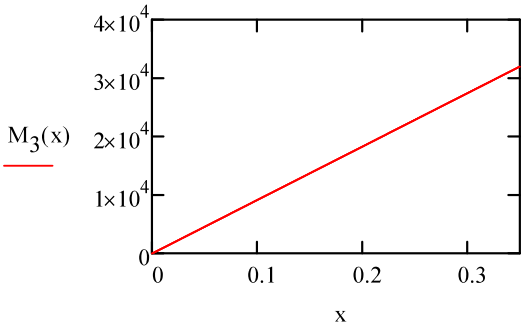

$P_{n.BI} := 51.06mm$ $P_{n.BO} := 51.48mm$ $P_{n.TI} := 51mm$ $P_{n.TO} := 51.13mm$

Length (unyielded zone):

$L_{uy.BI.left} := 13mm$ $L_{uy.BO.left} := 336mm$ $L_{uy.TI.left} := 65mm$ $L_{uy.TO.left} := 71mm$

$L_{uy.BI.right} := 367mm$ $L_{uy.BO.right} := 0mm$ $L_{uy.TI.right} := 219mm$ $L_{uy.TO.right} := 226mm$

Length (yielded zone):

$L_{y.BI} := 174mm$ $L_{y.BO} := 450mm$ $L_{y.TI} := 174mm$ $L_{y.TO} := 142mm$

$$d := 300mm - \frac{(41.5 + 71)mm}{2} = 0.244\,m$$

$A_{n.BI} := 203.75mm^2$ $F_{y.BI} := A_{n.BI}\cdot f_y = 51.345\cdot kN$

$A_{n.BO} := 209.46mm^2$ $F_{y.BO} := A_{n.BO}\cdot f_y = 52.784\cdot kN$

$A_{n.TI} := 202.92mm^2$ $F_{y.TI} := A_{n.TI}\cdot f_y = 51.136\cdot kN$

$A_{n.TO} := 207.38mm^2$ $F_{y.TO} := A_{n.TO}\cdot f_y = 52.26\cdot kN$

Mid-span:

$V_{mid.1} := V_1(35cm) = 57.5\cdot kN$ $M_{mid.1} := M_1(35cm) = 20.125\cdot kN\cdot m$ $F_{t.mid.1} := \frac{M_{mid.1}}{0.9\cdot d\cdot 2} = 45.869\cdot kN$

$V_{mid.2} := V_2(35cm) = 89\cdot kN$ $M_{mid.2} := M_2(35cm) = 31.15\cdot kN\cdot m$ $F_{t.mid.2} := \frac{M_{mid.2}}{0.9\cdot d\cdot 2} = 70.997\cdot kN$

$V_{mid.3} := V_3(35cm) = 91.5\cdot kN$ $M_{mid.3} := M_3(35cm) = 32.025\cdot kN\cdot m$ $F_{t.mid.3} := \frac{M_{mid.3}}{0.9\cdot d\cdot 2} = 72.991\cdot kN$

$F_t := \max\left(F_{t.mid.1}, F_{t.mid.2}, F_{t.mid.3}\right) = 72.991 \cdot kN$

Bond stress right:

$\tau_{y.BI.right} := \frac{F_t - F_{y.BI}}{L_{y.BI} \cdot P_{n.BI}} = 2.436 \cdot MPa$ $\tau_{y.BO.right} := \frac{F_t - F_{y.BO}}{L_{y.BO} \cdot P_{n.BO}} = 0.872 \cdot MPa$

$\tau_{y.TI.right} := 0.5 \cdot \frac{F_t - F_{y.TI}}{\left(\frac{L_{y.TI}}{2} \cdot P_{n.TI}\right)} = 2.463 \cdot MPa$ $\tau_{y.TO} := 0.5 \cdot \frac{F_t - F_{y.TO}}{\left(\frac{L_{y.TO}}{2} \cdot P_{n.TO}\right)} = 2.855 \cdot MPa$

$\alpha := 0.81$ $\beta := 0.416$ $\alpha_{cc} := 1$ $f_{ck} := 45.55MPa$

$E_s := 200GPa$ $\varepsilon_{cu} := 3.5 \cdot 10^{-3}$

$d_{BI} := 71mm$ $d_{BO} := 41.5mm$ $d_{TI} := 34mm$ $d_{TO} := 34mm$

$d_B := \frac{d_{BI} + d_{BO}}{2} = 56.25 \cdot mm$ $d_T := \frac{d_{TI} + d_{TO}}{2} = 34 \cdot mm$

Assume that neutral axis is between top and bottom reinforcement layers

$x := \frac{\left(F_{y.BI} + F_{y.BO} - F_{y.TI} - F_{y.TO}\right)}{b \cdot \alpha \cdot f_{ck}} = 0.08 \cdot mm$ $x > d_T = 0$

Assume that neutral axis is above the topreinforcement layer

$x := \frac{\left(F_{y.BI} + F_{y.BO} + F_{y.TI} + F_{y.TO}\right)}{b \cdot \alpha \cdot f_{ck}} = 22.499 \cdot mm$ $x < d_T = 1$

Compare to DIC above => acceptable

$\varepsilon_{sy} := \frac{f_y}{E_s} = 1.26 \times 10^{-3}$

$\varepsilon_{cu} \cdot \frac{d_T - x}{x} = 1.789 \times 10^{-3}$

$\varepsilon_{cu} \cdot \frac{h - d_B - x}{x} = 0.034$

$F_c := f_{ck} \cdot \alpha \cdot b \cdot x = 207.525 \cdot kN$

$d_m := h - d_B = 0.244\,m$

$M_{Rd} := f_{ck} \cdot \alpha \cdot b \cdot x \cdot (d_m - \beta \cdot x) - (F_{y.BI} + F_{y.BO}) \cdot (d_m - d_T) = 26.801 \cdot kN \cdot m$

Moment capacity of beam 19 $P_y := \frac{M_{Rd} \cdot 2}{35cm} = 153.147 \cdot kN$

$\frac{x}{d_m} = 0.092$

Development length:

Angles were greater than 150 deg, which means that the hook belong to standard hook accroding to EC

$\phi := 16mm$ According to the EC, the development length should to be longer than 5*ϕ

$L_{develop.min} := 5 \cdot \phi = 80 \cdot mm$

$L_{develop.TI} := 117mm$ $L_{develop.TO} := 87mm$

$L_{develop.BI} := 86mm$ $L_{develop.BO} := 116mm$

The unyielded straight part near the hook was shorter than development length. (BO)

Predicted anchorage strength:

Marques and Jirsa $f_h = 700(1-0.3d_b)\psi\sqrt{f_c'} \le f_y$

$\psi := 1$ $f_{ck} = 6.606 \times 10^3 \cdot psi$ $\phi = 0.63 \cdot in$

$f_h := 700(1 - 0.3 \cdot 0.63) \cdot \psi \cdot \sqrt{6.606 \cdot 10^3}\, psi = 318.132 \cdot MPa$

Hook strength:

$F_{H.TI} := f_h \cdot A_{n.TI} = 64.555 \cdot kN$

$F_{H.TO} := f_h \cdot A_{n.TO} = 65.974 \cdot kN$

$F_{H.BI} := f_h \cdot A_{n.BI} = 64.819 \cdot kN$

$F_{H.BO} := f_h \cdot A_{n.BO} = 66.636 \cdot kN$

Residual strength:

$A_{ave.aftercorrosion.BI} := 203.19mm^2$ $A_{ave.aftercorrosion.BO} := 206.94mm^2$

$A_{ave.aftercorrosion.TI} := 202.74mm^2$ $A_{ave.aftercorrosion.TO} := 204.62mm^2$

$$d_{after.BI} := 2\sqrt{\frac{A_{ave.aftercorrosion.BI}}{\pi}} = 0.633 \cdot in$$

$$f_{h.BI} := 700(1 - 0.3 \cdot 0.633) \cdot \psi \cdot \sqrt{6.606 \cdot 10^3}\ psi = 317.779 \cdot MPa$$

$$d_{after.BO} := 2\sqrt{\frac{A_{ave.aftercorrosion.BO}}{\pi}} = 0.639 \cdot in$$

$$f_{h.BO} := 700(1 - 0.3 \cdot 0.639) \cdot \psi \cdot \sqrt{6.606 \cdot 10^3}\ psi = 317.073 \cdot MPa$$

$$d_{after.TI} := 2\sqrt{\frac{A_{ave.aftercorrosion.TI}}{\pi}} = 0.633 \cdot in$$

$$f_{h.TI} := 700(1 - 0.3 \cdot 0.633) \cdot \psi \cdot \sqrt{6.606 \cdot 10^3}\ psi = 317.779 \cdot MPa$$

$$d_{after.TO} := 2\sqrt{\frac{A_{ave.aftercorrosion.TO}}{\pi}} = 0.635 \cdot in$$

$$f_{h.TO} := 700(1 - 0.3 \cdot 0.635) \cdot \psi \cdot \sqrt{6.606 \cdot 10^3}\ psi = 317.543 \cdot MPa$$

$$F_{h.BI} := f_h \cdot A_{ave.aftercorrosion.BI} = 64.641 \cdot kN$$

$$F_{h.BO} := f_h \cdot A_{ave.aftercorrosion.BO} = 65.834 \cdot kN$$

$$F_{h.TI} := f_h \cdot A_{ave.aftercorrosion.TI} = 64.498 \cdot kN$$

$$F_{h.TO} := f_h \cdot A_{ave.aftercorrosion.TO} = 65.096 \cdot kN$$

$$F_{u.BI} := F_{y.BI} - F_{h.BI} = -13.296 \cdot kN$$

$$F_{u.BO} := F_{y.BO} - F_{h.BO} = -13.05 \cdot kN$$

$$F_{u.TI} := F_{y.TI} - F_{h.TI} = -13.362 \cdot kN$$

$$F_{u.TO} := F_{y.TO} - F_{h.TO} = -12.836 \cdot kN$$

BBK 04 3.9.1.5a

$$f_{cm} := f_{ck} + 8MPa = 53.55 \cdot MPa$$

$$f_{ctm} := 0.3 \cdot \left(f_{ck} \cdot \frac{1}{MPa}\right)^{\frac{2}{3}} \cdot MPa = 3.826 \cdot MPa$$

$$f_{ctk.0.05} := 0.7 \cdot f_{ctm} = 2.678 \cdot MPa$$

$\xi := 90$ For plain bar

$F_{h.BBK.BI} := A_{ave.aftercorrosion.BI} \cdot \xi \cdot f_{ctk.0.05} = 48.98 \cdot kN$

$F_{h.BBK.BO} := A_{ave.aftercorrosion.BO} \cdot \xi \cdot f_{ctk.0.05} = 49.884 \cdot kN$

$F_{h.BBK.TI} := A_{ave.aftercorrosion.TI} \cdot \xi \cdot f_{ctk.0.05} = 48.872 \cdot kN$

$F_{h.BBK.TO} := A_{ave.aftercorrosion.TO} \cdot \xi \cdot f_{ctk.0.05} = 49.325 \cdot kN$

Sperry et al. $T_c = 304 f_{cm}^{0.29} \ell_{eh}^{1.1} d_b^{0.5}$

$f_{ck} = 6.606 \times 10^3 \cdot psi$

$d_{after.BI} = 0.633 \cdot in$ $L_{uy.BI.right} = 14.449 \cdot in$

$F_{h.BI.Sperry} := \left[304 \cdot \left(6.606 \times 10^3\right)^{0.29} \cdot 8.543^{1.1} \cdot 0.632^{0.5} \cdot lb\right] \cdot g = 145.872 \cdot kN$

$d_{after.BO} = 0.639 \cdot in$ $L_{uy.BO.right} = 0 \cdot in$

$F_{h.BO.Sperry} := \left[304 \cdot \left(6.606 \times 10^3\right)^{0.29} \cdot 0^{1.1} \cdot 0.633^{0.5} \cdot lb\right] \cdot g = 0 \cdot kN$

$d_{after.TI} = 0.633 \cdot in$ $L_{uy.TI.right} = 8.622 \cdot in$

$F_{h.TI.Sperry} := \left[304 \cdot \left(6.606 \times 10^3\right)^{0.29} \cdot 9.803^{1.1} \cdot 0.636^{0.5} \cdot lb\right] \cdot g = 170.242 \cdot kN$

$d_{after.TO} = 0.635 \cdot in$ $L_{uy.TO.right} = 8.898 \cdot in$

$F_{h.TO.Sperry} := \left[304 \cdot \left(6.606 \times 10^3\right)^{0.29} \cdot 9.646^{1.1} \cdot 0.635^{0.5} \cdot lb\right] \cdot g = 167.113 \cdot kN$

C.4 Beam 10D

10 D spliced hook bars Consider shear crack / bending crack

$b := 250\ mm$

$h := 300\ mm$

$L_{10D} := 92\ cm$

$P_{10D.max} := 204.956\ kN$ maximum applied force

$R_{10D} := \frac{P_{10D.max}}{2} = 102.478\ kN$ support

$a_s := 100\ mm$ distance between the edge and the support

$V_{10D} := R_{10D} = 102.478\ kN$

$M_{10D} := R_{10D} \cdot \frac{L_{10D} - 2 \cdot a_s}{2} = 36.892\ kN \cdot m$ moment in middle cross-section

$c_{top} := 34\ mm$

$c_{in.left} := 44\ mm$ $c_{in.right} := 45\ mm$

$c_{out.left} := 34\ mm$ $c_{out.right} := 25\ mm$ concrete cover

$c_{av} := \left(c_{in.left} + c_{in.right} + c_{out.left} + c_{out.right}\right) \cdot \frac{1}{4} = 37\ mm$

$d := h - c_{av} = 0.263\ m$

$F_{t1} := \frac{M_{10D}}{4 \cdot 0.9 \cdot d} = 38.965\ kN$ tensile force

Yield force

$f_y := 252\ MPa$ assumed yield strength

$A_{s.DI} := 203.82\ mm^2$ $A_{s.DO} := 200.92\ mm^2$

$A_{s.DICR} := 203.90\ mm^2$ $A_{s.DOCR} := 197.42\ mm^2$

$F_{y.DI} := f_y \cdot A_{s.DI} = 51.363\ kN$

$F_{y.DO} := f_y \cdot A_{s.DO} = 50.632\ kN$

$F_{y.DICR} := f_y \cdot A_{s.DO} = 50.632\ kN$

$F_{y.DOCR} := f_y \cdot A_{s.DOCR} = 49.75\ kN$

Bond in the unyielded zone

$l_{uy.DI} := 160\ mm$ $l_{uy.DO} := 187\ mm$ $l_{uy.DICR} := 273.74\ mm$ $l_{uy.DOCR} := 320\ mm$

$l_{a.DI} := 660\ mm$ $l_{a.DO} := 695\ mm$ $l_{a.DICR} := 717\ mm$ $l_{a.DOCR} := 815\ mm$

$P_{n.DI} := 50.59\ mm$ $P_{n.DO} := 50.40\ mm$ $P_{n.DICR} := 50.62\ mm$ $P_{n.DOCR} := 49.81\ mm$

Assume bond in unyielded zone

$\tau_{uy.DI} := 2\ MPa$

$\tau_{uy.DO} := 2\ MPa$

$\tau_{uy.DICR} := 2\ MPa$

$\tau_{uy.DOCR} := 2\ MPa$

$F_{u.DI} := \tau_{uy.DI} \cdot l_{uy.DI} \cdot P_{n.DI} = 16.189\ kN$

$F_{u.DO} := \tau_{uy.DO} \cdot l_{uy.DO} \cdot P_{n.DO} = 18.85\ kN$

$F_{u.DICR} := \tau_{uy.DICR} \cdot l_{uy.DICR} \cdot P_{n.DICR} = 27.713\ kN$

$F_{u.DOCR} := \tau_{uy.DOCR} \cdot l_{uy.DOCR} \cdot P_{n.DOCR} = 31.878\ kN$

$F_{h.DI} := F_{y.DI} - F_{u.DI} = 35.174\ kN$

$F_{h.DO} := F_{y.DO} - F_{u.DO} = 31.782\ kN$

$F_{h.DICR} := F_{y.DICR} - F_{u.DICR} = 22.918\ kN$

$F_{h.DOCR} := F_{y.DOCR} - F_{u.DOCR} = 17.871\ kN$

Bond strength in yielded zone (Assumed to be zero)

$$\tau_{y.DI} := \frac{F_{t1} - F_{y.DI}}{P_{n.DI} \cdot 32.63\ mm} = -7.51\ MPa$$

$$\tau_{y.DO} := \frac{F_{t1} - F_{y.DO}}{P_{n.DO} \cdot 36.87\ mm} = -6.278\ MPa$$

$$\tau_{y.DOCR} := \frac{F_{t1} - F_{y.DOCR}}{P_{n.DOCR} \cdot 57.22\ mm} = -3.784\ MPa$$

Marques and Jirsa

$\psi := 1 \qquad f_{ck} := 6.606 \cdot 10^3 \ \textit{psi} \qquad \phi := 0.63 \ \textit{in}$

$f_h := 700 \cdot (1 - 0.3 \cdot 0.63) \cdot \psi \cdot \sqrt{6.606 \cdot 10^3 \ \textit{psi}} = 318.132 \ \textit{MPa}$

Hook strength

$F_{MJ.DI} := f_h \cdot A_{s.DI} = 64.842 \ \textit{kN}$

$F_{MJ.DO} := f_h \cdot A_{s.DO} = 63.919 \ \textit{kN}$

$F_{MJ.DICR} := f_h \cdot A_{s.DICR} = 64.867 \ \textit{kN}$

$F_{MJ.DOCR} := f_h \cdot A_{s.DOCR} = 62.806 \ \textit{kN}$

Residual strength

$A_{c.DI} := 201.95 \ \textit{mm}^2 \quad A_{c.DO} := 200.27 \ \textit{mm}^2 \quad A_{c.DICR} := 201.79 \ \textit{mm}^2 \quad A_{c.DOCR} := 196.89 \ \textit{mm}^2$

$d_{after.DI} := 2 \cdot \sqrt{\frac{A_{c.DI}}{\pi}} = 0.631 \ \textit{in}$

$f_{h.DI} := 700 \cdot (1 - 0.3 \cdot 0.631) \cdot \psi \cdot \sqrt{6.606 \cdot 10^3 \ \textit{psi}} = 318.014 \ \textit{MPa}$

$d_{after.DO} := 2 \cdot \sqrt{\frac{A_{c.DO}}{\pi}} = 0.629 \ \textit{in}$

$f_{h.DO} := 700 \cdot (1 - 0.3 \cdot 0.629) \cdot \psi \cdot \sqrt{6.606 \cdot 10^3 \ \textit{psi}} = 318.25 \ \textit{MPa}$

$d_{after.DICR} := 2 \cdot \sqrt{\frac{A_{c.DICR}}{\pi}} = 0.631 \ \textit{in}$

$f_{h.DICR} := 700 \cdot (1 - 0.3 \cdot 0.631) \cdot \psi \cdot \sqrt{6.606 \cdot 10^3 \ \textit{psi}} = 318.014 \ \textit{MPa}$

$d_{after.DOCR} := 2 \cdot \sqrt{\frac{A_{c.DOCR}}{\pi}} = 0.623 \ \textit{in}$

$f_{h.DOCR} := 700 \cdot (1 - 0.3 \cdot 0.623) \cdot \psi \cdot \sqrt{6.606 \cdot 10^3 \ \textit{psi}} = 318.956 \ \textit{MPa}$

$F_{after.DI} := f_{h.DI} \cdot A_{c.DI} = 64.223 \ \textit{kN}$

$F_{after.DO} := f_{h.DI} \cdot A_{c.DO} = 63.689 \ \textit{kN}$

$F_{after.DICR} := f_{h.DICR} \cdot A_{c.DICR} = 64.172 \ \textit{kN}$

$F_{after.DOCR} := f_{h.DOCR} \cdot A_{c.DOCR} = 62.799 \ \textit{kN}$

$F_{u.a.DI} := F_{y.DI} - F_{after.DI} = -12.86 \ \textit{kN}$

$F_{u.a.DO} := F_{y.DO} - F_{after.DO} = -13.057 \ \textit{kN}$

$F_{u.a.DICR} := F_{y.DICR} - F_{after.DICR} = -13.54\ \boldsymbol{kN}$

$F_{u.a.DOCR} := F_{y.DOCR} - F_{after.DOCR} = -13.049\ \boldsymbol{kN}$

BBK

$f_{cm} := f_{ck} + 8\ \boldsymbol{MPa} = 53.547\ \boldsymbol{MPa}$

$f_{ctm} := 0.3 \cdot \left(f_{ck} \cdot \frac{1}{1\ \boldsymbol{MPa}} \right)^{\frac{2}{3}} \cdot 1\ \boldsymbol{MPa} = 3.826\ \boldsymbol{MPa}$

$f_{ctk0.05} := 0.7 \cdot f_{ctm} = 2.678\ \boldsymbol{MPa}$

$\xi := 90$

$F_{h.BBK.DI} := A_{c.DI} \cdot \xi \cdot f_{ctk0.05} = 48.679\ \boldsymbol{kN}$

$F_{h.BBK.DO} := A_{c.DO} \cdot \xi \cdot f_{ctk0.05} = 48.274\ \boldsymbol{kN}$

$F_{h.BBK.DICR} := A_{c.DICR} \cdot \xi \cdot f_{ctk0.05} = 48.641\ \boldsymbol{kN}$

$F_{h.BBK.DOCR} := A_{c.DOCR} \cdot \xi \cdot f_{ctk0.05} = 47.46\ \boldsymbol{kN}$

$\alpha := 0.81 \qquad \beta := 0.416 \qquad f_{ck} = 45.547\ \boldsymbol{MPa} \qquad E_s := 200\ \boldsymbol{GPa} \qquad \varepsilon_{cu} := 3.5 \cdot 10^{-3}$

$c_{in.left} := 44\ \boldsymbol{mm}$

$c_{out.left} := 34\ \boldsymbol{mm}$

$c_{in.right} := 45\ \boldsymbol{mm}$

$d_{bottom} := \frac{c_{in.left} + c_{out.left} + c_{in.right} + c_{out.right}}{4} = 37\ \boldsymbol{mm}$

$c_{out.right} := 25\ \boldsymbol{mm}$

$c_{top} = 34\ \boldsymbol{mm} \qquad d_{top} := \frac{c_{top} + c_{top}}{2} = 34\ \boldsymbol{mm}$

Assumption: n.a. is above the top reinforcement

$x := \frac{\left(F_{y.DI} + F_{y.DO} + F_{y.DICR} + F_{y.DOCR}\right) + \left(F_{y.DI} + F_{y.DO}\right)}{b \cdot \alpha \cdot f_{ck}} = 33\ \boldsymbol{mm}$

Considering the concrete spalling

$x_{spalling} := \frac{F_{y.DI} + F_{y.DO} + F_{y.DICR} + F_{y.DOCR}}{b \cdot \alpha \cdot f_{ck}} = 21.942\ \boldsymbol{mm}$

$$M_{Rd.1} := f_{ck} \cdot \alpha \cdot b \cdot x \cdot \left(d - \beta \cdot x\right) = 75.871 \ \boldsymbol{kN \cdot m}$$

$$M_{Rd.2} := \left(F_{y.DI} + F_{y.DO}\right) \cdot \left(d - c_{top}\right) = 23.357 \ \boldsymbol{kN \cdot m}$$

$$M_{Rd} := M_{Rd.1} - M_{Rd.2} = 52.514 \ \boldsymbol{kN \cdot m}$$

$$P_{yield} := \frac{M_{Rd} \cdot 2}{\left(\frac{L_{10D}}{2} - a_s\right)} = 291.746 \ \boldsymbol{kN}$$

C.5 Beam 13G

13 G spliced hook bars

$b := 250\ mm$

$h := 300\ mm$

$L_{13G} := 99.5\ cm$

$P_{13G.max} := 300.817\ kN$ maximum applied load

$R_{13G} := \frac{P_{13G.max}}{2} = 150.409\ kN$

$a_s := 100\ mm$

$V_{13G} := R_{13G} = 150.409\ kN$

$M_{13G} := R_{13G} \cdot \frac{L_{13G} - 2 \cdot a_s}{2} = 59.787\ kN \cdot m$

$c_{top} := 34\ mm$

$c_{in.left} := 38\ mm$ $c_{in.right} := 34\ mm$

$c_{out.left} := 24\ mm$ $c_{out.right} := 36\ mm$

$c_{av} := \left(c_{in.left} + c_{in.right} + c_{out.left} + c_{out.right}\right) \cdot \frac{1}{4} = 33\ mm$

$d := h - c_{av} = 0.267\ m$

$F_{t1} := \frac{M_{13G}}{4 \cdot 0.9 \cdot d} = 62.201\ kN$

Yield force

$f_y := 252\ MPa$

$A_{s.GI} := 202.36\ mm^2$ $A_{s.GO} := 199.44\ mm^2$

$A_{s.GICR} := 205.79\ mm^2$ $A_{s.GOCR} := 203.46\ mm^2$

$F_{y.GI} := f_y \cdot A_{s.GI} = 50.995\ kN$

$F_{y.GO} := f_y \cdot A_{s.GO} = 50.259\ kN$

$F_{y.GICR} := f_y \cdot A_{s.GICR} = 51.859\ kN$

$F_{y.GOCR} := f_y \cdot A_{s.GOCR} = 51.272\ kN$

Bond in the unyielded zone

$l_{uy.GI} := 329.5\ mm$ $l_{uy.GO} := 356.5\ mm$ $l_{uy.GICR} := 145\ mm$ $l_{uy.GOCR} := 193\ mm$

$l_{a.GI} := 840\ mm$ $l_{a.GO} := 867\ mm$ $l_{a.GICR} := 725\ mm$ $l_{a.GOCR} := 733\ mm$

$P_{n.GI} := 50.40\ mm$ $P_{n.GO} := 49.93\ mm$ $P_{n.GICR} := 50.79\ mm$ $P_{n.GOCR} := 50.38\ mm$

Assume bond in unyielded zone

$\tau_{uy.GI} := 2\ MPa$

$\tau_{uy.GO} := 2\ MPa$

$\tau_{uy.GICR} := 2\ MPa$

$\tau_{uy.GOCR} := 2\ MPa$

$F_{u.GI} := \tau_{uy.GI} \cdot l_{uy.GI} \cdot P_{n.GI} = 33.214\ kN$

$F_{u.GO} := \tau_{uy.GO} \cdot l_{uy.GO} \cdot P_{n.GO} = 35.6\ kN$

$F_{u.GICR} := \tau_{uy.GICR} \cdot l_{uy.GICR} \cdot P_{n.GICR} = 14.729\ kN$

$F_{u.GOCR} := \tau_{uy.GOCR} \cdot l_{uy.GOCR} \cdot P_{n.GOCR} = 19.447\ kN$

$F_{h.GI} := F_{y.GI} - F_{u.GI} = 17.781\ kN$

$F_{h.GO} := F_{y.GO} - F_{u.GO} = 14.659\ kN$

$F_{h.GICR} := F_{y.GICR} - F_{u.GICR} = 37.13\ kN$

$F_{h.GOCR} := F_{y.GOCR} - F_{u.GOCR} = 31.825\ kN$

Bond strength in yielded zone

$$\tau_{y.GICR} := \frac{F_{t1} - F_{y.GICR}}{P_{n.GICR} \cdot 93.68\ mm} = 2.174\ MPa$$

$$\tau_{y.GOCR} := \frac{F_{t1} - F_{y.GOCR}}{P_{n.GOCR} \cdot 55.5\ mm} = 3.909\ MPa$$

Marques and Jirsa

$\psi := 1$ $f_{ck} := 6.606 \cdot 10^3$ *psi* $\phi := 0.63$ *in*

$f_h := 700 \cdot (1 - 0.3 \cdot 0.63) \cdot \psi \cdot \sqrt{6.606 \cdot 10^3}$ *psi* $= 318.132$ *MPa*

Hook strength

$F_{MJ.GI} := f_h \cdot A_{s.GI} = 64.377$ *kN*

$F_{MJ.GO} := f_h \cdot A_{s.GO} = 63.448$ *kN*

$F_{MJ.GICR} := f_h \cdot A_{s.GICR} = 65.468$ *kN*

$F_{MJ.GOCR} := f_h \cdot A_{s.GOCR} = 64.727$ *kN*

Residual strength

$A_{c.GI} := 199.48$ mm^2 $A_{c.GO} := 196.96$ mm^2

$A_{c.GICR} := 205$ mm^2 $A_{c.GOCR} := 201.80$ mm^2

$d_{after.GI} := 2 \cdot \sqrt{\frac{A_{c.GI}}{\pi}} = 0.627$ *in*

$f_{h.GI} := 700 \cdot (1 - 0.3 \cdot 0.627) \cdot \psi \cdot \sqrt{6.606 \cdot 10^3}$ *psi* $= 318.485$ *MPa*

$d_{after.GO} := 2 \cdot \sqrt{\frac{A_{c.GO}}{\pi}} = 0.623$ *in*

$f_{h.GO} := 700 \cdot (1 - 0.3 \cdot 0.623) \cdot \psi \cdot \sqrt{6.606 \cdot 10^3}$ *psi* $= 318.956$ *MPa*

$d_{after.GICR} := 2 \cdot \sqrt{\frac{A_{c.GICR}}{\pi}} = 0.636$ *in*

$f_{h.GICR} := 700 \cdot (1 - 0.3 \cdot 0.636) \cdot \psi \cdot \sqrt{6.606 \cdot 10^3}$ *psi* $= 317.426$ *MPa*

$d_{after.GOCR} := 2 \cdot \sqrt{\frac{A_{c.GOCR}}{\pi}} = 0.631$ *in*

$f_{h.GOCR} := 700 \cdot (1 - 0.3 \cdot 0.631) \cdot \psi \cdot \sqrt{6.606 \cdot 10^3}$ *psi* $= 318.014$ *MPa*

$F_{after.GI} := f_{h.GI} \cdot A_{c.GI} = 63.531$ *kN*

$F_{after.GO} := f_{h.GO} \cdot A_{c.GO} = 62.822$ *kN*

$F_{u.a.GI} := F_{y.GI} - F_{after.GI} = -12.537$ *kN*

$F_{u.a.GO} := F_{y.GO} - F_{after.GO} = -12.563$ *kN*

$F_{after.GICR} := f_{h.GICR} \cdot A_{c.GICR} = 65.072\ kN$

$F_{after.GOCR} := f_{h.GOCR} \cdot A_{c.GOCR} = 64.175\ kN$

$F_{u.a.GICR} := F_{y.GICR} - F_{after.GICR} = -13.213\ kN$

$F_{u.a.GOCR} := F_{y.GOCR} - F_{after.GOCR} = -12.903\ kN$

BBK

$f_{cm} := f_{ck} + 8\ MPa = 53.547\ MPa$

$f_{ctm} := 0.3 \cdot \left(f_{ck} \cdot \frac{1}{1\ MPa} \right)^{\frac{2}{3}} \cdot 1\ MPa = 3.826\ MPa$

$f_{ctk0.05} := 0.7 \cdot f_{ctm} = 2.678\ MPa$

$\xi := 90$

$F_{h.BBK.GI} := A_{c.GI} \cdot \xi \cdot f_{ctk0.05} = 48.084\ kN$

$F_{h.BBK.GO} := A_{c.GO} \cdot \xi \cdot f_{ctk0.05} = 47.476\ kN$

$F_{h.BBK.GICR} := A_{c.GICR} \cdot \xi \cdot f_{ctk0.05} = 49.414\ kN$

$F_{h.BBK.GOCR} := A_{c.GOCR} \cdot \xi \cdot f_{ctk0.05} = 48.643\ kN$

$\alpha := 0.81 \qquad \beta := 0.416 \qquad f_{ck} = 45.547\ MPa \qquad E_s := 200\ GPa \qquad \varepsilon_{cu} := 3.5 \cdot 10^{-3}$

$c_{in.left} = 38\ mm$

$c_{out.left} = 24\ mm$

$c_{in.right} = 34\ mm$

$c_{out.right} = 36\ mm$

$d_{bottom} := \frac{c_{in.left} + c_{out.left} + c_{in.right} + c_{out.right}}{4} = 33\ mm$

$c_{top} = 34\ mm \qquad d_{top} := \frac{c_{top} + c_{top}}{2} = 34\ mm$

Assumption: n.a. is above the top reinforcement

$x := \frac{\left(F_{y.GI} + F_{y.GO} + F_{y.GICR} + F_{y.GOCR}\right) + \left(F_{y.GI} + F_{y.GO}\right)}{b \cdot \alpha \cdot f_{ck}} = 33.138\ mm$

$$M_{Rd.1} := f_{ck} \cdot \alpha \cdot b \cdot x \cdot \left(d - \beta \cdot x\right) = 77.392 \ \textbf{kN} \cdot \textbf{m}$$

$$M_{Rd.2} := \left(F_{y.GI} + F_{y.GO}\right) \cdot \left(d - c_{top}\right) = 23.592 \ \textbf{kN} \cdot \textbf{m}$$

$$M_{Rd} := M_{Rd.1} - M_{Rd.2} = 53.8 \ \textbf{kN} \cdot \textbf{m}$$

$$P_{yield} := \frac{M_{Rd} \cdot 2}{\left(\frac{L_{13G}}{2} - a_s\right)} = 270.692 \ \textbf{kN}$$

C.6 Beam 16K

16 K spliced hook bars

$b := 250\ mm$

$h := 300\ mm$

$L_{16K} := 89.5\ cm$

$P_{16K.max} := 300.561\ kN$ maximum applied force

$R_{16K} := \frac{P_{16K.max}}{2} = 150.281\ kN$

$a_s := 100\ mm$

$V_{16K} := R_{16K} = 150.281\ kN$

$M_{16K} := R_{16K} \cdot \frac{L_{16K} - 2 \cdot a_s}{2} = 52.222\ kN \cdot m$

$c_{top} := 34\ mm$

$c_{in.left} := 52\ mm$ $c_{in.right} := 68\ mm$

$c_{out.left} := 38\ mm$ $c_{out.right} := 35\ mm$

$c_{av} := \left(c_{in.left} + c_{in.right} + c_{out.left} + c_{out.right}\right) \cdot \frac{1}{4} = 48.25\ mm$

$d := h - c_{av} = 0.252\ m$

$F_{t1} := \frac{M_{16K}}{4 \cdot 0.9 \cdot d} = 57.622\ kN$

Yield force

$f_y := 252\ MPa$

$A_{s.KI} := 204.04\ mm^2$ $A_{s.KO} := 205.95\ mm^2$

$A_{s.KICR} := 204.24\ mm^2$ $A_{s.KOCR} := 202.70\ mm^2$

$F_{y.KI} := f_y \cdot A_{s.KI} = 51.418\ kN$

$F_{y.KO} := f_y \cdot A_{s.KO} = 51.899\ kN$

$F_{y.KICR} := f_y \cdot A_{s.KICR} = 51.468\ kN$

$F_{y.KOCR} := f_y \cdot A_{s.KOCR} = 51.08\ kN$

Bond in unyielded zone

$l_{uy.KI} := 304\ mm$ $l_{uy.KO} := 238\ mm$ $l_{uy.KICR} := 222.67\ mm$ $l_{uy.KOCR} := 234.67\ mm$

$l_{a.KI} := 690\ mm$ $l_{a.KO} := 640\ mm$ $l_{a.KICR} := 609\ mm$ $l_{a.KOCR} := 621\ mm$

$P_{n.KI} := 50.73\ mm$ $P_{n.KO} := 51\ mm$ $P_{n.KICR} := 50.77\ mm$ $P_{n.KOCR} := 50.81\ mm$

Assume bond in unyielded zone

$\tau_{uy.KI} := 2\ MPa$

$\tau_{uy.KO} := 2\ MPa$

$\tau_{uy.KICR} := 2\ MPa$

$\tau_{uy.KOCR} := 2\ MPa$

$F_{u.KI} := \tau_{uy.KI} \cdot l_{uy.KI} \cdot P_{n.KI} = 30.844\ kN$

$F_{u.KO} := \tau_{uy.KO} \cdot l_{uy.KO} \cdot P_{n.KO} = 24.276\ kN$

$F_{u.KICR} := \tau_{uy.KICR} \cdot l_{uy.KICR} \cdot P_{n.KICR} = 22.61\ kN$

$F_{u.KOCR} := \tau_{uy.KOCR} \cdot l_{uy.KOCR} \cdot P_{n.KOCR} = 23.847\ kN$

$F_{h.KI} := F_{y.KI} - F_{u.KI} = 20.574\ kN$

$F_{h.KO} := F_{y.KO} - F_{u.KO} = 27.623\ kN$

$F_{h.KICR} := F_{y.KICR} - F_{u.KICR} = 28.859\ kN$

$F_{h.KOCR} := F_{y.KOCR} - F_{u.KOCR} = 27.233\ kN$

Bond strength in yielded zone

$$\tau_{y.KI} := \frac{F_{t1} - F_{y.KI}}{P_{n.KI} \cdot 66.5\ mm} = 1.839\ MPa$$

$$\tau_{y.KO} := \frac{F_{t1} - F_{y.KO}}{P_{n.KO} \cdot 97\ mm} = 1.157\ MPa$$

Marques and Jirsa

$\psi := 1$ $f_{ck} := 6.606 \cdot 10^3$ *psi* $\phi := 0.63$ *in*

$f_h := 700 \cdot (1 - 0.3 \cdot 0.63) \cdot \psi \cdot \sqrt{6.606 \cdot 10^3}$ *psi* $= 318.132$ *MPa*

Hook strength

$F_{MJ.DI} := f_h \cdot A_{s.KI} = 64.912$ *kN*

$F_{MJ.DO} := f_h \cdot A_{s.KO} = 65.519$ *kN*

$F_{MJ.DICR} := f_h \cdot A_{s.KICR} = 64.975$ *kN*

$F_{MJ.DOCR} := f_h \cdot A_{s.KOCR} = 64.485$ *kN*

Residual strength

$A_{c.KI} := 203.93$ *mm*^{2} $A_{c.KO} := 205.09$ *mm*^{2}

$A_{c.KICR} := 203.54$ *mm*^{2} $A_{c.KOCR} := 204.27$ *mm*^{2}

$d_{after.KI} := 2 \cdot \sqrt{\frac{A_{c.KI}}{\pi}} = 0.634$ *in*

$f_{h.KI} := 700 \cdot (1 - 0.3 \cdot 0.634) \cdot \psi \cdot \sqrt{6.606 \cdot 10^3}$ *psi* $= 317.661$ *MPa*

$d_{after.KO} := 2 \cdot \sqrt{\frac{A_{c.KO}}{\pi}} = 0.636$ *in*

$f_{h.KO} := 700 \cdot (1 - 0.3 \cdot 0.636) \cdot \psi \cdot \sqrt{6.606 \cdot 10^3}$ *psi* $= 317.426$ *MPa*

$d_{after.KICR} := 2 \cdot \sqrt{\frac{A_{c.KICR}}{\pi}} = 0.634$ *in*

$f_{h.KICR} := 700 \cdot (1 - 0.3 \cdot 0.634) \cdot \psi \cdot \sqrt{6.606 \cdot 10^3}$ *psi* $= 317.661$ *MPa*

$d_{after.KOCR} := 2 \cdot \sqrt{\frac{A_{c.KOCR}}{\pi}} = 0.635$ *in*

$f_{h.KOCR} := 700 \cdot (1 - 0.3 \cdot 0.635) \cdot \psi \cdot \sqrt{6.606 \cdot 10^3}$ *psi* $= 317.543$ *MPa*

$F_{after.KI} := f_{h.KI} \cdot A_{c.KI} = 64.781$ *kN*

$F_{after.KO} := f_{h.KI} \cdot A_{c.KO} = 65.149$ *kN*

$F_{after.KICR} := f_{h.KICR} \cdot A_{c.KICR} = 64.657$ *kN*

$F_{after.KOCR} := f_{h.KICR} \cdot A_{c.KOCR} = 64.889$ *kN*

$F_{u.a.KICR} := F_{y.KICR} - F_{after.KICR} = -13.188\ \boldsymbol{kN}$

$F_{u.a.KOCR} := F_{y.KO} - F_{after.KOCR} = -12.989\ \boldsymbol{kN}$

BBK

$f_{cm} := f_{ck} + 8\ \boldsymbol{MPa} = 53.547\ \boldsymbol{MPa}$

$f_{ctm} := 0.3 \cdot \left(f_{ck} \cdot \frac{1}{1\ \boldsymbol{MPa}} \right)^{\frac{2}{3}} \cdot 1\ \boldsymbol{MPa} = 3.826\ \boldsymbol{MPa}$

$f_{ctk0.05} := 0.7 \cdot f_{ctm} = 2.678\ \boldsymbol{MPa}$

$\xi := 90$

$F_{h.BBK.KI} := A_{c.KI} \cdot \xi \cdot f_{ctk0.05} = 49.157\ \boldsymbol{kN}$

$F_{h.BBK.KO} := A_{c.KO} \cdot \xi \cdot f_{ctk0.05} = 49.436\ \boldsymbol{kN}$

$F_{h.BBK.KICR} := A_{c.KICR} \cdot \xi \cdot f_{ctk0.05} = 49.063\ \boldsymbol{kN}$

$F_{h.BBK.KOCR} := A_{c.KOCR} \cdot \xi \cdot f_{ctk0.05} = 49.238\ \boldsymbol{kN}$

$\alpha := 0.81 \qquad \beta := 0.416 \qquad f_{ck} = 45.547\ \boldsymbol{MPa} \qquad E_s := 200\ \boldsymbol{GPa} \qquad \varepsilon_{cu} := 3.5 \cdot 10^{-3}$

$c_{in.left} = 52\ \boldsymbol{mm}$

$c_{out.left} = 38\ \boldsymbol{mm}$

$c_{in.right} = 68\ \boldsymbol{mm}$

$d_{bottom} := \frac{c_{in.left} + c_{out.left} + c_{in.right} + c_{out.right}}{4} = 48.25\ \boldsymbol{mm}$

$c_{out.right} = 35\ \boldsymbol{mm}$

$c_{top} = 34\ \boldsymbol{mm} \qquad d_{top} := \frac{c_{top} + c_{top}}{2} = 34\ \boldsymbol{mm}$

Assumption: n.a. is above the top reinforcement

$x := \frac{\left(F_{y.KI} + F_{y.KO} + F_{y.KICR} + F_{y.KOCR}\right) + \left(F_{y.KI} + F_{y.KO}\right)}{b \cdot \alpha \cdot f_{ck}} = 33.522\ \boldsymbol{mm}$

$$M_{Rd.1} := f_{ck} \cdot \alpha \cdot b \cdot x \cdot \left(d - \beta \cdot x\right) = 73.525 \ \boldsymbol{kN \cdot m}$$

$$M_{Rd.2} := \left(F_{y.KI} + F_{y.KO}\right) \cdot \left(d - c_{top}\right) = 22.497 \ \boldsymbol{kN \cdot m}$$

$$M_{Rd} := M_{Rd.1} - M_{Rd.2} = 51.028 \ \boldsymbol{kN \cdot m}$$

$$P_{yield} := \frac{M_{Rd} \cdot 2}{\left(\frac{L_{16K}}{2} - a_s\right)} = 293.686 \ \boldsymbol{kN}$$

C.7 Shear capacity

$h := 300mm \qquad b := 250mm$

$c_{top} := 34mm$

$d := h - c_{top} = 0.266\,m$

$z := 0.9 \cdot d = 239.4 \cdot mm$

$s_w := 300mm$

$f_{ywd} := \frac{252}{1}MPa = 252 \cdot MPa$

$\theta_{10D} := \operatorname{atan}\left(\frac{8}{10.5}\right) = 37.304 \cdot deg$ $\qquad$ $\theta_{13G} := \operatorname{atan}\left(\frac{8.5}{10.5}\right) = 38.991 \cdot deg$

$n_{10D} := 1$ $\qquad$ $n_{13G} := 1$

$A_{sw} := \frac{(6mm)^2 \cdot \pi}{4} = 28.274 \cdot mm^2$

$V_{Rd.10D} := n_{10D} \cdot f_{ywd} \cdot A_{sw} \cdot 2 = 14.25 \cdot kN$ $\qquad$ $V_{Rd.13G} := n_{13G} \cdot f_{ywd} \cdot A_{sw} \cdot 2 = 14.25 \cdot kN$

$P := 2 \cdot V_{Rd.10D} = 28.501 \cdot kN$ $\qquad$ $P := 2 \cdot V_{Rd.13G} = 28.501 \cdot kN$

Assumption: without stirrups if stirrups were not activated

$b_w := b$ $\qquad$ $b_w := b \qquad d_{10} :=$

$\gamma_c := 1.5$ $\qquad$ $\gamma_c := 1.5$

$C_{Rd.c} := \frac{0.18}{\gamma_c} = 0.12$ $\qquad$ $C_{Rd.c} := \frac{0.18}{\gamma_c} = 0.12$

$k := 1 + \sqrt{\frac{200}{d \cdot \frac{1}{...}}} = 28.42$ $\qquad$ $k := 1 + \sqrt{\frac{200}{d_{10} \cdot \frac{1}{...}}} = 28$

$A_{sl} := (16mm)^2 \cdot \frac{\pi}{4} = 201.062 \cdot mm^2$ $\qquad$ $A_{sl} := (16mm)^2 \cdot \frac{\pi}{4} = 20$

$\rho_l := \frac{A_{sl}}{b_w \cdot d} = 3.023 \times 10^{-3}$ $\qquad$ $\rho_l := \frac{A_{sl}}{b_w \cdot d_{10}} = 3.064 \times$

$f_{ck} := 45.5MPa$

$\upsilon_{min} := 0.035 \cdot k^{\frac{3}{2}} \cdot \left(f_{ck}\right)^{\frac{1}{2}} = 3.611 \times 10^{4} \frac{kg^{0.5}}{m^{0.5} \cdot s}$

$V_{Rd.min} := \upsilon_{min} \cdot b_w \cdot d = 2.402 \times 10^{3} \frac{m^{1.5} \cdot kg^{0.5}}{s}$

$V_{Rd.c} := \left[C_{Rd.c} \cdot k \cdot \left(100 \cdot \rho_l \cdot f_{ck}\right)\right]^{\frac{1}{3}} \cdot b_w \cdot d = 24.142 \frac{m^{1.667} \cdot kg^{0.333}}{s^{0.667}}$

$f_{ck} := 45.5MPa$

$\upsilon_{min} := 0.035 \cdot k^{\frac{3}{2}} \cdot \left(f_{ck}\right)$

$V_{Rd.min} := \upsilon_{min} \cdot b_w \cdot d$

$V_{Rd.c} := \left[C_{Rd.c} \cdot k \cdot \left(100\right.\right.$

$\theta_{16K} := \operatorname{atan}\left(\frac{8.5}{9.1}\right) = 43.047 \cdot \text{deg}$

$n_{16K} := 1$

$V_{Rd.16K} := n_{16K} \cdot f_{ywd} \cdot A_{sw} \cdot 2 = 14.25 \cdot \text{kN}$

$P := 2 \cdot V_{Rd.16K} = 28.501 \cdot \text{kN}$

: 262.5mm

.603

)1.062·mm^2

10^{-3}

$$\frac{1}{2} = 3.611 \times 10^{4}\ \frac{kg^{0.5}}{m^{0.5}\cdot s}$$

$$10 = 2.37 \times 10^{3}\ \frac{m^{1.5}\cdot kg^{0.5}}{s}$$

$$\cdot\rho_l\cdot f_{ck}\right)\Big]^{\frac{1}{3}}\cdot b_w\cdot d_{10} = 23.824\ \frac{m^{1.667}\cdot kg^{0.333}}{s^{0.667}}$$